

ScholarWorks@GSU

Endothelial Cell Factors Involved in Bartonella Bacilliformis Pathogenesis

Authors	Soni, Tanushree
Citation	Soni, Tanushree. 2009. "Endothelial Cell Factors Involved in Bartonella Bacilliformis Pathogenesis." Georgia State University. https://doi.org/10.57709/1063875
DOI	https://doi.org/10.57709/1063875
Rights	I hereby certify that, if appropriate, I have obtained and attached hereto a written permission statement from the owner(s) of each third party copyrighted matter to be included in my thesis, dissertation, or project report, allowing distribution as specified below. I certify that the version I submitted is the same as that approved by my advisory committee. I hereby grant to Georgia State University or its agents the non-exclusive license to archive and make accessible, under the conditions specified below, my thesis, dissertation, or project report in whole or in part in all forms of media, now or hereafter known. I retain all other ownership rights to the copyright of the thesis, dissertation or project report. I also retain the right to use in future works (such as articles or books) all or part of this thesis, dissertation, or project report.
Download date	2026-05-20 03:55:25
Link to Item	https://hdl.handle.net/20.500.14694/2105

ENDOTHELIAL CELL FACTORS INVOLVED IN *BARTONELLA BACILLIFORMIS*
PATHOGENESIS

by

TANUSHREE SONI

Under the Direction of Dr. Barbara Baumstark, Ph.D.

ABSTRACT

The genus *Bartonella* comprises emerging pathogens that are causative agents of a wide range of clinical manifestations such as cat scratch disease, bacillary angiomatosis, and Carrion's disease. All species are transmitted by blood-sucking arthropods and infect erythrocytes and endothelial cells of hosts. Carrion's disease is a bi-phasic infection caused by *Bartonella bacilliformis* which is characterized by hemolysis of infected erythrocytes followed by invasion of the vascular endothelium. This provokes pronounced cellular proliferation, angiogenesis and skin eruptions called verruga peruana. Endothelial cells are thought to be the primary niche wherein bacteria reside between inoculation and erythrocyte infection. This study aims to elucidate some of the endothelial factors involved during the verruga peruana phase of Carrion's disease.

In order to adhere to and invade human microvascular endothelial cells (HMEC-1), *B. bacilliformis* engages a family of cell receptors called integrins. We used anti-integrin antibodies to show that the primary integrin involved is the fibronectin receptor $\alpha_5\beta_1$, although the vitronectin receptor $\alpha_V\beta_3$ also plays a minor role. We show *B. bacilliformis* invasion is also dependent on integrin ligands, fibronectin and vitronectin as antibodies against these proteins

decreased invasion and attachment, whereas pre-treatment of the bacteria with these molecules enhanced infection of endothelial cells. Bacterial uptake requires various host cytoplasmic signaling pathways to work in tandem, and our study identified three mitogen activated protein kinases involved. Apart from MAPKs, phosphatidylinositol 3 kinase plays a role during invasion and cell survival. PI3K inhibitors blocked bacterial internalization and *B. bacilliformis* infected cells showed accelerated apoptosis. Lastly, microarray analysis was performed to study the gene expression profile of *B. bacilliformis* infected HMEC-1 cells. Numerous molecules of the integrin signaling pathways are involved, suggesting integrins as the major receptor recruited for the successful infection by *B. bacilliformis*.

In summary this is the first study to demonstrate the role of integrins as *B. bacilliformis* receptors and integrin ligands as facilitators of infection. Gene expression analysis suggests the possibility that integrin mediated signaling pathways are the key modulators of cellular alterations during *B. bacilliformis* infection. This hypothesis is supported by the identification of some members of the integrin signaling pathway necessary for *B. bacilliformis* entry into endothelial cells.

INDEX WORDS: *Bartonella*, Endothelial cells, Integrins, Invasion, Extracellular Matrix Proteins, Kinases, Microarray Analysis

ENDOTHELIAL CELL FACTORS INVOLVED IN *BARTONELLA BACILLIFORMIS*
PATHOGENESIS

by

TANUSHREE SONI

A Dissertation Presented in Partial Fulfillment of Requirements for the Degree of

Doctor of Philosophy

in the College of Arts and Sciences

Georgia State University

2008

Copyright by
Tanushree Soni
2008

ENDOTHELIAL CELL FACTORS INVOLVED IN *BARTONELLA BACILLIFORMIS*
PATHOGENESIS

by

TANUSHREE SONI

Committee Chair: Barbara Baumstark

Committee: PC Tai
Zehava Eichenbaum
Julia Hilliard

Electronic Version Approved:

Office of Graduate Studies
College of Arts and Sciences
Georgia State University
May 2008

Acknowledgements

This dissertation would not have been completed without the good wishes and love of some wonderful people. I would like to express my gratitude to them all.

I would like to thank Dr Barbara Baumstark for providing me an environment that developed my scientific skills and ability to think independently. I am grateful to Dr P.C. Tai and Dr Zehava Eichenbaum for their patience and guidance during the completion of my dissertation. I am pleased to thank Dr Julia Hilliard who gave me much needed confidence, encouragement and valuable insights that helped shape this project.

I am blessed to have the most loving parents, sister and brother in law. You all have been pillars of support and inspiration thorough out my life. Thank you, mummy, papa, Sonu and Dhiraj. I am also very fortunate to receive endless support and encouragement from mummyji, papaji, bhaiya and bhabhi.

I owe a huge debt of gratitude to my friends: Kavita, Pradeep, Goutam and Madhavi for giving me the strength, love and their invaluable friendship. I would like to thank Griselle, Feda, and Drew who laughed and cried with me and made this journey so memorable.

This testament of gratitude is incomplete without mentioning my husband, Samit. I am so grateful to God for having you in my life. You have given me unconditional love and confidence that not only helped me complete my dissertation but also enriched my life and made me a better person. Thank you for loving me.

TABLE OF CONTENTS

Acknowledgements	iv
List of Tables	vii
List of Figures	viii
List of Abbreviations	x
General Introduction	12
History of Carrion's disease	14
Bacteriology	16
Clinical manifestations of <i>Bartonella</i> infections	17
Oroya Fever and verruga peruana	17
Trench Fever	18
Cat Scratch Disease (CSD)	19
Bacillary angiomatosis and endocarditis	19
Virulent factors involved in adhesion and invasion	20
Erythrocyte infection by <i>B. bacilliformis</i>	21
Interactions of <i>B. bacilliformis</i> with endothelial cells	22
Interactions of <i>B. henselae</i> and <i>B. quintana</i> with endothelial cells	24
Concluding remarks	28
Chapter I: Role of Integrins in <i>B. bacilliformis</i> infection of endothelial cells	30
Introduction	30
Integrins involved in bacterial pathogenesis	31
Fibronectin	34
Vitronectin	36
Bacterial cell adhesion molecules that engage integrins	37
Materials and Methods	39
Results	54
Discussion	89
Chapter II: Role of cell signal molecules during <i>B. bacilliformis</i> infection. 98	98
Introduction	98
Involvement of Mitogen Activated Protein Kinases in bacterial pathogenesis	99
Involvement of Phosphoinositidine 3 Kinase in bacterial pathogenesis	100
Materials and Methods	102
Results	107
Discussion	134
Chapter III: Expression patterns of genes involved in <i>B. bacilliformis</i> uptake	142
Introduction	142
Materials and Methods	145

Results	151
Discussion.....	173
Summary and conclusions	188
Bibliography	194

List of Tables

Table 1. <i>Bartonella</i> species, their natural reservoir and vector, and the resulting human diseases	13
Table 1.1. Effect of anti-integrin antibodies on <i>B. bacilliformis</i> invasion of HMEC-1 cells.	57
Table 1.2. Effect of anti-integrin antibodies on <i>B. bacilliformis</i> adhesion of HMEC-1 cells.	60
Table 1.3a. Effect of fibronectin-treated <i>B. bacilliformis</i> on invasion of HMEC-1 cells.	73
Table 1.3b. Effect of vitronectin-treated <i>B. bacilliformis</i> on invasion of HMEC-1 cells.	74
Table 1.4. Effect of anti-ECM antibodies on <i>B. bacilliformis</i> invasion of HMEC-1 cells.	78
Table 1.5. Effect of human serum on <i>B. bacilliformis</i> invasion into HMEC-1 cells.....	81
Table 1.6. Effect of fetal calf serum on <i>B. bacilliformis</i> invasion into HMEC-1 cells....	83
Table 2.1a. Effect of MEK inhibitor PD98059 on <i>B. bacilliformis</i> invasion into endothelial cells.	110
Table 2.1b. Effect of MEK inhibitor U0126 on <i>B. bacilliformis</i> invasion into HMEC-1 cells.	112
Table 2.2. Effect of p38 kinase inhibitor, SB203580 on <i>B. bacilliformis</i> invasion into HMEC-1 cells.	115
Table 2.3. Effect of JNK inhibitor SP600125 on <i>B. bacilliformis</i> invasion into HMEC-1 cells.	118
Table 2.4a. Effect of PI3K inhibitor wortmannin on <i>B. bacilliformis</i> invasion into HMEC-1 cells.	121
Table 2.4b. Effect of PI3K inhibitor LY294002 on <i>B. bacilliformis</i> invasion into HMEC-1 cells.	123
Table 2.5. Effect of PI3K inhibitor LY294002 on the viability of infected HMEC-1 cells.	127
Table 3.1a. Highly differentially expressed functional HMEC-1 transcriptomes, 30 minutes after <i>B. bacilliformis</i> infection.	157
Table 3.1b. Highly differentially expressed functional HMEC-1 transcriptomes, one hour after <i>B. bacilliformis</i> infection.	159
Table 3.1c. Highly differentially expressed functional HMEC-1 transcriptomes, three hours after <i>B. bacilliformis</i> infection.	161
Table 3.1d. Highly differentially expressed functional HMEC-1 transcriptomes, six hours after <i>B. bacilliformis</i> infection.	164
Table 3.2. Integrin subunits and integrin signaling component HMEC-1 transcriptomes.	168
Table 3.3. Validation of gene expression data obtained from microarray studies.....	172

List of Figures

Figure 1.1. Effect of anti-integrin antibodies on <i>B. bacilliformis</i> infection of HMEC-1 cells.	56
Figure 1.2. Effect of anti-integrin antibodies on <i>B. bacilliformis</i> adhesion to HMEC-1 cells.	59
Figure 1.3a. Determination of integrin α_5 and integrin β_1 gene expression in <i>B. bacilliformis</i> infected HMEC-1 cells.	62
Figure 1.3b. Determination of integrin α_v and integrin β_3 gene expression in <i>B. bacilliformis</i> infected HMEC-1 cells.	63
Figure 1.4. <i>B. bacilliformis</i> binding to ECM proteins studied by ELISAs.....	65
Figure 1.5a. <i>B. bacilliformis</i> binding to soluble fibronectin studied by ELISAs.....	67
Figure 1.5b. <i>B. bacilliformis</i> binding to soluble vitronectin studied by ELISAs.....	68
Figure 1.6a. Effect of fibronectin-coated <i>B. bacilliformis</i> invasion into HMEC-1 cells.	71
Figure 1.6b. Effect of vitronectin-coated <i>B. bacilliformis</i> invasion into HMEC-1 cells.	72
Figure 1.7. Effect of anti-ECM protein antibodies on <i>B. bacilliformis</i> infection of HMEC-1 cells.	77
Figure 1.8. Effect of human serum on <i>B. bacilliformis</i> invasion into HMEC-1 cells.	80
Figure 1.9. Effect of fetal calf serum on <i>B. bacilliformis</i> invasion into HMEC-1 cells.	82
Figure 1.10. Western immunoblot showing the presence of the 43kDa antigen in the outer membrane preparations from <i>B. bacilliformis</i> and recombinant <i>E. coli</i> expressing NlpD _{Bb}	85
Figure 1.11. Western immunoblot of recombinant <i>E. coli</i> expressing wild type NlpD _{Bb} and mutant NlpD _{Bb}	87
Figure 2.1a. Effect of MEK1/2 inhibitors PD98059 on <i>B. bacilliformis</i> invasion into HMEC-1 cells.	109
Figure 2.1b. Effect of MEK1/2 inhibitor U0126 on <i>B. bacilliformis</i> invasion into HMEC-1 cells.	111
Figure 2.2. Effect of p38 kinase inhibitor SB203580 on <i>B. bacilliformis</i> invasion into HMEC-1 cells.	114
Figure 2.3. Effect of JNK1/2/3 inhibitor SP600125 on <i>B. bacilliformis</i> invasion into HMEC-1 cells.	117
Figure 2.4a. Effect of PI3K inhibitor wortmannin on <i>B. bacilliformis</i> invasion into HMEC-1 cells.	120
Figure 2.4b. Effect of PI3K inhibitor LY294002 on <i>B. bacilliformis</i> invasion into HMEC-1 cells.	122
Figure 2.5a. Effect of LY294002 on HMEC-1 cells infected with <i>B. bacilliformis</i>	126
Figure 2.5b. Effect of PI3K inhibitor, LY294002, on endothelial cell viability, two hours post-infection.	128
Figure 2.5c. Effect of PI3K inhibitor, LY294002, on <i>B. bacilliformis</i> -infected endothelial cell viability, two hours post-infection.	129
Figure 2.5d. Effect of PI3K inhibitor, LY294002, on endothelial cell viability, six hours post-infection.	130
Figure 2.5e. Effect of PI3K inhibitor, LY294002, on <i>B. bacilliformis</i> -infected endothelial cell viability, six hours post-infection.....	131

Figure 2.5f. Effect of PI3K inhibitor, LY294002, on endothelial cell viability, 24 hours post-infection.	132
Figure 2.5g. Effect of PI3K inhibitor, LY294002, on <i>B. bacilliformis</i> -infected endothelial cell viability, 24 hours post-infection.	133
Figure 3.1a. Endothelial gene expression at various time points.....	152
Figure 3.1b. Endothelial gene expression at various time points.	154
Figure 3.2a. <i>Bartonella bacilliformis</i> binding to integrins.	192
Figure 3.2b. Integrin mediated signaling events occurring after <i>B. bacilliformis</i> attachment to integrins.	193

List of Abbreviations

ADAM12	A Disintegrin and Metalloprotease 12
ANGPT	Angiopoetin
AP	Alkaline Phosphatase
BA	Bacilliary Angiomatosis
BadA	Bartonella adhesion A
BadA	Bcl2 Antagonist of Death
BAX	Bcl2 Associated X Protein
Bep	Bartonella translocated effector protein
BSA	Bovine Serum Albumin
CASP9	Caspase 9
Cdc42	Cell division cycle 42
CEACAM	Carcinoembryonic antigen-related cell adhesion molecule 1
Cel	Cell Intensity File
CFU	Colony Forming Unit
CSD	Cat Scratch Disease
DMSO	Dimethyl Sulfoxide
DPM	Disintegrations Per Minute
ECM	Extra Cellular Matrix
ELISA	Enzyme Linked Immuno Sorbent Assay
ERK	Extracellular signal Regulated Kinase
FAK	Focal Adhesion Kinase
FBS	Fetal Bovine Serum
FCS	Fetal Calf Serum
FGF	Fibroblast Growth Factor
FGFR4	Fibroblast Growth Factor Receptor 4
FnBp	Fibronectin binding protein
GCOS	GeneChip Operating System
GFP	Green Flurescent Protein
HHV8	Human Herpes Virus 8
HIF-1	Hypoxia Inducible Factor-1
HIV	Human Immunodeficiency Virus
HMEC-1	Human Microvascular Endothelial Cell
HRK	Harakiri
Ial	Invasion-associated locus
ICAM1	Intercellular adhesion molecule 1
IGF	Insulin like Growth Factor
ILK	Integrin Linked Kinase
Ipas	Invasion plasmid antigens

IPTG	Isopropyl β -D-1-thiogalactopyranoside
KS	Kaposi's Sarcoma
LPS	Lippopolysaccharide
m.o.i	mulitplicity of infection
MAPK	Mitogen Activated Kinase
MAPKK	MAPK kinase
MAPKKK	MAPKK kinase
NlpD	Novel lipoprotein D
NR	Normalized Ratio
OD	Optical Density
OMP	Outer Membrane Protein
Opa	Opacity associated protein
PAK	p21 Activating Kinase
PBS	Phosphate Buffered Saline
PECAM	Platelet/endothelial cell adhesion molecule
PI3K	Phosphotidylinositide 3 kinase
PMN	Polymorphonuclear lymphocytes
p-NPP	p-Nitrophenyl Phosphate
PtdIns(4,5)P2	Phophatidylinositol 4,5 bis-phosphate
PTKs	Protein Tyrosine Kinases
PVDF	Polyvinylidene Fluoride
Rac	ras-related C3 botulinum toxin substrate 1
RBC	Red Blood Cell
RGD	Arginine-Glycine-Aspartate
Rho	ras homolog gene family
RQ	Relative Quotient
SAPK/JNK	Stress Activated Protein Kinase/ c-Jun N-terminal Kinase
SEM	Standard Error Mean
T4SS	Type-IV secretion system
TLR7	Toll Like Receptor 7
TNF α	Tumour Necrosis Factor α
TRAF3	TNF Receptor Associated Factor 3
VEGF	Vascular Endothelial Growth Factor
VOMP	Variably expressed OMP
YadA	Yersinia adhesin A

General Introduction

Bartonella (formerly *Rochalimaea*) is a genus of facultative intracellular parasites that consists of 20 species (spps), eight of which are known human pathogens (Table.1.). These bacteria employ an arthropod mode of transmission; the blood-sucking vectors include sandflies, ticks, fleas, and mosquitoes. *Bartonella* spp cause a wide range of diseases that can induce acute onset (e.g., Oroya phase of *B. bacilliformis* infection) or chronic disease (e.g., bacillary angiomatosis during *B. henselae* infection). The invasion and persistent colonization of erythrocytes in the mammalian reservoir is unique to the *Bartonella* genus. Erythrocytic infection also can be asymptomatic, representing an exception to Koch's postulate, which states that "Bacteria do not occur in the blood or tissues of healthy animals or humans" (Brock, 1999). In this chapter, we review some of the virulent factors of the human pathogens *B. bacilliformis*, *B. henselae*, and *B. quintana*, with a predominant focus on *B. bacilliformis*.

Table 1. *Bartonella* species, their natural reservoir and vector, and the resulting human diseases

Bartonella species	Reservoir	Vector	Human disease(s)
Human-specific species			
<i>B. bacilliformis</i>	Human	Sandfly	Carrión's disease: Oroya fever and verruga peruana
<i>B. quintana</i>	Human	Body louse	Trench fever, endocarditis, bacillary angiomatosis
Zoonotic species			
<i>B. clarridgeiae</i>	Cat	Cat flea	Cat-scratch disease
<i>B. elizabethae</i>	Rat	?	Endocarditis, neuroretinitis
<i>B. grahamii</i>	Mouse, vole	?	Neuroretinitis
<i>B. henselae</i>	Cat	Cat flea	CSD, endocarditis, BA, BP, neuroretinitis, bacteremia with fever
<i>B. vinsonii</i> subsp. <i>arupensis</i>	Mouse	Ticks	Bacteremia with fever
<i>B. washoensis</i>	Ground squirrels	?	Myocarditis
Animal-specific species			
<i>B. alsatica</i>	Rabbit	?	?
<i>B. birtlesii</i>	Mouse	?	?
<i>B. bovis</i> (= <i>B. weissii</i>)	Cattle/cat	?	?
<i>B. capreoli</i>	Roe deer	?	?
<i>B. chomelii</i>	Cattle	?	?
<i>B. doshiae</i>	Vole	?	?
<i>B. koehlerae</i>	Cat	?	?
<i>B. peromysci</i>	Deer, mouse	?	?
<i>B. schoenbuchensis</i>	Roe deer	Deer ked	?
<i>B. talpae</i>	Mole	?	?
<i>B. taylorii</i>	Mouse, vole	?	?
<i>B. tribocorum</i>	Rat	?	?
<i>B. vinsonii</i> subsp. <i>berkhoffii</i>	Dog	Ticks	?
<i>B. vinsonii</i> subsp. <i>vinsonii</i>	Vole	Vole ear mite	?

Source : Molecular and Cellular Basis of *Bartonella* Pathogenesis. Christoph Dehio. Annual Review of Microbiology. 2004. 58: 365-90.

History of Carrion's disease

Carrion's disease is a bi-phasic infection named after Daniel Carrion, a medical student, who first linked the two phases of the disease, namely, Oroya fever and verruga peruana. The first, acute-onset, phase of the disease was documented in 1870 when thousands of rail workers succumbed to fever and anemia caused by unknown factors. A railway was being built in the Andean region from Lima to La Oroya, and because the disease was contained within this region, authorities called it "Oroya fever" in reference to the final point of the rail (Cueto, 1996). The second phase of the disease is characterized by nodular skin lesions. These lesions have been described for centuries, and are represented on artifacts from pre-Incan civilizations. These lesions last anywhere from a few weeks to months. Because these lesions were unique to the Peruvian region, they were given the simple nomenclature Peruvian warts or verruga peruana. Cases of Carrion's disease also have been recorded in arid regions of Ecuador and Colombia (Alexander, 1995). For many years, Oroya fever and verruga peruana were believed to be manifestations of two separate infections. Daniel Carrion demonstrated their relationship by inoculating himself with blood from an eruptive verruga lesion. Within three weeks, he suffered from acute febrile anemia, a hallmark of the Oroya phase. Unfortunately, Carrion died while in the acute phase of the disease, though his fatal self-experimentation provided proof that the two stages had the same origin.

The causative agent of Carrion's disease remained unidentified until the establishment of local bacteriological institutes in the early 1900s. Alberto Barton, a British immigrant, first described the causative agent in his thesis and then, after extensive research, announced the discovery of a novel microbe in the blood of Oroya

fever patients in 1909. He observed that the fever coincided with an increase in bacteremia. This was followed by a decrease in the number of bacteria and ultimately their complete absence from the blood stream; only later did the blood-filled warts characteristic of verruga peruana make their appearance. Barton's conclusions were not accepted until 1913, when Richard P. Strong confirmed his findings and proposed the new genus *Bartonella bacilliformis* (Strong *et al.*, 1915). Subsequently, the genus *Bartonella* was merged with *Rochalimaea* (*B. quintana*, *B. henselae*, *B. elizabethae*, and *B. vinsonii*) and *Grahamella* (*B. talpae*, *B. peromysci*, *B. grahamii*, *B. taylori*, and *B. doshiae*) (Birtles *et al.*, 1995; Brenner *et al.*, 1993), based on DNA hybridization and 16S rRNA similarities to produce a genus currently containing 20 species.

All *Bartonella* species are transmitted by blood-sucking arthropods. Bueno and colleagues first proposed sandflies as a common vector for the transmission of the causative agent of Carrion's disease and cutaneous leishmaniasis (Herrer *et al.*, 1975). Townsend then identified *Phlebotomus verrucarum* (now known as *Lutzomyia verrucarum*), a nocturnal sandfly, as the vector of Oroya fever (Townsend, 1913). *B. bacilliformis* also were isolated from the proboscis of the sandfly, which further confirmed it as the arthropod vector (Hertig, 1942). The source for *B. bacilliformis* colonization of *Lutzomyia verrucarum* remains unknown. So far, no mammalian reservoirs have been discovered, though a mammalian reservoir cannot be ruled out because of the phylogenetic relation to *Grahamella*, which are harbored by small woodland animals. The primary reservoirs for the zoonotic pathogen *B. henselae* are cats. *B. henselae* causes intraerythrocytic bacteremia in cats; the cat flea *Ctenocephalides felis* is responsible for feline-to-feline transmission (Higgins *et al.*, 1996; Kordick *et al.*,

1995). Incidental transfer of the bacteria from cats to humans occurs through cat bites and scratches and indirectly via cat fleas. The arthropod vector for *B. quintana* transmission is the human body louse, *Pediculus humanus*. *B. quintana* can multiply within the intestines of the lice and is present in their feces. Fecal transmission into the skin occurs when a body louse bite induces pruritis and scratching of the host skin (Raoult *et al.*, 1999). Humans are thought to be the only reservoirs necessary for *B. quintana* because infections can lead to prolonged, asymptomatic bacteremia. However, since the bacteria have been detected in cat teeth, cat fleas, and monkey fleas, additional reservoirs also have been proposed (Raoult *et al.*, 1994).

Bacteriology

The genus *Bartonella* consists of small (0.3–0.5µm wide, 1–1.7 µm long), Gram negative, pleomorphic, aerobic rods. *Bartonella*, along with *Afipia*, *Agrobacterium*, and *Brucella*, constitute the alpha-2 subgroup of the class Proteobacteria. Biochemically, they are catalase and oxidase negative. They also are fastidious and extremely slow-growing organisms that can be recovered from primary isolates on blood agar only after 12–14 days. Subculture reduces the colony formation time to 3–5 days. *B. bacilliformis* has an optimal growth temperature of approximately 26°C, which could explain why the lesions are localized to bodily extremities, as well as its survival within an insect vector. The other two widely studied *Bartonellae*, *B. henselae* and *B. quintana*, need 5% CO₂ at 37°C to grow optimally. Fresh clinical isolates of *B. henselae* and *B. quintana* produce dry colonies that are deeply embedded in agar. These strains also have increased autoagglutination properties in suspension, which can be attributed to the presence of surface, type-IV pili. Higher passaged strains produce smooth mucoid colonies without

any agar indentations and do not agglutinate in liquid (Batterman *et al.*, 1995). With the exception of *B. bacilliformis* and *B. clarridgeiae*, the species are non-flagellated and non-motile. *B. henselae* and *B. quintana* have surface pili that represent important virulence factors. The genome size of *B. bacilliformis* is relatively small at just 1600kbp, with a GC content of 39–40% (Brenner *et al.*, 1991). *B. henselae* and *B. quintana* genomes are believed to have originated from *Brucella melitensis*. The genome of *B. henselae* has a slightly larger genome (1.9Mb) than *B. quintana*. The *B. quintana* genome appears to have been derived from that of *B. henselae* through the deletion of genomic islands (Alsmark *et al.*, 2004). The complete genomes of *B. bacilliformis*, *B. henselae*, and *B. quintana* are now available.

Clinical manifestations of *Bartonella* infections

Oroya Fever and verruga peruana

Oroya fever, the first phase of Carrion's disease, is characterized by the presence of *B. bacilliformis*-infected erythrocytes and develops 3 to 12 weeks after inoculation from the bite of the sandfly (Strong *et al.*, 1915). Almost 80% of circulating red blood cells (RBCs) can be parasitized with *B. bacilliformis*. *B. bacilliformis* is the only species in its genus to have hemolytic properties, as a result of which the infected erythrocytes undergo hemolysis *in vivo*, leading to severe hemolytic anemia. The fatality rate of untreated cases is extremely high, and survivors of the acute infection have asymptomatic persistent bacteremia. Patients recovering from the Oroya phase also suffer decreased immuno-competency. The two most common infections occurring in such patients are salmonellosis and toxoplasmosis (Cuadra, 1956; Garcia-Caceres *et al.*, 1991). The verruga peruana stage sets in within six weeks of an acute infection. During this phase,

the bacteria show tropism for the vascular endothelial cells. Vasculature infection provokes endothelial cell hyperplasia and neovascularization, resulting in the formation of new blood capillaries, a process defined as angiogenesis. The proliferating endothelial cells, along with inflammatory and growth factors induced by *B. bacilliformis*, culminate in pyogenic granulomatous hemangiomas, referred to as verruga peruana. These nodular lesions are primarily localized on limb extremities and the face and neck, though they can be found on the mucosal lining and, rarely, internal organs. Histologically, they are very similar to Kaposi's sarcoma (KS) lesions associated with infection by human herpes virus 8 (HHV8) (Caceres-Rios *et al.*, 1995). Most newly formed capillaries in the verrugas do not have lumens, and those that do feature open lumens that allow blood to collect in the papules. Dendrocytes and neutrophils are also seen, along with the proliferating endothelial cells, and bacteria are concentrated in extracellular and interstitial spaces (Arias-Stella *et al.*, 1986b; Arrese Estrada *et al.*, 1992). Electron micrographs of cells from the verruga lesions show membrane-bound *B. bacilliformis* in the process of being phagocytosed, though intracellular bacteria were rare (Arias-Stella *et al.*, 1986b). Treatment with oral antibiotics can temporarily resolve the lesions; however, due to the chronic infection of the host cells, relapse is common. Prolonged antibiotic therapy is required to eliminate the infection completely.

Trench Fever

Trench fever was prevalent in World War I as a result of poor sanitary conditions that allowed for the infestation of body lice, the vector for the causative pathogen, *B. quintana*. Recently, this infection, which is characterized by recurrent, high-fever episodes that last 1–3 days, has been reported among homeless people with poor

unsanitary conditions across the globe. The condition, renamed “urban” trench fever, is self-limiting and accompanied by pre-tibial pain, dizziness, and chronic bacteremia, which then lead to bacillary angiomatosis (BA) and endocarditis.

Cat Scratch Disease (CSD)

The most common disease caused by *B. henselae* in all age groups and people across the world, CSD is a benign, self-limiting condition transmitted by *B. henselae*-infected cat scratches or bites or indirectly by cat fleas. Regional lymphadenopathy (swollen, enlarged lymph nodes) and suppurative papules at the site of inoculation are characteristic clinical manifestations of CSD. Symptoms can occur within a couple of weeks or months and resolve spontaneously. Immunocompromised patients may present more complications. Antibiotic therapy has been used successfully to treat CSD.

Bacillary angiomatosis and endocarditis

Bacillary angiomatosis and endocarditis are caused by various *Bartonella* species. Verruga peruana-like lesions, which are manifestations of *B. henselae* or *B. quintana* infections, are referred to as epithelioid angiomatosis or bacillary angiomatosis. In appearance, they are blood filled, ulcerated, crusted, subcutaneous, or dermal nodules. Unlike verruga peruana, BA occurs only in immunocompromised patients, particularly those infected by human immunodeficiency virus (HIV). The other difference between verruga lesions and BA is that a variety of internal organs, such as the liver, spleen, brain, lungs, and bowel, can be affected (Cockerell *et al.*, 1987). Finally, BA differs from verruga because the bacteria are easily cultured and detected in BA lesions by PCR amplification of the 16sRNA sequence, histochemical staining, and electron microscopy.

The condition, in which the internal organs present with cystic lesions due to *B. henselae* or *B. quintana* infection is called bacillary peliosis. The peliotic space is partially lined with endothelium, which is separated from the parenchymal cells by a mixture of inflammatory cells and clumps of bacilli (Relman *et al.*, 1991).

The causative *Bartonella* species for endocarditis include *B. henselae*, *B. quintana*, *B. elizabethae*, and *B. vinsonii subsp. berkhoffii* and *subsp. arupensis*. Patients with preexisting valvulopathies suffer increased risk of endocarditis through transmission of *B. henselae* via cats and/or cat fleas. *B. quintana*-associated endocarditis does not correlate with any preexisting conditions. The antibodies from people suffering from *Bartonella*-induced endocarditis are cross-reactive with *Chlamydia* spp., often resulting in the misdiagnosis of the pathogen (Maurin *et al.*, 1997). Aminoglycoside treatment results in full recovery from *Bartonella* endocarditis.

Virulent factors involved in adhesion and invasion

All *Bartonella* spp. can infect erythrocytes in the specific mammalian host and therefore are spread easily by blood-sucking arthropods. The course of erythrocytic infection has been described in great detail for *B. tribocorum*, an organism found in rats (Schulein *et al.*, 2001). Briefly, a synchronous wave of erythrocyte infection occurs five days after the initial inoculation with the bacterium. Following invasion, eight rounds of bacterial replication take place. The number of bacteria remains unchanged for the life span of the erythrocytes. Because RBC infection is recurrent at five-day intervals, it ensures the presence of erythrocytic bacteria for efficient vector transmission. Erythrocytic infection subsides spontaneously, and at no point do the cells undergo hemolysis. This model is extremely useful for explaining what might occur in *B.*

quintana infections but not *B. bacilliformis* infections, because the latter condition is marked by severe hemolysis. *In vitro*, hemolysis is contact dependent, and the hemolysis factor is protease sensitive (Hendrix, 2000).

Erythrocyte infection by B. bacilliformis

B. bacilliformis infection of erythrocytes depends primarily on the presence of multiple, unipolar flagella. Non-motile bacteria exhibit decreased binding capacity and are unable to invade erythrocytes; *B. bacilliformis* pretreated with anti-flagellin antibodies also are deficient in erythrocytic invasion (Scherer *et al.*, 1993). The case in support of the flagella requirement was further strengthened when site-directed mutagenesis of the flagellin gene reduced bacterial binding by 75% (Battisti *et al.*, 1999). The mechanism of flagella-mediated invasion is not well understood, but motility may enhance *B. bacilliformis*–erythrocyte interactions, in which case the twirling motion of the flagella would help the bacteria force their way into the erythrocytes. This idea is supported by the observation that binding is reduced in the presence of proton motive force and respiration inhibitors (Benson *et al.*, 1986).

The function of a *B. bacilliformis* – encoded invasion-associated locus (*ial*) in erythrocyte invasion has been demonstrated by cloning the genes into *E. coli*, where they confer a marginally invasive phenotype to the recombinant *E. coli* (Mitchell *et al.*, 1995). The locus consists of two genes, *ialA* and *ialB*. *IalA* is a nucleoside polyphosphatase hydrolase of the MutT family is thought to be involved in nucleotide regulation and the metabolism. The *ialB* gene product is an 18kDa inner membrane protein (Cartwright *et al.*, 1999; Coleman *et al.*, 2001). Mutations of *ialB* were found to decrease *B. bacilliformis* binding to erythrocytes by 50% and the function was restored in

transcomplementation mutants, thus establishing the role for IalB in erythrocyte infections (Coleman *et al.*, 2001).

B. bacilliformis entry into erythrocytes also can be triggered by bacterial-mediated alterations in the cell membrane. Deformin, a bacterial protein found in *B. bacilliformis* and *B. henselae* culture supernatants, is a small, hydrophobic, albumin-bound substance (Derrick *et al.*, 2001). Deformin is responsible for producing deep invaginated pits and trenches in the erythrocyte membrane. Electron micrographs reveal the presence of *B. bacilliformis* within these indentations, where they are ultimately internalized (Derrick *et al.*, 2001). Deformin function is reversible in the presence of the ATPase inhibitor vanadate, the phospholipid dilauroylphosphatidylcholine, and ionophores that increase intracellular calcium levels (Xu *et al.*, 1995). The erythrocyte receptors for *B. bacilliformis* have been identified using immunoblots and include the carbohydrate moieties alpha, beta spectrin, and glycophorins A and B (Buckles *et al.*, 2000).

Interactions of B. bacilliformis with endothelial cells

Vascular endothelial cells are not only the principal targets for *B. bacilliformis*, but also may serve as a bacterial niche during the asymptomatic phase. *B. bacilliformis* adhere to and invade endothelial cells, as seen in tissues from verruga lesions and *in vitro* using primary cell lines (Arias-Stella *et al.*, 1986b; Hill *et al.*, 1992). Invasion is an actin-dependent process and occurs over a period of a few hours. The key regulators of actin restructuring are the small GTPases: Rho, Rac, and Cdc42. The first GTPase to be activated during *B. bacilliformis* infection is Cdc42, followed by Rac. Activated Cdc42 and Rac stimulate the formation of filopodia and lamellipodia. Various bacterial

aggregates are associated with leading membrane protrusions, which surround the bacteria and finally engulf them through a phagocytic mechanism (Verma *et al.*, 2002b). Pretreatment of the host cell with Rac or Cdc42 inhibitors markedly reduces *B. bacilliformis* invasion. In addition, Rho inhibition hampers bacterial uptake (Verma *et al.*, 2001). During the course of the infection, internal vesicles with single or clumped bacilli can be detected with florescent microscopy. The vesicles are colocalized with the Golgi complex in the perinuclear region, so that the disruption of the Golgi complex leads to bacterial dispersion throughout the cytoplasm (Verma *et al.*, 2001). Various host cell kinases, such as protein tyrosine kinases and mitogen-activated protein kinases that regulate actin organization, also are involved during *B. bacilliformis* internalization (Verma *et al.*, 2002b; Williams-Bouyer *et al.*, 1999). The only host receptor identified in epithelial cells thus far is the fibronectin receptor $\alpha_5\beta_1$ integrin (Williams-Bouyer *et al.*, 1999). Endothelial cell receptors and bacterial factors required for endothelial parasitization remain unidentified.

The most striking effect of *B. bacilliformis* infection of endothelial cells is the ability of the bacteria to induce proliferation and angiogenesis. The angiogenic effects appear with live bacteria and bacterial supernatants (Garcia *et al.*, 1990; Garcia, F. U. *et al.*, 1992). Early studies lead to the suggestion that the angiogenic factor is a protein due to its heat liability and precipitation with 45% ammonium sulfate (Garcia *et al.*, 1990). A recent report also proposes the molecular chaperone GroEL as a potential vasoproliferative candidate (Minnick *et al.*, 2003). The function of GroEL has been confirmed in studies with purified GroEL from *B. bacilliformis* culture supernatants and anti-GroEL antibodies, which inhibit neovascularization (Kohlhorst, D., personal

communication). The inflammatory infiltrates also could be mitogen sources *in vivo*, because *B. henselae*-infected macrophages release certain angiogenic factors, and the conditioned medium can trigger endothelial cell proliferation (Resto-Ruiz *et al.*, 2002). Studies of clinical specimens of verruga peruana show that the primary source of the vascular endothelial growth factor (VEGF) is the overlying epidermis (Cerimele *et al.*, 2003). Therefore, multiple sources of both bacterial and host origins may be required for vasoproliferation and angiogenesis *in vivo*.

Interactions of B. henselae and B. quintana with endothelial cells

B. henselae and *B. quintana* can invade nucleated cells, such as endothelial and epithelial cells, by phagocytosis (Batterman *et al.*, 1995; Brouqui *et al.*, 1996). When they get inside, these bacteria can multiply within the host cell's membrane-bound vesicle. In addition to classical phagocytosis, *B. henselae* can be internalized through a unique structure called invasome (Dehio *et al.*, 1997), a slow process that takes 24 hours, during which the leading lamella of endothelial cells aggregate the surface-bound bacteria. The bacteria enclosed within the lamella then are engulfed and internalized in an actin-dependent and microtubule-independent process (Dehio *et al.*, 1997). The bacterial factors facilitating infection by *B. henselae* and *B. quintana* are better defined than those of *B. bacilliformis*. Both these bacteria possess type-IV pili, which confer a twitching motility and self-aggregation properties (Batterman *et al.*, 1995). Pili also play an important role in host cell adhesion, a crucial step that precedes invasion. Bacteria that have been passaged many times have decreased or no pili, and thus are unable to attach to or invade host cells (Batterman *et al.*, 1995). Pili structures mediate host cell attachment. In addition, *B. henselae* pili are associated with VEGF production, which

leads to host cell proliferation (Kempf *et al.*, 2001). An outer membrane afimbrial protein encoded by *B. henselae*, Bartonella adhesion A (BadA) represents another bacterial factor with multiple functions. Only *B. henselae* strains that express BadA can adhere to endothelial cells and fibronectin, an extracellular matrix protein (Riess *et al.*, 2007). The expression of *BadA* undergoes phase variation and, like the pili, can be lost as a result of extensive passaging. Because BadA binds fibronectin, the putative host cell receptors are predicted to be integrins. Indeed, *B. henselae* binds with decreased avidity to cells that do not express the β_1 integrin (Riess *et al.*, 2004). The immunodominant BadA also has a critical function in the activation of hypoxia-inducible factor 1 (HIF-1) and pro-angiogenic cytokines such as VEGF in host cells (Riess *et al.*, 2004). A few other outer membrane proteins (OMP), ranging from 23kDa to 58 kDa, also interact with endothelial cells, though the 43kDa protein provides the major adhesin (Burgess *et al.*, 1998). *B. quintana* also has outer membrane proteins that are homologous to BadA. These variably expressed outer membrane proteins (Vomp) are immunodominant and undergo phase variation *in vivo*. The four genes belonging to Vomp family are absent from strains isolated from animal models and patients who have undergone prolonged bacteremia (Zhang *et al.*, 2004). The Vomp A and C proteins are involved in autoaggregation and, when expressed in *E. coli*, are able to confer a collagen-binding phenotype (Zhang *et al.*, 2004). Their exact role in adhesion and invasion is unclear, because *B. quintana* expressing Vomp A, B and C do not demonstrate increased adhesion; however, these proteins are critical for VEGF expression in host cells (Schulte *et al.*, 2006).

The type-IV secretion systems (T4SS) are transport machineries in Gram-negative bacteria that are related to bacterial conjugation systems. Bacterial conjugation systems originally functioned in DNA transfer among different bacteria, and virulent pathogens have adopted T4SS to transfer DNA and virulence factors into host cells (Cascales *et al.*, 2003). A T4SS called *virB/virD4* in *Bartonella* spp. was first identified in an analysis of the locus of the 17kDa protein, a highly antigenic protein of *B. henselae* (Padmalyam *et al.*, 2000). Since then, *virB/virD4* has been identified in other *Bartonella* spp. that cause human diseases (Kohlhorst, personal communication) and may be acquired through a process of lateral gene transfer (Saenz *et al.*, 2007). The operon consists of 10 genes, *virB2-10*, and *virD4*, located downstream of the operon. With the exception of *virB5*, which encodes the 17kDa antigen, and *virB7*, all genes are homologous with the T4SS loci of other bacteria. Because the *virB5* product is immunodominant, it may be a component of the pili and may function as an adhesin. *B. tribocorum* harboring mutations in the *virB4* and *virD4* genes cannot infect erythrocytes in experimental rat models. Moreover, *virB4/virD4* is required even before intraerythrocytic infection, and is thus necessary to establish the infection in the primary niche, probably the endothelial cells (Schulein *et al.*, 2002). The *B. henselae* *virB* operon is induced during infection of endothelial cells *in vitro* (Schmiederer *et al.*, 2001). The induced operon then is responsible for mediating the transfer of seven substrates BepA-G (Bartonella-translocated effector proteins), of which BepA has been characterized as having anti-apoptotic properties (Schmid *et al.*, 2006; Schulein *et al.*, 2005). The *B. henselae* *virB/D4* locus mediates the physiological changes seen in infected endothelial cells (Schmid *et al.*, 2004). The *virB4* mutants cannot induce invasome-mediated

internalization, NF- κ B–dependent pro-inflammatory response, or the anti-apoptotic pathway. Moreover, the cytostatic and cytotoxic effects seen at high bacterial titres are mediated by the *virB* system (Schmid *et al.*, 2004). The *virB* system of *B. quintana* has not been characterized, though it resembles *B. henselae* in genetic makeup and pathogenesis, so the gene products may have similar functions. Interestingly, *virB/D4* is not present in *B. bacilliformis*, so the mechanism of host cell alterations mediated by *B. bacilliformis* must differ significantly from that of *B. henselae* (Saenz *et al.*, 2007).

The *Bartonella*-induced vasoproliferation of vascular cells *in vivo* and *in vitro* depends on mitogen factors and enhanced cell survival. *B. henselae* and *B. quintana* each inhibit apoptosis by different mechanisms (Kirby *et al.*, 2002a; Liberto *et al.*, 2004). As mentioned previously, the *virB* system is critical for host cell survival, and the *virB* effector protein BepA suppresses apoptosis (Schmid *et al.*, 2004; Schulein *et al.*, 2005). No other proteins that affect cell survival have been identified in other *Bartonella* spp. *Bartonella* spp. also have a mitogenic effect on infected endothelial cells. Thus far, the only bacterial protein identified with mitogenic potential is GroEL in *B. bacilliformis* (Kohlhorst, D., personal communication; Minnick *et al.*, 2003).

The vasoproliferative skin eruptions that occur during *Bartonella* infections are indicative of a chronic inflammation, characterized by the presence of mixed infiltrates of monocytes, macrophages, leukocytes, and polymorphoneutrophils (PMN). The acute inflammatory response that leads to chronic inflammation has been studied in *B. henselae*-infected endothelial cells. This inflammation is mediated by the activation and nuclear translocation of NF- κ B (Fuhrmann *et al.*, 2001). The infected cells have increased and prolonged expression of the adhesion receptors E-selectin and the

intercellular cell adhesion molecule 1 (ICAM1), which results in increased PMN rolling on and attachment to the infected endothelial cultures (Fuhrmann *et al.*, 2001). *B. henselae* also interacts with activated macrophages to produce pro-angiogenic cytokines, such as VEGF and interleukin-1beta (IL-1 β), that are present in chronically inflamed tissues attempting to heal (Resto-Ruiz *et al.*, 2002). High levels of pro-inflammatory cytokine productions of tumor necrosis factor alpha (TNF- α), IL-1 β , and interleukin 6 (IL-6) in *B. henselae* infected murine macrophage cell lines have been recorded (Musso *et al.*, 2001). Thus, the macrophages recruited at the site of infected endothelium *in vivo* could serve as a major source of inflammatory cytokines and be involved in the development of chronic inflammation.

Concluding remarks

Recent advances in molecular tools have helped scientists improve their understanding of some of the complicated interactions between *Bartonella* and its host cells. Endothelial cells are colonized by all *Bartonella* spps., and in humans these cells undergo pathological angiogenesis and have a pro-inflammatory phenotype during the later stages of infection. However, many experiments suggest a role for endothelial cells as the primary niche in the host reservoir. Although endothelium is a major target for the *Bartonella*-induced pathogenic response, nothing has been reported about the cell surface receptors involved in *Bartonella* adhesion and invasion. These bacterial receptors could be involved in not only invasion but also the mitogenic and angiogenic stimulation of infected cells. This study therefore attempts to elucidate the endothelial cell surface receptors and cell signaling molecules involved in *B. bacilliformis* infections. Microarray profiling of the genes from *B. bacilliformis*-infected endothelial cells provides a means to

understand some of the pathways recruited during the infection. These studies improve our understanding of host cell responses during infections elicited by these fascinating pathogens.

Chapter I: Role of Integrins in *B. bacilliformis* infection of endothelial cells

Introduction

An established infectious disease occurs when a pathogen colonizes and multiplies within specific host tissue. Adherence of the pathogen to the cell surface and its subsequent internalization is a prerequisite for colonization. *B. bacilliformis*, a bacterium that grows intracellularly, specifically targets erythrocytes in the first phase of infection and then endothelial cells in the second phase (Minnick *et al.*, 1996). The semi-permeable cellular barrier at the blood–tissue interphase consists of endothelial cells. Due to its location, the multifunctional endothelium provides an easy target for blood-borne pathogens and pathogen products. In addition to *Bartonella* spps, *Rickettsiae* specifically target endothelial cells for infections (Valbuena *et al.*, 2002). Endothelium infection benefits the pathogen because it allows for an easy transition from the blood stream to the internal tissues. From there, the infection can follow several pathways. Some organisms use cell surface receptors and preexisting cell-signaling pathways for adhesion and invasion. Alterations in membrane integrity, the endothelial matrix, and intracellular junctions represent alternatives ways in which bacteria can infect endothelial cells. In the following sections, we discuss the role of endothelial integrins and their extracellular matrix ligands in *B. bacilliformis* infection. Integrins are expressed by endothelial cells both *in vivo* and *in vitro*. Various bacteria initiate endothelial cell infection by attachment to integrins; direct interaction involves bacterial adhesins expressed on their surface, whereas indirect integrin contacts are established via integrin ligands.

Integrins involved in bacterial pathogenesis

Integrins are cell-surface receptors that link intracellular and extracellular environments. A family of glycosylated, heterodimeric receptors, integrins are formed by the non-covalent association of α and β subunits. Integrins play an important role in maintaining cell shape, migration, growth, survival, and differentiation; in addition, they are highly conserved from sponges to humans, in which there are 19 α and 8 β subunits (Burke, 1999; Hynes *et al.*, 2000). The combination of these subunits gives rise to 25 different receptors, in which the α - β pairing determines ligand specificity (Hynes, 2002). mRNA splice variants and post-translational modifications diversify the integrin repertoire. The globular head domains formed by α and β subunits constitute the ligand binding site and are attached to the cell membrane through a single transmembrane helix. The small cytoplasmic integrin tail consists of only 30–50 amino acids. Integrin–ligand binding represents a promiscuous event, because different integrins interact with the same ligands, and different ligands recognize the same integrin. The majority of the integrin ligands belong to the extracellular matrix (ECM) protein group. Integrins can also associate with other integrins, cell receptors, plasma proteins, and complement factors (van der Flier *et al.*, 2001). Ligand affinity depends on the cell types expressing the integrin. Divalent cations also play critical roles in integrin–ligand interactions, as indicated by the observation that integrins cannot bind molecules in the presence of metal chelators (Gailit *et al.*, 1988). The α chains present three cation-binding sites, of which one is permanently occupied with either calcium or magnesium at their physiological concentrations, and the other two are occupied upon ligand binding. In its inactive form, the α subunit inhibits the interaction of β integrin with cytoskeletal proteins. Integrin

engagement by ligands induces a conformational change that dissociates the α - β subunits, activates the integrins, and initiates intracellular signaling (Hughes *et al.*, 1996; Vinogradova *et al.*, 2000). Integrin activation triggers clustering, which in turn leads to greater affinity for their ligands. The integrins cluster at cell attachment sites, called focal adhesion or focal contacts, where bidirectional signaling occurs. Focal contacts consist of integrins, cytoskeletal components, and signaling molecules. Integrins lack intrinsic enzyme activity and rely on adaptor kinases for signal transduction. Activated integrins recruit protein tyrosine kinases (PTKs), focal adhesion kinase (FAK), and small GTPases (Rho, Rac and Cdc42), with the small GTPases being the key factors for outside-inside-outside signaling.

Several bacteria and viruses exploit integrins and integrin-modulated signaling for adhesion and invasion. The efficiency of pathogen invasion depends on the integrin density and affinity for the bacterial binding site. The most common pathogen receptors are the fibronectin and vitronectin integrins ($\alpha_5\beta_1$ and $\alpha_v\beta_3$, respectively). Infectious agents either express integrin-binding proteins that stimulate direct integrin binding or synthesize ECM protein-binding molecules that allow pathogens to access integrins. For example, *Yersinia* species express an invasion protein that engages up to five different integrins with the β_1 subunit (Hamzaoui *et al.*, 2004). *Shigella* species directly interact with $\alpha_5\beta_1$ through invasion plasmid antigens (Ipas) (Watarai, M. *et al.*, 1996). Enteropathogenic *E. coli*, *Borrelia burgdorferi* and *Bordetella* spp provide other examples of bacterial-expressing integrin-binding proteins (Coburn *et al.*, 2003b; Coburn *et al.*, 2003a; Coburn *et al.*, 2003c; Frankel *et al.*, 1996; Ishibashi *et al.*, 2001). *Bartonella* spp can mediate host cell entry via integrins; in particular, *Bartonella* adhesin

A (BadA) is a trimeric autotransporter that plays a critical role in endothelial cell adhesion (Riess *et al.*, 2004). BadA is homologous to other adhesins of *Yersinia* (YadA) and *Neisseria* (NadA) and, like YadA is thought to interact with β_1 . *B. henselae* experiences reduced binding to fibroblasts lacking β_1 integrins, suggesting that BadA binds to β_1 (Riess *et al.*, 2004). In addition, *B. bacilliformis* invasion is reduced when epithelial β_1 and α_5 antibodies are used (Williams-Bouyer *et al.*, 1999). However, the endothelial receptors for *B. bacilliformis* adherence and invasion are unknown. This study therefore attempts to determine the cell surface molecules involved in *B. bacilliformis* pathogenesis. Functional blocking antibodies against integrins provide a means to study the hypothesis that *B. bacilliformis* internalization is an integrin-mediated event.

Extracellular matrix proteins involved in bacterial pathogenesis

Integrins rest at the heart of numerous biological processes and function by coupling ECM proteins to the interior milieu of the cell. Cell adherence to the substrate is vital for multicellular organisms' survival. Integrins provide the primary receptors that not only attach the cell to ECM but also modulate the cell functions by sensing environmental signals. As a scaffold of proteins that provides a stable base for cell growth, ECM includes the basal membrane and interstitial matrix and is composed of proteoglycans, collagen, elastin, and glycoproteins. The glycoproteins include fibronectin, vitronectin, thrombospondin, tenascin, and laminin. These proteins are secreted by the cells and organize themselves into a fibrous mesh within the preexisting matrix. In addition to providing a platform for cell attachment, ECM is rich in growth factors that mediate cellular functions. The protein-rich environment of ECM also serves

as a safe haven for bacterial colonization and multiplication. In this report, we concentrate on the two most widely used ECM proteins in bacterial infections, namely, fibronectin and vitronectin.

Fibronectin

Fibronectin is a high molecular weight glycoprotein found in the plasma (soluble form); the insoluble form in ECM is associated with fibrils. Fibronectin consists of two, disulfide-linked polypeptide chains with three internal repeats. Splice variants from a single gene generate various fibronectin isoforms. The most notable function of fibronectin involves embryonic cell migration in the neural crest. It also has a therapeutic role in wound healing and appears in large concentrations associated with fibrin. Moreover, fibronectin maintains cell shape through integrin-mediated microfilament and actin organization. At least six integrins recognize fibronectin, of which $\alpha_5\beta_1$ is the most significant and well characterized (Johansson *et al.*, 1997). Although fibronectin can be found in glycosylated, phosphorylated, or sulfated form, only the degree of phosphorylation modulates its binding properties. Six peptide sites mediate cell adhesion; of which the most significant is the tripeptide motif arginine-glycine-aspartate (RGD). Secondary sequences work in synergy with the RGD motif, especially for binding to $\alpha_5\beta_1$. Two heparin-binding domains appear at the C-terminal and N-terminal ends of the fibronectin molecule. The C-terminal domain binds to heparin with stronger affinity, whereas the N-terminal domain can bind to fibrin, which allows cell migration in fibrin clots during wound healing. Also, fibronectin has a collagen-binding domain that is evolutionary conserved, suggesting that it could have an important biological function. Fibronectin molecules undergo a two-step polymerization process to form fibronectin

fibrils in ECM environment. The key integrin in fibrillogenesis is $\alpha_5\beta_1$, and antibodies against the $\alpha_5\beta_1$ receptor binding domain curtail matrix assembly. Intracellular bacteria often colonize the extracellular space, where they utilize ECM proteins to their advantage to gain entry into the host cells. Bacterial surface proteins that interact with ECM molecules bind to integrins via these proteins. The mostly commonly recognized ECM component is fibronectin, and the function of fibronectin in *Staphylococcus aureus* and *Streptococcus pyogenes* pathogenesis has been well established. The fibronectin binding protein (Fnbp) A and B proteins of *S. aureus* indirectly link the cocci to $\alpha_5\beta_1$ integrin, which promotes bacterial uptake (Jonsson *et al.*, 1991a). In addition, the fibronectin-mediated attachment of *S. aureus* alters the integrin-dependent signal cascade, which triggers cytoskeletal rearrangement and leads to its internalization. *Streptococcus* spp. can adhere to $\alpha_5\beta_1$ directly via the M-protein or indirectly through a high-affinity fibronectin binding protein (Cue *et al.*, 2000). The Gram negative *Neisseria meningitidis* expresses an outer membrane fibronectin binding protein called Opc that mediates endothelial cell attachment (Unkmeir *et al.*, 2002). Experiments with anti-integrin and anti-ECM protein antibodies have demonstrated the role of $\alpha_5\beta_1$ and fibronectin during *Pseudomonas aeruginosa* invasion of respiratory cells (Leroy-Dudal *et al.*, 2004; Yilmaz *et al.*, 2002). Another Gram negative bacterium *Campylobacter jejuni* expresses CadF, an OMP that binds fibronectin and induces alterations in actin filaments (Moser *et al.*, 1997). *B. henselae* strains that express BadA can bind fibronectin. BadA expression is phase variant, and the loss of BadA results in the loss of host cell attachment and fibronectin interaction (Riess *et al.*, 2006). The addition of anti-fibronectin, anti-*B. henselae* antibodies, and exogenous fibronectin during *B. henselae* infection of

endothelial cells decreases the effectiveness of bacterial pathogenesis (Dabo *et al.*, 2006). This research also identified Pap31, Omp43, and Omp89 as the three major surface proteins that bind fibronectin; however, the role of fibronectin in *B. bacilliformis* infection of endothelial cells remains undetermined. We performed binding assays with immobilized and soluble fibronectin; in addition, we performed invasion assays with fibronectin-coated *B. bacilliformis* and anti-fibronectin antibodies to examine the function of fibronectin.

Vitronectin

Vitronectin is a multifunctional glycoprotein abundantly found in the blood and ECM. It is not as well characterized as fibronectin but has similar functions in cell adhesion. It represents a major component of platelets and plays an important role in hemostasis in that it prevents cells from cytolytic destruction by complement and protects thrombin inactivation by anti-thrombinIII. In its fibrillar form, vitronectin is often co-localized with fibronectin. The three known vitronectin integrins are $\alpha_V\beta_3$, $\alpha_{IIb}\beta_3$, and $\alpha_V\beta_5$, all of which bind vitronectin through the RGD motif. *In vitro*, the cell adhesive activity of serum is due to vitronectin; at low serum concentrations, fibronectin becomes functional. A few of the previously mentioned bacteria can capture both fibronectin and vitronectin and use them to their advantage. The phase-variable, opacity-associated proteins (Opa) of *Neisseria* spps interact with vitronectin, facilitating its $\alpha_V\beta_3$ and $\alpha_V\beta_5$ mediated uptake of the bacteria (Dehio *et al.*, 1998). Vitronectin forms a bridge connecting *P. aeruginosa* to $\alpha_V\beta_5$ integrins, contributing to bacterial invasion of alveolar cells (Leroy-Dudal *et al.*, 2004). Little information is available about the interaction of vitronectin with *Bartonella* spps. Although it has been reported that *B. henselae* binds

vitronectin only in the presence of glycosaminoglycans, little is known about how the ligand affects invasion (Dabo *et al.*, 2006). We used vitronectin-binding studies, vitronectin-opsonised *B. bacilliformis*, and anti-vitronectin antibodies to elucidate the role of this ECM protein in *B. bacilliformis* pathogenesis.

Bacterial cell adhesion molecules that engage integrins

Several pathogens express surface proteins that recognize host receptors and help translocation into non-phagocytic cells. These proteins are termed adhesins, and their interaction with the receptors initiates a signal cascade involving tyrosine kinases, adaptor proteins, and cytoskeletal molecules. The activation of these proteins leads to the formation of phagocytic cups, which engulf the surface-bound pathogen. Almost all bacterial adhesins that interact with integrins have the tripeptide RGD, the same motif used by the integrin ligands fibronectin and vitronectin. Many of the pathogen molecules with RGD are secreted by the type IV secretory pathway. The Gram negative bacteria belonging to *Bordetella* spp cause respiratory infection and have several proteins that adhere to and invade host cells via RGD attachment to integrins. The fimbrial surface proteins of *B. pertussis* filamentous hemagglutinin (FHA) show decreased adhesion and invasion when their RGD motif is mutated (Ishibashi *et al.*, 2001). These mutants also have decreased ICAM1 expression capabilities (Ishibashi *et al.*, 2002). Site-directed mutagenesis of the RGD motif in P 69/ pertactin-secreted toxin prevents the efficient invasion of *B. pertussis* into mammalian cells (Everest *et al.*, 1996). A variant of the mature form of *Streptococcal* pyrogenic exotoxin (mSpeB2) that is crucial for invasive disease also contains RGD. Exotoxin mSpeB mediates binding to vitronectin integrin $\alpha_V\beta_3$ on endothelial cells and $\alpha_{IIb}\beta_3$ on platelets (Stockbauer *et al.*, 1999). The RGD

motifs in *Serratia marcescens* protein Ssp and *E. coli* antigen 43 also associate with integrins on their host cells (Ohnishi *et al.*, 1997; Owen *et al.*, 1996). However, *B. bacilliformis* adhesins that participate in host cell invasion remain unknown. A highly antigenic protein, novel lipoprotein D (NlpD_{Bb}) has been identified as a potential outer membrane protein that contains the RGD motif in the C-terminal domain (Padmalayam *et al.*, 2000b). In our studies, we used *E. coli* expressing NlpD_{Bb} and NlpD_{Bb}, containing a site-directed mutation in the RGD motif, to determine the role of this tripeptide in *B. bacilliformis* pathogenesis.

Materials and Methods

HMEC-1 cell line growth and culturing.

The immortalized human microvascular endothelial cell line (HMEC-1) was a kind gift from Dr. Ades of the Centers for Disease Control (CDC), Atlanta (Ades EW *et al.*, 1992). The HMEC-1 cells from passages 19-27 were grown in 15ml of growth media consisting of 50% M199 (Cambrex), 15% FBS (Fetal Bovine SerumHyclone), 2% Penicillin/Streptomycin (Cellgro), and 50% EGM-2 (Cambrex). Cells were grown and maintained in T-75 flasks (Starstedt) at 37°C under 5% CO₂ and humid conditions. This medium was changed every 2–3 days until 70–80% confluence was reached. The cells were maintained in 10ml of maintenance media (M199 +15%FBS+2% Penicillin-Streptomycin) between passages. For cell detachment, confluent cells were washed twice with PBS (Phosphate Buffered Saline pH 7.4) to remove all traces of serum before the addition of 10ml/ 75²mm Cell stripper (Cellgro). Cells were incubated at 37°C for 10 minutes and then gently scraped with cell scrapers (Starstedt). Detached cells were collected in 15-ml Falcon tubes and centrifuged at 700xg for 10 minutes at 25°C. Cells were resuspended in 1ml of maintenance media and enumerated microscopically using the hemocytometer before seeding the T-25, T-75, or T-150 flasks or 6- or 24- well plates. Cells were allowed to adhere for 1six hours before use.

To prepare frozen stocks, cell pellets were resuspended in DMSO (dimethyl sulfoxide) freeze medium (Cellgro) to obtain a final concentration of 1x10⁵ cells/ml. The vials were allowed to freeze at -80°C in a cryofreezing container (Nalgene) for 24 hours and then transferred to a liquid N₂ tank facility.

Bacterial growth and culturing.

B. bacilliformis KC584 was obtained from ATCC (35686) and grown on brain heart infusion (BHI) plates supplemented with 10% sheep blood (BD Bioscience) at 26°C for 4–7 days. Low-passaged bacteria (1–3 passages) were used for all experiments. After the confluent colonies became visible, plates were overlaid with 7ml of PBS. The bacteria were gently scraped off the plate with a loop. Bacterial suspension was centrifuged at 2000xg for 10 minutes at 25°C. Pellets were washed once with PBS and centrifuged as previously described. The final suspension was in 1ml BHI broth, unless otherwise noted.

The *E. coli* HMS174 strain was a kind gift from Dr. Parjit Kaur. *E. coli* HMS174 was grown on Luria Bertani (LB) plates at 37°C for 16–20 hours. *E. coli* strains containing the pET20b (+) plasmid were grown on LB plates or LB broth supplemented with 100µg/ml ampicillin at 37°C for 16–20 hours.

Radiolabeling *B. bacilliformis* with ³⁵S-methionine.

In the method adapted from Williams-Bouyer *et al* (Williams-Bouyer *et al.*, 1999), *B. bacilliformis* was harvested and pelleted as described previously. The bacterial pellet was resuspended in 1ml methionine free RPMI (Cellgro) containing 2% FBS and 0.2% sheep erythrocyte lysate. ³⁵S-labeled methionine (Perkin-Elmer) was added to a final concentration of 50µCi/ml. *B. bacilliformis* was allowed to incorporate the radioactivity for one hour at 26°C, after which the bacteria were washed twice with PBS to remove unbound radioactivity. *B. bacilliformis* was resuspended in 1ml PBS containing 10mM glucose. The number of bacteria was determined microscopically using a hemocytometer.

Antibodies.

The functional blocking, anti-integrin antibodies used were polyclonal anti- $\alpha_5\beta_1$, monoclonal anti- $\alpha_v\beta_3$, and monoclonal anti- β_4 , purchased from Chemicon International. Anti- β_1 monoclonal antibodies came from Labvision Corp. The monoclonal anti-human fibronectin (clone IST-3) antibody was purchased from Sigma, and the polyclonal anti-human fibronectin antibodies were from Biomeda. Monoclonal and polyclonal anti-human vitronectin (Clone BE10) antibodies were supplied by ICN Biomedicals and Chemicon, respectively. Polyclonal and monoclonal antibodies against green fluorescent protein (GFP) (Invitrogen) served as controls. All antibodies used were at a 5 μ g/ml (final) concentration in M199 media containing 1%BSA (Bovine Serum Albumin).

Generation of anti-*B. bacilliformis* antibodies.

B. bacilliformis were harvested from two plates and washed thoroughly in PBS, as described previously. The final suspension was in 1ml of PBS. Washed bacteria were killed by the addition of 10% formalin (final concentration 0.1%) at 25°C for four hours. Killed bacteria were centrifuged at 1000xg for five minutes and washed six times with 1ml of PBS. After removing all traces of formalin, the bacteria were resuspended in 1ml PBS and emulsified with an equal volume of complete Freund's adjuvant. An aliquot of 0.1ml of the emulsified antigen was injected subcutaneously into two female New Zealand rabbits. The rabbits were injected at 10 sites along the spine. A second booster shot of bacterial emulsification in an incomplete Freund's adjuvant was given after 15 days. Serum was collected every three weeks for three months. The IgG fraction was concentrated and purified by SACRI antibody services at the University of Calgary, Canada. The optimal antibody titers were determined using standard ELISA.

Extracellular matrix proteins.

Human plasma fibronectin and vitronectin were from Chemicon. BSA fraction V and fetuin were purchased from Sigma.

Invasion assays with anti-integrin antibodies.

HMEC-1 cells were seeded in 24 well plates containing maintenance media at a concentration of 1×10^6 cells/ml. HMEC-1 cells were grown to 80% confluency, after which they were washed twice with PBS before adding media. M199 plus 1%BSA (500 μ l) with 5 μ g/ml antibodies was added to the experimental wells an hour before bacterial infections. Control wells received media with GFP antibodies (5 μ g/ml) or media without antibodies. HMEC-1 cells were infected with radiolabeled bacteria at a m.o.i of 1:100. Infection was allowed to proceed for six hours at 37°C in a 5% CO₂ incubator. The steps to recover intracellular bacteria involved extensive washing of the wells (6X) with PBS to remove any unbound bacteria. Cells were then treated with 500 μ l of 0.08% trypsin-EDTA for 10–15 minutes at 37°C. This mild trypsin treatment gently detached the cells and cleaved externally bound bacteria. Trypsinization was arrested by the addition of 500 μ l of maintenance media. The well contents were transferred to microfuge tubes and centrifuged at 1000xg for 10 minutes at room temperature to pellet the eukaryotic cells. The supernatant was removed, and the pellet was resuspended in 500 μ l of 1% TritonX-100. Cells were lysed by vortexing briefly and were then mixed with 5ml of liquid scintillation fluid (Optima GoldXR, Perkin-Elmer). The volume of bacteria used to infect the cells was added to the scintillation fluid to determine the amount of radioactivity added. Radioactivity (DPM: disintegrations per minute) was measured with a LS2500 scintillation counter (Beckman Coulter). Percent invasion was calculated as follows:

(DPM recovered/DPM added)×100. The percent invasion results of the control experiments were normalized to 100, and the invasion experimental values were calculated in relation to the normalized control. Percent inhibition was calculated as normalized percent invasion – 100.

Invasion assays with ECM opsonised *B. bacilliformis* and anti-ECM antibodies.

B. bacilliformis was harvested and washed by the method described previously. *B. bacilliformis* was resuspended in 2.5ml methionine-free RPMI without serum or blood lysate with 50µCi/ml of ³⁵S methionine (final concentration), and 500µl was aliquoted into fresh microfuge tubes. Fibronectin at final concentrations of 5, 10, 25, 50, 100, and 200µg/ml or vitronectin at 0.5, 2.5, 7.5, and 10µg/ml was added to each tube. The tubes were incubated at 26°C for one hour. The unbound radioactivity and protein were removed by washing the bacteria three times with PBS. The bacteria were resuspended in 500µl of PBS containing 10mM glucose. Bacterial enumeration was done using a hemocytometer, and HMEC-1 cells were infected at 1:100 m.o.i for six hours. Intracellular *B. bacilliformis* was recovered and percent invasion was determined as explained previously. Invasion assays were also carried out with ³⁵S-methionine labeled *B. bacilliformis* in the presence of 5µg/ml (final concentration) of polyclonal and monoclonal anti-fibronectin and vitronectin antibodies.

Invasion assays in the presence of human serum.

Pooled human serum was a kind gift from Dr. Yuang Liu. Serum was heated for 30 minutes in a 50°C water bath to inactivate serum complement proteins. The serum was triple filtered through a 0.22µm syringe filter. Filtered serum was diluted in M199 media to achieve final concentrations of 1%, 2.5%, 5%, 7.5%, and 10%. Semi-confluent

HMEC-1 cells in 24 wells were infected with ^{35}S -methionine labeled *B. bacilliformis* in the presence of different human serum concentrations. Percent invasion was calculated as described in the previous sections.

Adhesion assays.

Infection assays were performed with ^{35}S -methionine labeled *B. bacilliformis*, as described. After treating the cells with 0.08% trypsin-EDTA, the reaction was terminated by the addition of maintenance media. The cells were spun down at 1000xg to settle host cells with intracellular bacteria. Supernatant containing the externally bound bacteria was collected in clean microfuge tubes. Bacteria from the supernatant were pelleted at 2000xg for 10 minutes. The bacteria were resuspended in 500 μl of 1% TritonX-100 and mixed with liquid scintillation fluid. Radioactivity was measured with a LS2500 scintillation counter. Percent adhesion was calculated as follows: $(\text{DPM recovered}/\text{DPM added}) \times 100$. The percent adhesion results of control experiments again were normalized to 100, and the adhesion experimental values were calculated in relation to the normalized control. Percent inhibition thus was calculated as normalized percent adhesion – 100.

Infection of HMEC-1 cells with *B. bacilliformis* for RT-PCR studies.

HMEC-1 cells were grown in T150 flasks containing 30ml of growth media, incubated at 37°C, 5% CO₂, under conditions of saturated humidity. The HMEC-1 cells were allowed to reach 90% confluence, after which the media were replaced with 30ml of M199 containing 5% FBS, and the cells were incubated for 24 hours. Cells from a single flask were counted to give an approximation of the growth in the remaining flasks. *B. bacilliformis*, at a m.o.i. of 100:1 in 100 μl of PBS, was added to each experimental flask,

and 100 μ l of sterile PBS, pH 7.4, was added to each control flask. The media were aspirated at 30 minutes, one hour, three hours, and six hours post infection, and the flasks were washed three times to remove detached cells and unbound bacteria. The cells were detached from the flasks, as described previously, and centrifuged at 700xg for 10 minutes at 25°C. The cells were immediately processed for total RNA.

Preparation of HMEC-1 total RNA.

Total RNA from HMEC-1 cells was extracted using the Qiagen RNeasy column (Qiagen). Briefly, the harvested HMEC-1 cells were resuspended gently in 600 μ l of lysis buffer with β -mercaptoethanol. The lysate was pipetted into a QIAshredder spin column (Qiagen) for homogenization and centrifuged at 14,000xg for two minutes. The spin columns were washed with 700 μ l of 70% ethanol and mixed well with a pipette. Next, 700 μ l of the lysate-ethanol mixture was added, and the column was centrifuged at 14,000xg for 24 seconds, after which the flow-through was discarded. Into the spin column, 700 μ l of wash buffer was added, and the spin column was again centrifuged at 14,000xg for 24 seconds. This flow through also was discarded. The bound RNA was then washed twice with 500 μ l of wash buffer. The first wash required centrifugation at 14,000xg for 24 seconds, and the second needed two minutes. The RNA was eluted with 30 μ l of RNase-free water into a fresh 1.5ml of RNase-free microcentrifuge tube (USA Scientific). To increase the elution efficiency, the tubes were incubated at room temperature for five minutes, and then centrifuged at 14,000xg for one minute. The elutate was pipetted back into the spin column and allowed to incubate for 30 minutes at room temperature, after which the tubes were centrifuged again at 14,000xg for one

minute. The RNA concentrations were determined by BioPhotometer (Eppendorf), and the total HMEC-1 RNA was stored at -80°C until needed.

Real-time RT-PCR.

cDNA was synthesized from 500ng of cellular RNA using the High-Capacity cDNA reverse transcription kit (Applied Biosystems). The reverse transcriptase (RT) Master Mix (2X) was prepared with $2\mu\text{l}$ of 10XRT buffer, $0.8\mu\text{l}$, 25XdNTP mix (100mM), $2\mu\text{l}$ of 10X RT random primers, $1\mu\text{l}$ of MultiScribeTM reverse transcriptase, $1\mu\text{l}$ RNase inhibitor, and $3.2\mu\text{l}$ of nuclease-free DEPC-treated water (Ambion). The Master Mix was kept on ice after gentle mixing. Individual reactions for cellular RNA from each time point were prepared by mixing $10\mu\text{l}$ of RNA with $10\mu\text{l}$ of 2X Master Mix. The reverse transcription was performed in an Eppendorf thermal cycler under the following conditions: 25°C for 10 minutes, 37°C for 120 minutes, and 85°C for five seconds. cDNA was stored at -20°C until further use. Real-time quantitative PCR (rt-qPCR) was performed with the synthesized cDNA using the TaqMan Universal PCR Master Mix (Applied Biosystems) protocol. Briefly, $1\mu\text{l}$ of cDNA was diluted with $8\mu\text{l}$ of DEPC-treated water, followed by the addition of $10\mu\text{l}$ of Master Mix and $1\mu\text{l}$ of the assay primer (TaqMan Gene Expression Assay, Applied Biosystem). The catalog numbers of the assay primer used for the genes (in parenthesis) were Hs002337443_m1 (integrin α_5), Hs00236976_m1 (integrin β_1), Hs00233808_m1 (integrin α_v), and Hs01001469_m1 (integrin β_3). The RNA was quantified in an Applied Biosystem 7500 using the following cycling settings: 48°C for 30 minutes, AmpliTaq activation at 95°C for 10 minutes, denaturation at 95°C for 15 seconds, and, finally, annealing/extension at 60°C for 1 minute (40 cycles). Cyclophin A (PPIA, Hs99999904_m1) was used as the

endogenous control. All reactions were performed in triplicate, and the comparative threshold values ($\Delta\Delta C_T$) were calculated in Microsoft Excel. All threshold values (C_T) were first normalized to the endogenous reference (PPIA). $\Delta\Delta C_T$ was calculated by subtracting the control (uninfected) C_T from the experimental (infected) C_T . Relative quantification (RQ) for mRNA for each sample was determined by $2^{(-\Delta\Delta C_T)}$. The p-value was then calculated using Student's t-test for unequal variances; a value of ≤ 0.1 was considered significant.

***B. bacilliformis* binding to immobilized ECM.**

Fibronectin, vitronectin, and fetuin were diluted in bicarbonate coating buffer (1.59g Na_2CO_3 , 2.93g NaHCO_3 , and 1000ml distilled H_2O , pH 9.6) to give a final concentration of 5 $\mu\text{g}/\text{ml}$. Then, 100 μl was added to EIA/RIA plates (Corning), and the plates were incubated at 4°C for 16 hours. The wells were washed three times with 200 μl of PBST (phosphate-buffered saline with 1% Tween), then blocked with PBST containing 5%BSA for two hours at 37°C. The wells were washed three times with PBST to remove blocking buffer. *B. bacilliformis* was diluted to 2×10^6 - 1×10^7 CFU/ml in blocking buffer, and 100 μl was added to the wells and incubated for three hours at 37°C. The wells were washed, and anti-*B. bacilliformis* antibodies (diluted 1:1000) were added for one hour at 37°C. Unbound antibodies were removed with PBST washes, and 100 μl of secondary alkaline phosphatase (AP)-conjugated anti-rabbit antibodies (diluted 1:5000) were added for one hour at 37°C. Excess, unbound secondary antibody was washed out with PBST. Alkaline phosphatase substrate p-NPP (p-Nitrophenyl Phosphate) tablet (5mg) (KPL) was dissolved in 10ml of diethanolamine buffer (48.5ml diethanolamine, 500ml distilled H_2O , pH9.8, 0.5mM MgCl_2), of which 75 μl was added to

each well. Color was allowed to develop in the dark for 15 minutes at room temperature. The reaction was stopped by the addition of 25µl of 0.2M EDTA. Plates were read with a Biomek plate reader at 405 nm.

ECM protein binding to immobilized *B. bacilliformis*.

B. bacilliformis pellets were diluted in bicarbonate coating buffer to give a final concentration of 1×10^6 cells/ml. *E. coli* at log phase were diluted in bicarbonate buffer so that the final cell counts were 1×10^6 cells/ml. Next, 100µl of the bacteria were added to wells of EIA/RIA plates that were incubated at 4°C for 16 hours. Unbound bacteria were removed by washing the well three times with 200µl of PBST, and then blocked for two hours with 100µl of PBST+5%BSA. Various dilutions of fibronectin (0.1-100 µg/ml), vitronectin (0.1-10 µg/ml), or fetuin were prepared in blocking buffer, and 100µl of the diluted proteins were added to the wells for three hours at 37°C. Unbound proteins were removed by washing with PBST, and 100µl of anti-ECM antibody (diluted 1:1000) was added for one hour at 37°C. The wells were washed as described previously; then, 100µl of secondary, AP-conjugated anti-rabbit antibody (diluted 1:5000) was allowed to react with the primary antibody for one hour at 37°C. Alkaline phosphatase substrate was added and allowed to develop as described. Plates again were read in a Biomek plate reader at 405 nm.

Plasmids and DNA manipulations.

The cloning and expression vector pET20b(+) was a kind gift from Dr. Zellers. The vector was propagated in *E. coli* XL-1 Blue cells and expressed in *E. coli* HMS174 strains. Plasmids were isolated using the Plasmid Midi Kit (Qiagen), according to the manufacturer's protocol. The *nlpD* gene was amplified from the pKK-223 vector

containing the *nlpD* gene that had been constructed Dr. Padmalayam (Padmalayam *et al.*, 2000a). The following primers were synthesized at the Georgia State University (GSU) DNA/Protein core facility:

5'CCCCCAAGCTTTGAGTTCTCTAAATACTG3' (*nlpD*_{Rvc})

5'CCCCCGAATTCATGAGAAGATTCA3' (*nlpD*_{Fwd})

The underlined sequences are the *HindIII* and *EcoRI* restriction enzyme-cutting sites in the reverse and forward primers, respectively.

Restriction enzyme digestion, ligation, and transformation.

Purified amplicons and pET20b(+) were digested with *HindIII* and *EcoRI* for four hours at 37°C. All digested products were gel purified (Qiagen), and ligation was performed overnight at 16°C with T4 ligase (New England Biolabs). The CaCl₂ competent *E. coli* HMS174 were transformed with 5µl of the ligation mixture, and transformants were plated on LB ampicillin plates. Plasmids were isolated from transformed colonies and sequenced to confirm the presence of the *nlpD* gene. The *E. coli* BL21 strains were transformed with pKK223-3, pKK-NlpD, or pKK223-3 containing mutant *nlpD*, as described. Sequencing was performed at the GSU core facility using an ABI 3100 Genetic Analyzer. The recombinant plasmid containing *nlpD*_{Bb} was named pNlpD₂₀.

Protein expression.

Recombinant *E. coli* strains were grown at 37°C in LB-ampicillin broth to an OD₆₀₀ of 0.6. Cells were then induced by incubating with 0.5mM IPTG for three hours. The cells were subsequently collected by centrifugation at 8000xg for 10 minutes at 4°C. Bacterial pellets were stored at -80°C if not used immediately. Pellets were resuspended

in an appropriate volume of 1XQAE buffer (25mM Tris-HCl, pH7.5, 20% glycerol w/v, 2mM EDTA and 1mM DTT) and disrupted in a French pressure cell at 10^8 Pa (1.5×10^4 lbf in.⁻²). Cell debris was removed by centrifugation at 9000xg for 15 minutes at 4°C. The supernatant was aspirated for further use. Proteins from the cell lysates were separated by SDS-PAGE, and then transferred to PVDF membranes for Western blot analysis. Membranes were probed with anti-NlpD antibodies (diluted 1:5000) to determine protein expression.

Site-directed mutagenesis.

A two-step overlap extension PCR method was used to introduce a point mutation in the aspartate residue of NlpD. Two separate reactions were performed with a set of the following primers:

Set 1: 5'CAAAGAGTAAAACGTGGTGAGGAAATTGCTAAATCGGGT3'

(RGEFwd) and 5'CCCCCAAGCTTTGAGTTCTCTAAATACTG3' (nlpD_{Rvc})

Set 2: 5'ACCCGATTTAGCAATTTCTCACCACGTTTTACTCTTTG3'

(RGERvc) and 5'CCCCCGAAATTCATGAGAAGATTCA3' (nlpD_{Fwd})

The bolded nucleotides differ from the wild type to mutate the aspartate (D) residue to a glutamate (E) residue, whereas the underlined sequences indicate the restriction enzyme sites for *HindIII* and *EcoRI*, respectively. The PCR products from the first step were gel purified and used as DNA templates for the second PCR reaction, along with nlpD_{Fwd} and nlpD_{Rvc} primers. The products from this reaction were also gel purified and then ligated with *HindIII/EcoRI* digested pET20b(+). Ligation, transformation, sequence analysis, and protein expression were carried out as described previously. The plasmid containing

the mutant *nlpD* gene was designated as pNlpD.E₂₀. This plasmid was used to amplify mutant *nlpD* to sub-clone into pKK223-3 vector as described.

Isolation of inner and outer bacterial membranes.

Bacterial cell lysates from induced *E. coli* cultures were prepared as described in the previous section. The supernatant obtained after cell disruption was subjected to ultracentrifugation at 40,000xg for one hour at 4°C in a Ti75 Rotor. The supernatant was discarded, and the pellet fraction, which contains the total membrane fraction, was resuspended in 1ml of ice-cold 20% sucrose-3mM EDTA solution. The resuspended mixture was overlaid on a 70–53% sucrose gradient in SW41 polyallomer tubes. The tubes were spun in a SW41 rotor at 37,000xg for 24 hours at 4°C. The inner membrane, separated at the 20–53% sucrose interface, and the outer membrane fraction, at the 53–70% sucrose interface, were carefully transferred out with a Pasteur pipette into ultracentrifuge tubes. The samples were diluted with two volumes of water and one-quarter volume of 10mM MgCl₂. The tubes were centrifuged for one hour at 47,000 xg in a Ti70 rotor to concentrate the membrane fractions. Membrane pellets were resuspended in 500 µl of 1XQAE and subjected to Western blots to determine the presence of NlpD, as described previously. Membrane fractions were also probed with anti-OmpA antibodies to determine the purity of the outer membrane fractions.

Gentamicin protection assays.

E. coli HMS174 and BI21 harbouring the pET20 b(+) vector, or recombinant plasmids expressing wild-type *B. bacilliformis* NlpD or NlpD RGD mutants were grown and induced as described. Cells from 1ml of the induced culture were spun down at 7000xg for 5 minutes. The cells were washed twice with 1X PBS and

resuspended in 1ml of M199 media containing 0.5% D-mannose. Bacteria were enumerated microscopically. Semi-confluent HMEC-1 cells were infected with 100 bacteria/cell for three hours at 37°C in a CO₂ incubator. The media were then replaced with fresh M199 media. The infection was allowed to proceed for another three hours, after which the cells were washed three times. M199 media containing 100µg/ml of gentamicin was added to the washed cells, and the plates were incubated for three hours. The cells then were washed six times with PBS, detached using a cell stripper (Mediatech), and then lysed with sterile 1% Triton X100 to release intracellular bacteria. Serial dilutions of the released bacteria were plated on LB-ampicillin plates. Plates were incubated at 37°C for 16 hours. The next day colonies on the plates were counted.

Adhesion assays with recombinant *E. coli*.

Recombinant *E. coli* were grown and prepared for HMEC-1 cell infections as described in the invasion assay section. HMEC-1 cells were grown to 80% confluency on chamber slides (Nunc). *E. coli* were allowed to infect HMEC-1 cells at 1:100 m.o.i for three hours. The wells were washed six times with PBS. The cells were then fixed with ice-cold 70% methanol for 15 minutes. The methanol was rinsed out and stained with fresh 10% Giemsa in distilled H₂O for 30–45 minutes. The slides were rinsed with distilled H₂O and then destained by dipping four times in 1% acetic acid. After a last rinse in distilled H₂O, the slides were air dried and examined microscopically to determine bacterial adherence to host cells.

Statistical analysis

All experiments were performed in triplicate. Standard error means for each data set were calculated in Microsoft Excel. Confidence levels (p-values) were determined in Microsoft Excel using Student's test for unequal variances.

Results

Integrin blocking antibodies decrease *B. bacilliformis* invasion

Endothelial cells are the primary target for *B. bacilliformis* infection during the secondary phase of Bartonellosis. The bacterium is found on and in the endothelial cells of patients with verruga peruana. *In vitro*, *B. bacilliformis*-infected endothelial cells suffer altered morphology and undergo proliferation (Verma *et al.*, 2001). However, the endothelial cell receptors involved in *B. bacilliformis* invasion remain unidentified. Epithelial cell infection in the presence of antibodies against epithelial α_5 and β_1 integrins reduced the number of intracellular *B. bacilliformis* (Williams-Bouyer *et al.*, 1999). We have used the same approach to determine which integrins could be required for *B. bacilliformis* invasion into endothelial cells. Endothelial cells were pre-incubated with antibodies against $\alpha_5\beta_1$, $\alpha_v\beta_3$, β_1 , and β_4 . Polyclonal and monoclonal antibodies against GFP represent the controls and thus eliminate the effects of a non-specific interaction of an antibody with the bacteria. Microvascular cells were infected with radiolabeled bacteria for six hours, after which the externally bound *B. bacilliformis* was removed by mild trypsinization. Host cells were lysed, and the amount of radiolabeled bacteria released was determined in terms of the DPM recovered. Invasion was inhibited in the presence of anti-integrin antibodies, signifying the need for integrins during invasion. Invasion was significantly decreased by 84%, 27%, and 31% in the presence of anti- $\alpha_5\beta_1$, anti- $\alpha_v\beta_3$, and β_1 , respectively (Figure 1.1. and table 1.1.). The maximum number of intracellular bacteria was recovered from those cells treated with anti- β_4 antibodies; the level of inhibition observed with these antibodies was not significant (p-value = 0.11). No inhibition was seen in cells infected with the control anti-GFP antibody. These

observations demonstrate the involvement of endothelial cell integrins in *B. bacilliformis* invasion.

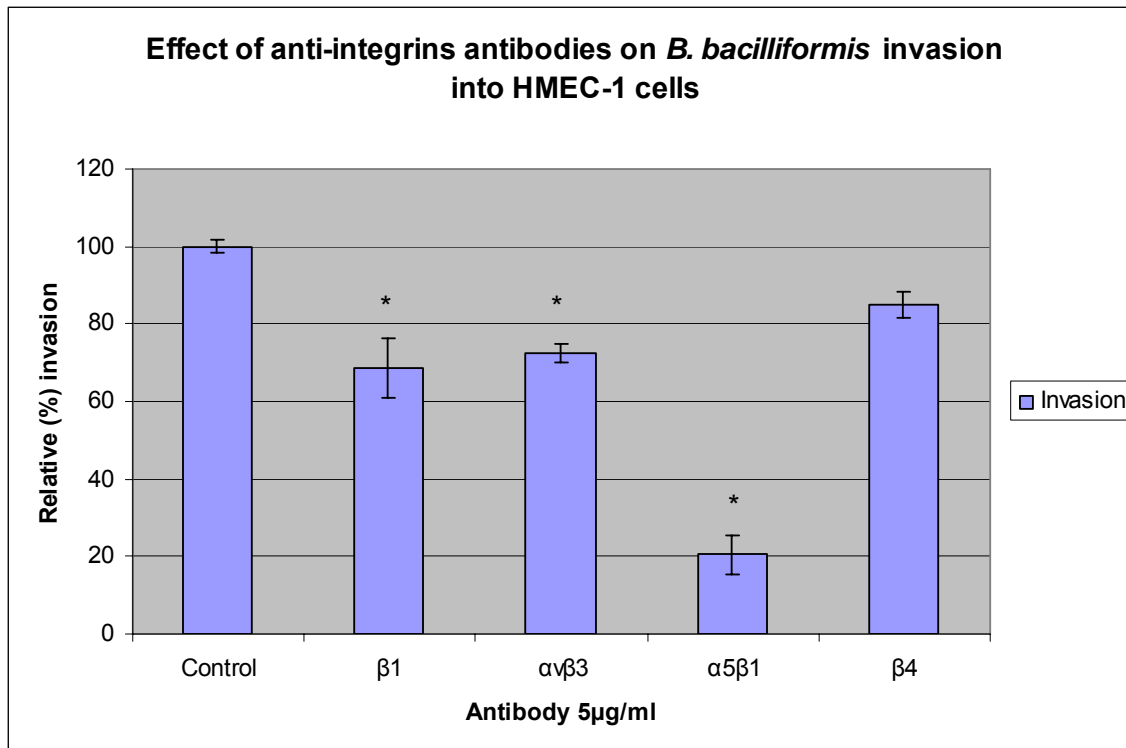


Figure 1.1. Effect of anti-integrin antibodies on *B. bacilliformis* infection of HMEC-1 cells.

HMEC-1 cells were grown in 24-well plates and infected with ^{35}S -methionine labeled *B. bacilliformis* at 1:100 m.o.i in the presence or absence of anti-integrin or control antibodies. Cell lysates were prepared six hours post infection and used to determine the radiolabeled intracellular bacterial content. The radioactivity recovered indicated the number of internalized bacteria. The percent invasion was calculated as (recovered DPM/added DPM) $\times 100$; that in the control experiments was set to 100, and the percent invasion of the treated samples was calculated in relation to 100%. The X-axis denotes the antibody used, whereas the relative percent invasion is plotted on the Y-axis. The numbers are the average of three replicates; error bars represent standard error mean (SEM). The p-value was obtained with Student's t-test, such that a p-value (*) ≤ 0.05 was considered significant, relative to the control.

Table 1.1. Effect of anti-integrin antibodies on *B. bacilliformis* invasion of HMEC-1 cells.

HMEC-1 cells were infected with ^{35}S -methionine labeled *B. bacilliformis* for six hours in the presence of 5 $\mu\text{g/ml}$ of anti-integrin or control antibodies and serum-free M199 media with 1% BSA. Percent invasion and percent inhibition values are the means \pm SEM of three experiments. Invasion values were calculated as (recovered DPM/added DPM) \times 100, set to 100 for untreated samples. Percent invasion from treated samples was calculated in relation to the 100% invasion in untreated samples. Percent inhibition was determined by normalized invasion – 100. Student's t-test was performed with data from both treated and untreated samples. The p-value < 0.05 is considered significant, and NA indicates not applicable.

Antibody used	Percent Invasion	Percent Inhibition	p-Value
Control	100 \pm 1.33	NA	NA
Anti- β_1	68.52 \pm 7.77	31.62 \pm 7.82	0.03
Anti- $\alpha_v\beta_3$	72.39 \pm 2.29	27.82 \pm 2.21	0.01
Anti- $\alpha_5\beta_1$	20.56 \pm 5.07	84.20 \pm 5.80	0.01
Anti- β_4	84.94 \pm 3.22	13.00 \pm 3.52	0.11

Integrins are involved in *B. bacilliformis* attachment to endothelial cells

Ubiquitous integrins can serve as bacterial receptors (Scibelli *et al.*, 2007). In the previous section, we showed that masking of integrins affects *B. bacilliformis* invasion. Here, we analyze whether the unavailability of integrins also affects the attachment of *B. bacilliformis* to host cells. Mild trypsin treatment released the externally bound bacteria into the media and these bacteria were separated from intact host cells by centrifugation. This trypsin treatment removes extracellular bacteria without affecting the intracellular bacteria (Hill *et al.*, 1992). Bacterial pellets were then measured for their radioactive content. The results showed that the extracellular bacterial numbers decreased significantly in assays containing anti-integrin antibodies. Adhesion was dramatically reduced by 63% when infection was performed with anti- $\alpha_5\beta_1$ antibodies (Figure 1.2., table 1.2). Blocking antibodies for $\alpha_v\beta_3$ and β_1 inhibited adherence by 28% and by 23%, respectively. Anti- β_4 did not affect bacterial attachment. The adhesion inhibition pattern correlates well with the invasion inhibition values, which suggests that integrins prevent bacterial internalization by obstructing their adherence to integrins.

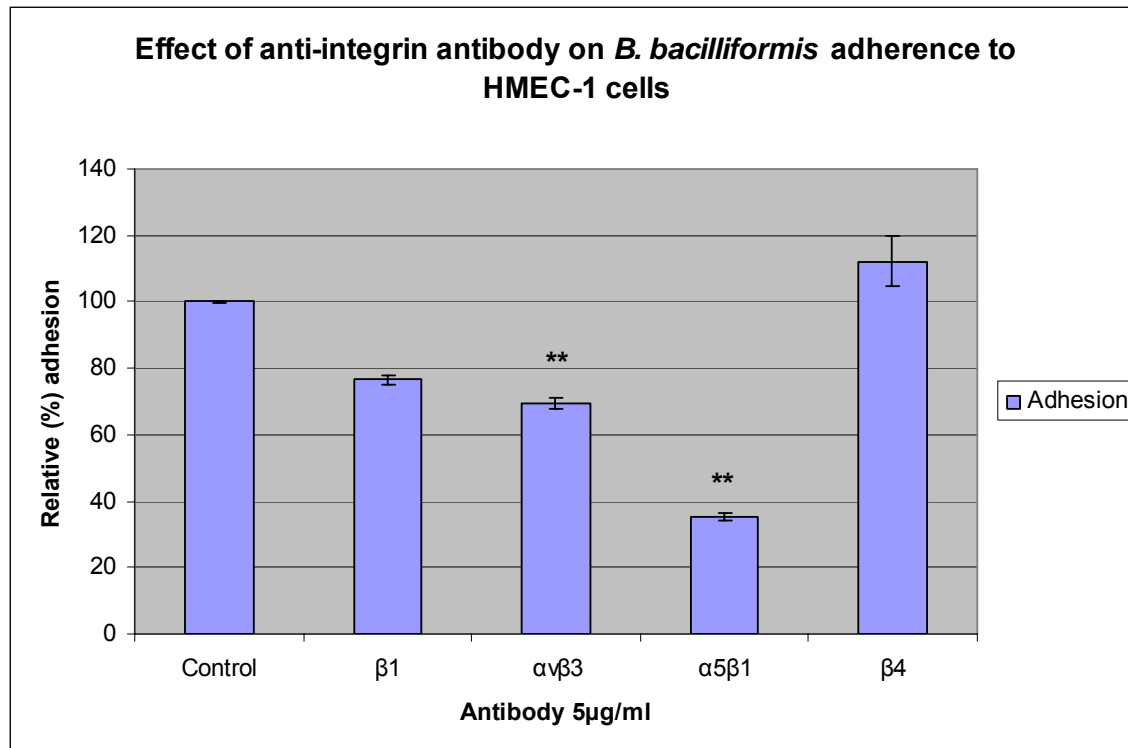


Figure 1.2. Effect of anti-integrin antibodies on *B. bacilliformis* adherence to HMEC-1 cells.

HMEC-1 cells were grown in 24-well plates and infected with ^{35}S -methionine labeled *B. bacilliformis* at 1:100 m.o.i in the presence or absence of anti-integrin antibodies. Six hour post infection, cell were treated with 0.08% trypsin treatment, and cell supernatants were collected. *B. bacilliformis* were centrifuged at 2000xg for 10 minutes and then resuspended in liquid scintillation fluid to determine the amount of radioactivity incorporated; the radioactivity recovered indicated the number of externally bound bacteria. Percent adhesion was calculated as (recovered DPM/added DPM) \times 100, and the percent adhesion from the control experiments was set to 100, whereas the percent adhesion of the treated samples was calculated in relation to 100%. The X-axis denotes the antibody used, and the Y-axis represents the relative percent adhesion. The numbers depict the average of three replicates; error bars represent the SEM. The p-value was obtained by Student's t-test, such that p-values (*) \leq 0.05 and (**) \leq 0.01 are considered significant.

Table 1.2. Effect of anti-integrin antibodies on *B. bacilliformis* adhesion of HMEC-1 cells.

HMEC-1 cells were infected with ^{35}S -methionine labeled *B. bacilliformis* for six hours in the presence of $5\mu\text{g/ml}$ of anti-ECM protein antibodies or control antibodies in serum-free M199 media containing 1% BSA. Percent adhesion and percent inhibition values are means \pm SEM of three experiments. Adhesion values were calculated as (recovered DPM/added DPM) \times 100, set to 100 for untreated samples. Percent adhesion from treated samples was calculated in relation to 100% invasion of untreated samples. Percent inhibition was determined by normalized adhesion – 100. Student's t-test was performed with data from treated and untreated samples. The p-value < 0.05 is considered significant, and NA indicates not applicable.

Antibody Used	Percent Adhesion	Percent Inhibition	p-Value
Control	100 \pm 0.12	NA	NA
Anti- β_1	76.54 \pm 1.41	23.23 \pm 1.41	0.057
Anti- $\alpha_v\beta_3$	69.61 \pm 1.65	28.48 \pm 1.19	0.003
Anti- $\alpha_5\beta_1$	35.14 \pm 1.14	63.93 \pm 1.82	0.003
Anti- β_4	112.16 \pm 7.46	NA	NA

***B. bacilliformis* affects the gene expression of integrins**

Real time RT-PCR was done to study the integrin gene expression in infected HMEC-1 cells. Inventoried primers for integrins α_5 , β_1 , α_v , and β_3 internal control PPIA (cyclophilin A, CAG32988) were used to study the gene expression. PPIA expression in experimental and control cells was comparable according to RT-PCR and microarray analysis; therefore, we choose it as the internal control. The comparative threshold method was used to determine the relative quantification (RQ). First, the threshold values (Ct) obtained for each sample (control, uninfected and experimental, infected) were normalized against the endogenous control, PPIA. Second, the normalized Ct (Δ Ct) of the control was subtracted from the treated dCt to obtain the comparative threshold value ($\Delta\Delta$ Ct). The relative quantification was obtained by the formula $2^{(-\Delta\Delta Ct)}$. The integrin α_5 expression in infected samples increased significantly by 2.2-fold at 30 minutes post infection, then gradually decreased over time. At six hours post infection, the expression remained unchanged (Figure 1.3a). Integrin β_1 gene expression increased slightly but significantly at 30 minutes, after which the expression between infected and uninfected cells appeared comparable (Figure 1.3a). Integrin α_v mRNA levels were marginally elevated at 30 minutes, but the RQ values were not significant, and the expression was down-regulated in infected cells at one, three, and six hours post infection (Figure 1.3b). The same trend can be observed with Integrin β_3 gene expression (Figure 1.3b).

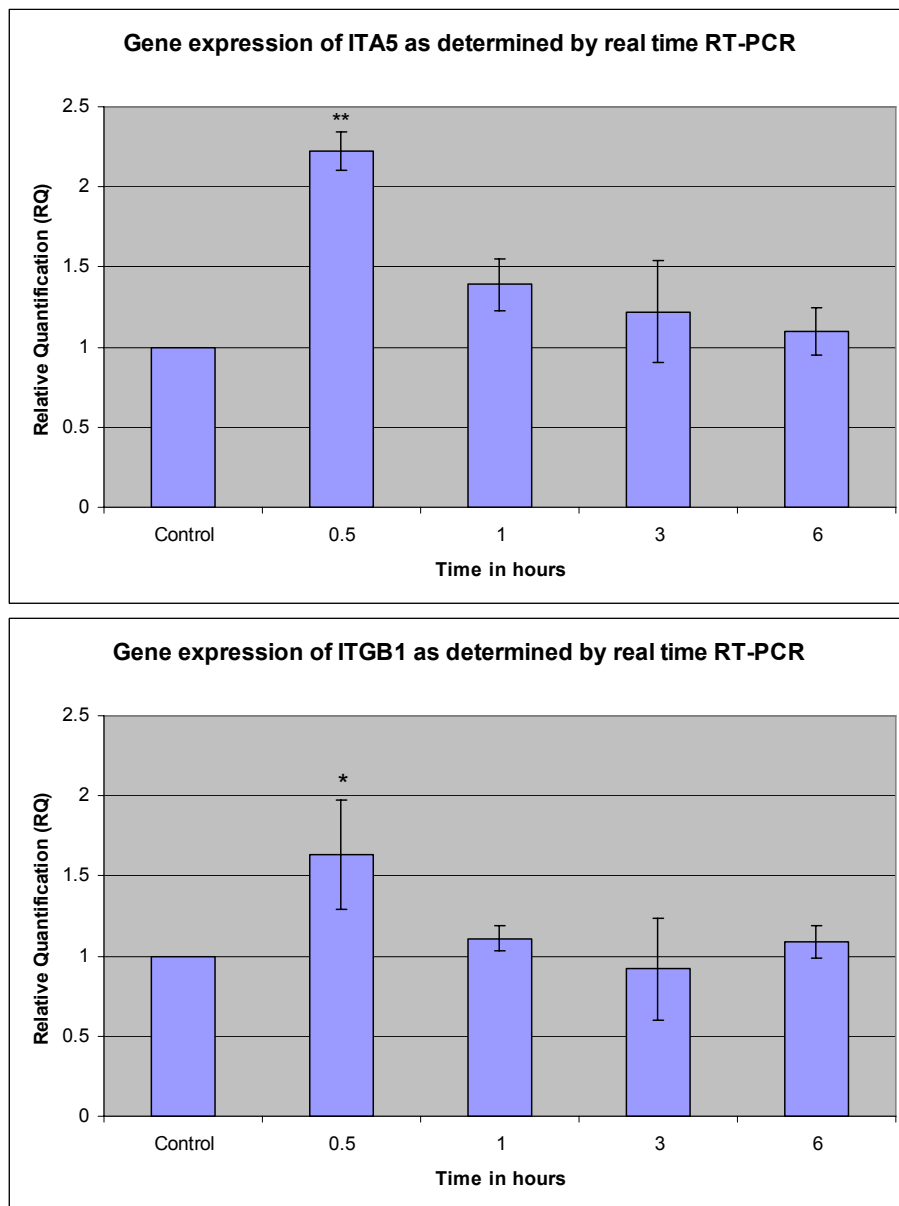


Figure 1.3a. Determination of integrin α_5 and integrin β_1 gene expression in *B. bacilliformis* infected HMEC-1 cells.

Real-time RT-PCR analysis was done to profile the expression of integrin genes using total RNA from infected HMEC-1 cells at various times points. The relative quantification (RQ) of mRNA from infected cells was calculated after normalization to internal control (PPIA) and in relation to threshold values obtained from mock-infected cells. The time in hours is plotted on the X-axis, and RQ is depicted on the Y-axis. Data points are the average of three replicates, and error bars represent the SEM. The p-values obtained by Student's t-test indicate p-values (*) ≤ 0.05 is significant.

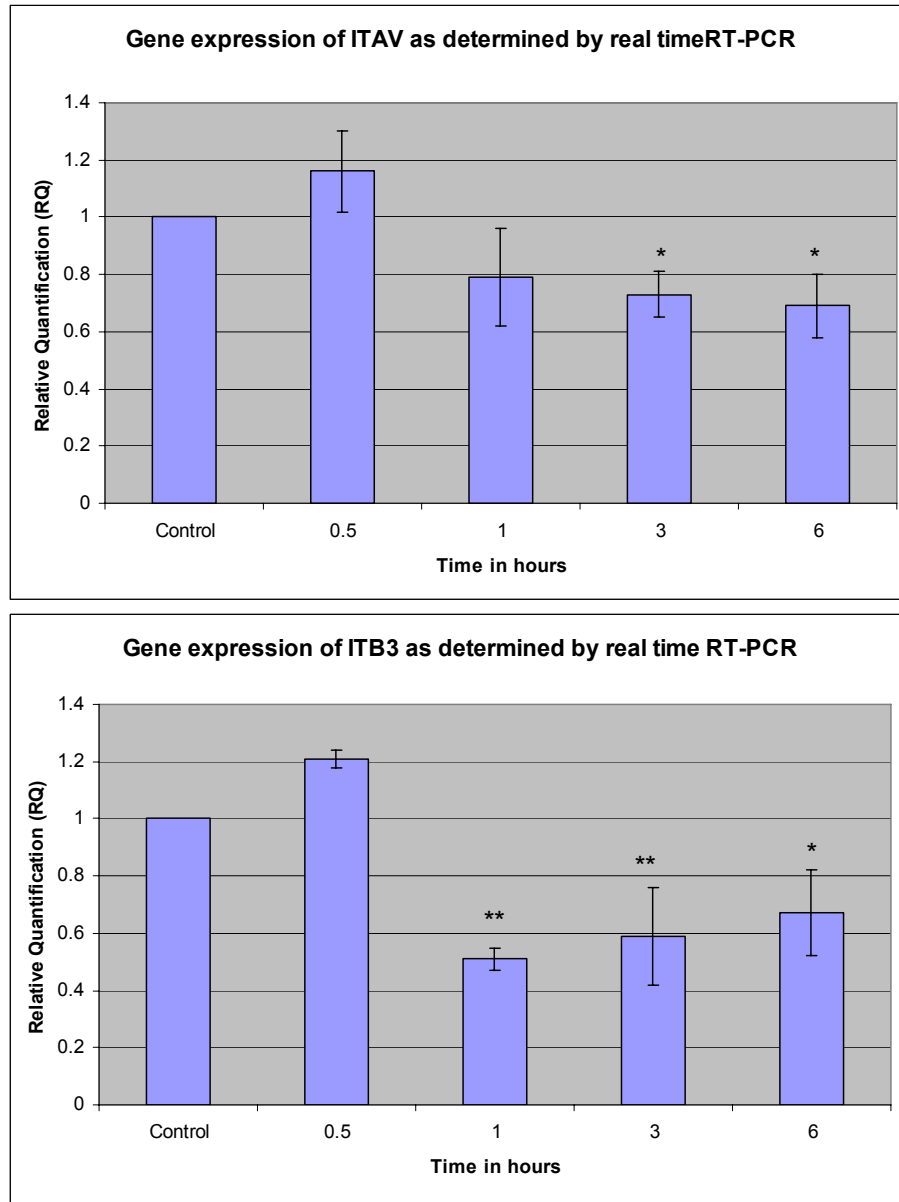


Figure 1.3b. Determination of integrin α_v and integrin β_3 gene expression in *B. bacilliformis* infected HMEC-1 cells.

Real-time RT-PCR analysis helped profile the expression of integrin genes using total RNA from infected HMEC-1 cells at various times points. The relative quantification (RQ) of mRNA from infected cells was calculated after normalization to internal control PPIA and in relation to threshold values obtained from mock-infected cells. The time in hours is plotted on the X-axis, and RQ is depicted on the Y-axis. Data points are the average of three replicates; error bars represent the SEM. The p-value was obtained by Student's t-test, and p-values (*) ≤ 0.05 and (**) ≤ 0.01 were considered significant.

***B. bacilliformis* binds to immobilized fibronectin and vitronectin**

Fibronectin and vitronectin are the optimal natural ligands for $\alpha_5\beta_1$ and $\alpha_v\beta_3$, respectively. Bacteria synthesize proteins that bind fibronectin and vitronectin, which in turn interact with their receptors. In this study, we examine the interaction of *B. bacilliformis* with immobilized or soluble fibronectin and vitronectin. Fibronectin, vitronectin, or the control protein fetuin (5 μ g/ml), a serum glycoprotein, was coated on EIA/RIA plates. The wells were blocked with PBST containing 5% BSA. Various dilutions of *B. bacilliformis* were added to the bound proteins. Bound *B. bacilliformis* were detected with anti-*B. bacilliformis* antibodies, followed by alkaline phosphatase conjugated secondary antibodies. The color intensity of the enzyme substrate p-NPP was proportional to the amount of secondary antibody bound to anti-*B. bacilliformis* antibodies. *B. bacilliformis* interacted with immobilized fibronectin, as seen in the significant increase in absorbance (Figure 1.4.). A bacteria dose-dependent response binding to fibronectin and vitronectin was obtained from 2×10^6 - 5×10^6 CFU/ml, after which binding reaches saturation. *B. bacilliformis* also bound to control protein fetuin, but the absorbance remained low, regardless of the amount of bacteria in the assays. These observations indicate that *B. bacilliformis* is able to bind to immobilized ECM proteins.

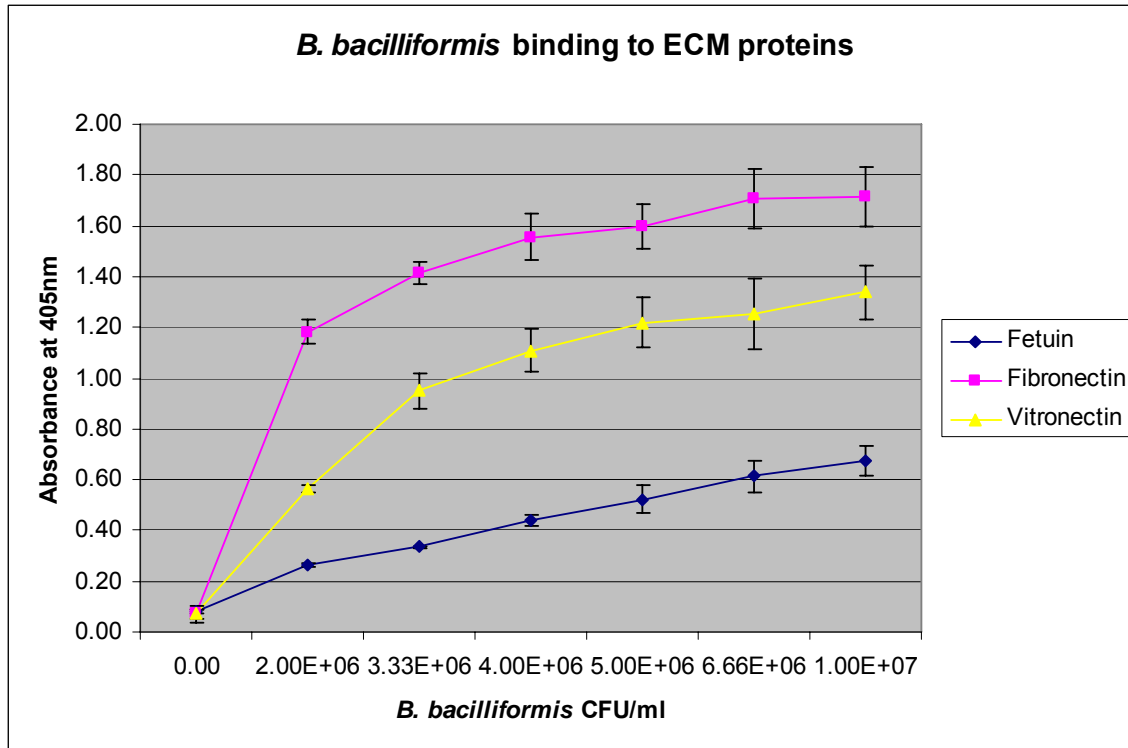


Figure 1.4. *B. bacilliformis* binding to ECM proteins studied by ELISAs.

Fibronectin, vitronectin, or fetuin (control) was coated on EIA plates. After blocking with 5%BSA, *B. bacilliformis* dilutions were incubated with bound proteins. Unbound bacteria were washed and bound bacteria were detected with anti-*B. bacilliformis* antibodies, followed by AP-conjugated secondary antibodies. The p-NPP substrate was allowed to react with AP-conjugated antibodies, and then absorbance was read at 405 nm. The binding event correlated with the increase in absorbance compared with the control wells. All experiments were performed in triplicate, and the p-value calculated by Student's t-test was <0.05.

***B. bacilliformis* binding to soluble fibronectin and vitronectin**

Immobilized proteins could have different interaction domains compared with the free soluble form. *B. bacilliformis*-coated EIA plates were used to investigate the effect of increasing concentrations of soluble ECM proteins on bacterial binding patterns. A sharp increase in absorbance was recorded at 0.1 $\mu\text{g/ml}$ of fibronectin. The binding reached a plateau, followed by a second phase of increased absorbance from 1 $\mu\text{g/ml}$ to 75 $\mu\text{g/ml}$. The increase in absorbance after 10 $\mu\text{g/ml}$ of fibronectin probably is due to the addition of excess fibronectin and not bacteria binding (Figure 1.5a.). *B. bacilliformis* did not bind to the control protein fetuin, and no fibronectin was detected in *E. coli*-coated wells. Soluble vitronectin's attachment to *B. bacilliformis* also was detected (Figure 1.5b). A linear increase occurs from 0.5 $\mu\text{g/ml}$ to 10 $\mu\text{g/ml}$, followed by a decrease at 25 $\mu\text{g/ml}$. *E. coli* used as a control does not show any binding to ECM proteins. Taken together these results suggest that *B. bacilliformis* has the capacity to capture soluble ECM proteins as well as bind immobilized ECM proteins.

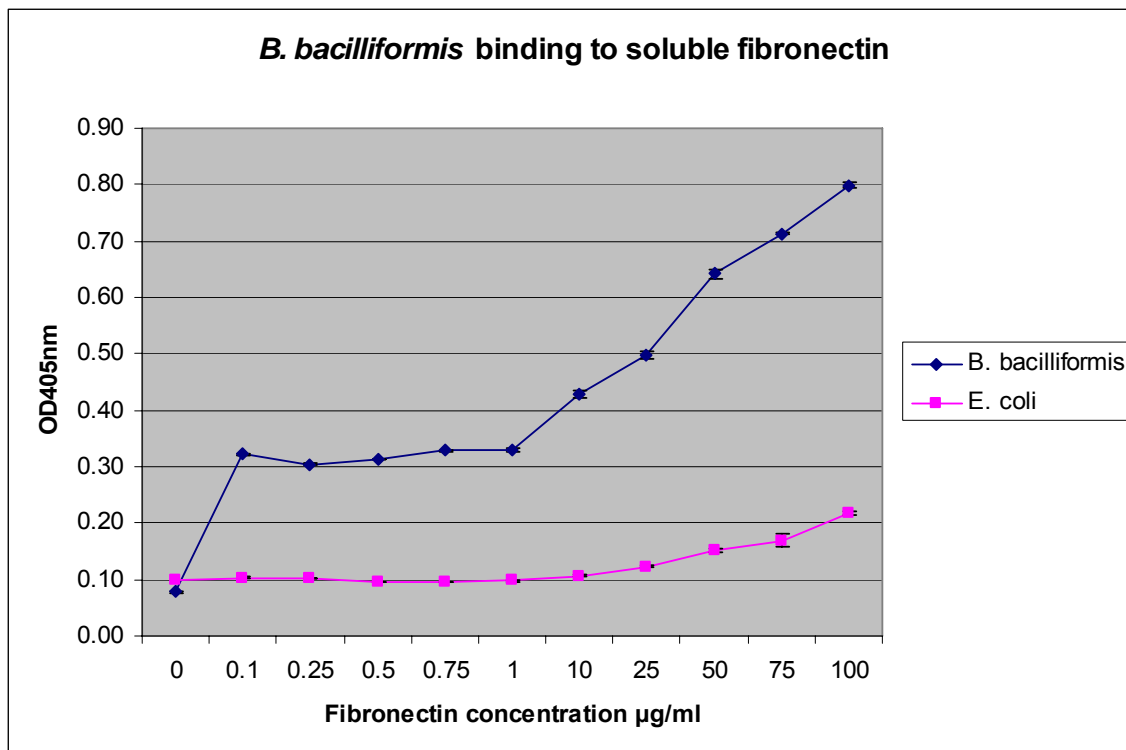


Figure 1.5a. *B. bacilliformis* binding to soluble fibronectin studied by ELISAs.

B. bacilliformis and *E. coli* (1×10^6 cells/ml) were coated on EIA plates. After blocking with 5% BSA, 5 µg/ml of fibronectin was incubated with bound bacteria. Unbound proteins were washed and detected with anti-fibronectin, followed by AP-conjugated secondary antibodies. The p-NPP substrate was allowed to react with AP-conjugated antibodies; absorbance was read at 405 nm. The binding event correlates with the increase in absorbance compared with the control wells. All experiments were performed in triplicate, and the p-value calculated by Student's t-test was 0.0001.

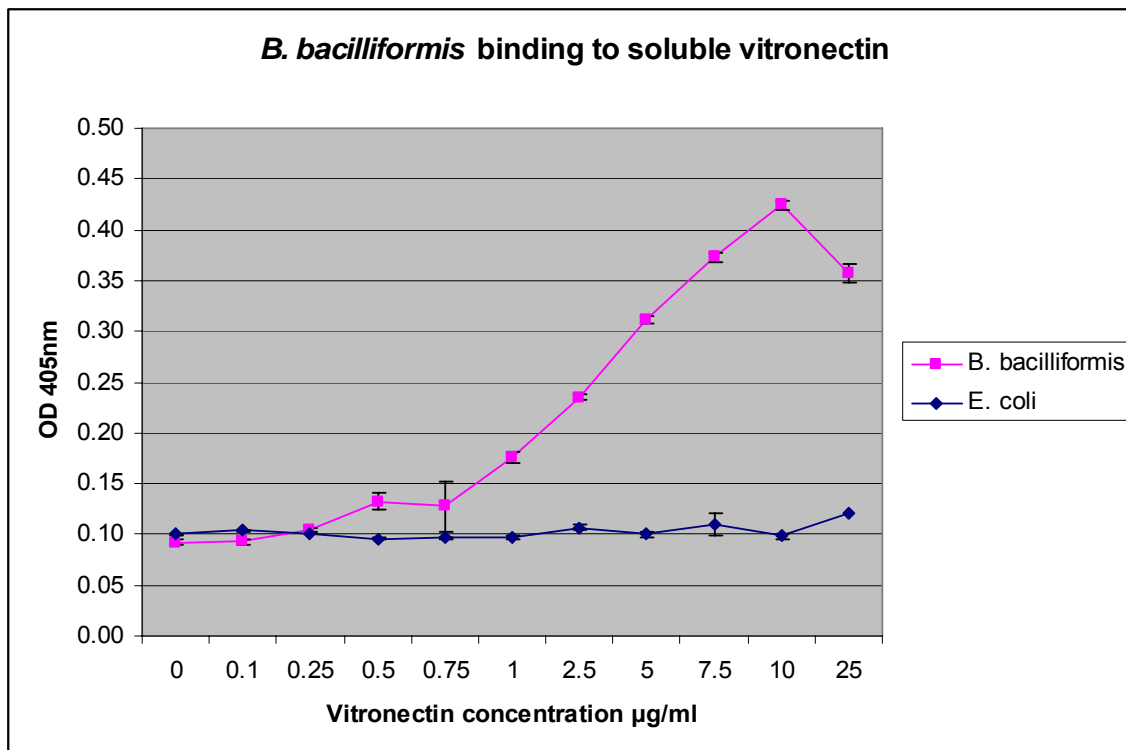


Figure 1.5b. *B. bacilliformis* binding to soluble vitronectin studied by ELISAs.

B. bacilliformis and *E. coli* (1×10^6 cells/ml) were coated on EIA plates. After blocking with 5% BSA, 5 µg/ml of vitronectin was incubated with bound bacteria. Unbound proteins were washed and detected with anti-vitronectin, followed by AP-conjugated secondary antibodies. The p-NPP substrate was allowed to react with AP-conjugated antibodies, and absorbance was read at 405 nm. The binding event correlates with the increase in absorbance compared with the control wells. All experiments were performed in triplicate, and the p-value calculated by Student's t-test was 0.0001.

Effect of ECM-coated *B. bacilliformis* on HMEC-1 cell invasion

B. bacilliformis has the ability to bind fibronectin and vitronectin, as determined by ELISAs. These two proteins are freely available in the serum and extracellular matrix surrounding the endothelial cells. Histological examination of tissues from verruga lesions showed that *B. bacilliformis* is localized in and around endothelial cells (Arias-Stella *et al.*, 1986a). According to these findings, the bacteria have easy access to fibronectin and vitronectin in and around the endothelial cells. Because fibronectin and vitronectin are ligands for integrins believed to be involved in *B. bacilliformis* pathogenesis and because they interact with the bacterial surface, we studied their role in endothelial cell infections. *B. bacilliformis* were pre-incubated with varying concentrations of fibronectin or vitronectin. ECM protein-coated bacteria were then used to infect HMEC-1 cells, following the standard protocol. Fibronectin-opsinised *B. bacilliformis* showed enhanced invasion, depending on the protein concentration (Figure 1.6a.). A 51% increase in the number of intracellular bacteria was observed when bacteria were treated with 25µg/ml of fibronectin. Increases in fibronectin concentration above 25µg/ml did not result in additional invasion. This result suggested that the fibronectin-binding sites on *B. bacilliformis* probably were saturated at this concentration.

B. bacilliformis pre-treated with vitronectin also invaded with greater efficiency than the untreated bacteria (Figure 1.6b.); however, the degree of invasion enhancement was much less pronounced than that seen with fibronectin. This relatively low level of increase was probably due at least in part to the need to use lower vitronectin concentrations for these studies, since the ELISAs showed that beyond 2.5µg/ml of vitronectin, *B. bacilliformis*-protein interaction was inhibited (Figure 1.6b). The

maximum increase in invasion occurred at 5 μ g/ml of vitronectin and remained unchanged at further concentrations. At equal concentrations of 10 μ g/ml of both ECM proteins, the internalization efficiency of fibronectin- and vitronectin-coated bacteria were comparable at 11% for vitronectin and 13% for fibronectin (Table 3a and 3b).

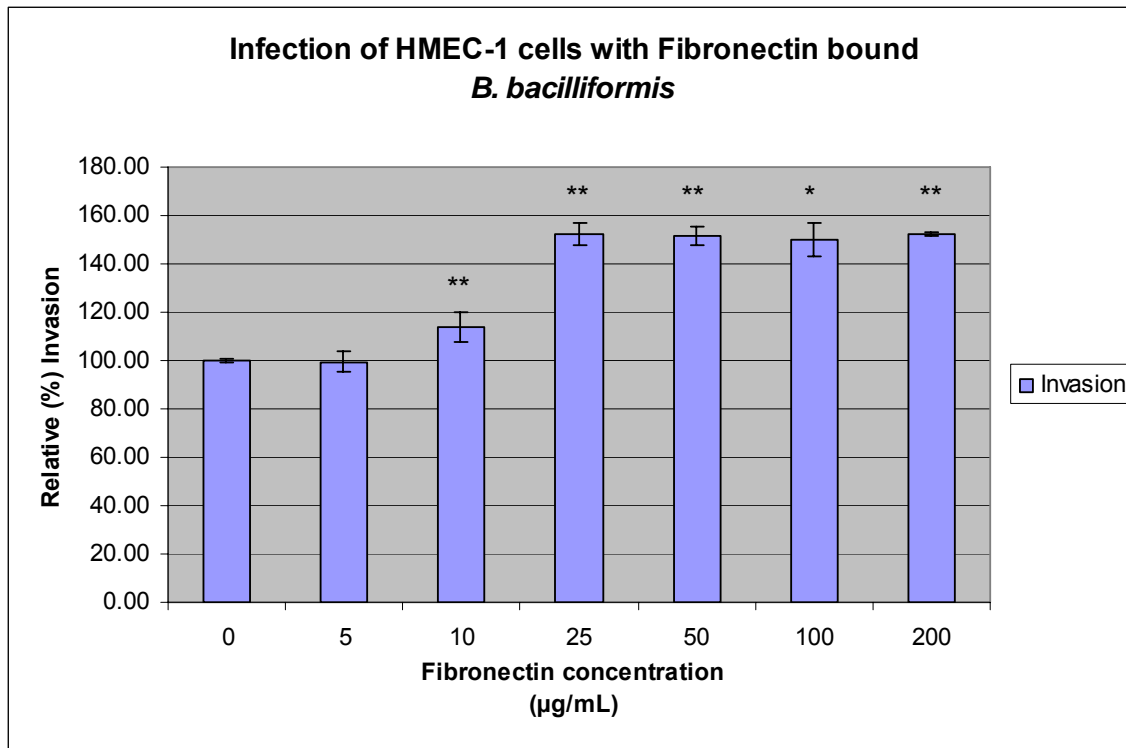


Figure 1.6a. Effect of fibronectin-coated *B. bacilliformis* invasion into HMEC-1 cells.

HMEC-1 cells were grown in 24-well plates and infected at 1:100 m.o.i with ^{35}S -methionine labeled *B. bacilliformis*, pretreated with varying concentrations of fibronectin. Cell lysates were prepared six hours post infection, then used to determine the radiolabeled intracellular bacteria. The radioactivity recovered indicated the number of internalized bacteria. Percent invasion was calculated as $(\text{recovered DPM}/\text{added DPM}) \times 100$. Again, percent invasion from the control experiments was set to 100, and the percent invasion of the treated samples was calculated in relation to 100%. The X-axis denotes the concentration of fibronectin used in contrast to the bacteria used, and the Y-axis reveals the relative percent invasion. The numbers are the average of three replicates, and error bars represent the SEM. The p-values were obtained by Student's t-test; those values of (*) ≤ 0.05 and (**) ≤ 0.01 were significant.

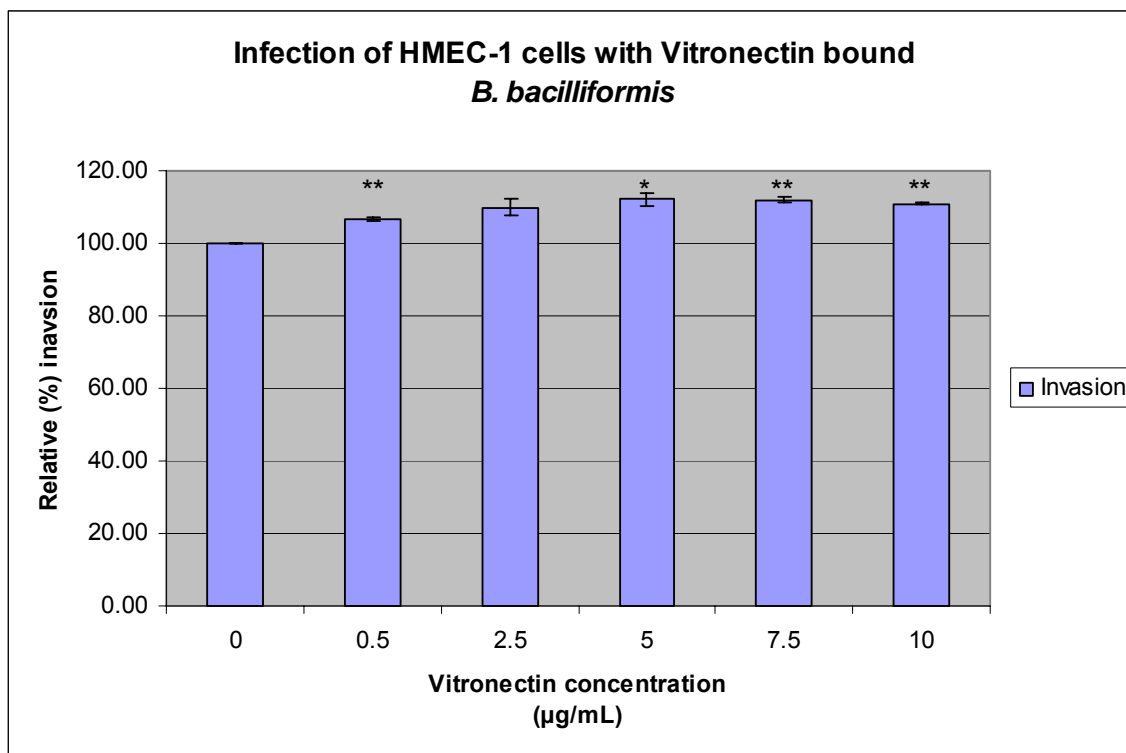


Figure 1.6b. Effect of vitronectin-coated *B. bacilliformis* invasion into HMEC-1 cells.

HMEC-1 cells were grown in 24-well plates and infected at 1:100 m.o.i with ^{35}S -methionine labeled *B. bacilliformis* that were pre-treated with varying concentrations of vitronectin. Cell lysates were prepared after six hours, and then used to determine the number of intracellular bacteria. The radioactivity recovered indicated the number of internalized bacteria. The percent invasion was calculated as (recovered DPM/added DPM) $\times 100$. Whereas the percent invasion from the control experiments was set to 100, the percent invasion of the treated samples was calculated in relation to 100%. The X-axis denotes the concentration of vitronectin used to opsonize the bacteria; the relative percent invasion is plotted on the Y-axis. The numbers are the average of three replicates, and error bars represent the SEM. The p-value was obtained by Student's t-test, and p-values (*) ≤ 0.05 and (**) ≤ 0.01 were significant.

Table 1.3a. Effect of fibronectin-treated *B. bacilliformis* on invasion of HMEC-1 cells.

HMEC-1 cells were infected with, fibronectin-opsonised, ^{35}S -methionine labeled *B. bacilliformis* for six hours in serum-free M199 media. Percent invasion and percent increase values are the means \pm SEM of three experiments. Invasion values were calculated as (recovered DPM/added DPM) \times 100 and were set to 100 for untreated samples. Percent invasion from treated samples was calculated in relation to 100% invasion of untreated samples. Percent increase was determined by normalized invasion – 100. Student's t-test was performed with data from treated and untreated samples. The p-value of <0.05 is considered significant, and NA indicates not applicable.

Fibronectin Concentration ($\mu\text{g/ml}$)	Percent Invasion	Percent Increase	p-Value
0	100 \pm 0.83	NA	NA
5	99.42 \pm 4.07	0.58 \pm 4.07	NA
10	113.86 \pm 5.86	13.80 \pm 5.86	NA
25	151.97 \pm 4.72	51.97 \pm 4.71	0.002
50	151.14 \pm 3.78	51.14 \pm 3.90	0.001
100	151.08 \pm 6.91	50.10 \pm 6.91	0.011
200	152.17 \pm 0.76	52.17 \pm 0.89	0.002

Table 1.3b. Effect of vitronectin-treated *B. bacilliformis* on invasion of HMEC-1 cells.

HMEC-1 cells were infected with vitronectin-opsinised, ^{35}S -methionine labeled *B. bacilliformis* for six hours in serum-free M199 media. Percent invasion and percent increase values are the means \pm SEM of three experiments. Invasion values were calculated as (recovered DPM/added DPM) \times 100, set to 100 for untreated samples. Percent invasion from treated samples was calculated in relation to 100% invasion of untreated sample. Percent increase was determined by normalized invasion – 100. Student's t-test was performed with data from treated and untreated samples, and p-values <0.05 were considered significant.

Vitronectin Concentration ($\mu\text{g/ml}$)	Percent Invasion	Percent Increase	p-Value
0	100 \pm 0.83	NA	NA
0.5	106.55 \pm 0.67	6.63 \pm 0.67	0.007
2.5	109.78 \pm 2.29	9.78 \pm 2.29	0.058
5	112.05 \pm 2.04	12.05 \pm 2.04	0.002
7.5	111.92 \pm 0.79	11.92 \pm 0.79	0.001
10	111.00 \pm 0.19	11.00 \pm 0.19	0.011

Cellular ECM involved in *B. bacilliformis* internalization

Endothelial cells synthesize extracellular matrix proteins (Berge *et al.*, 1992; Jaffe *et al.*, 1978). These proteins are secreted into the extracellular environment, where they interact with themselves, with other extracellular proteins, and with cell receptors.

Histological analysis of tissues from verruga lesion detected the presence of *B. bacilliformis* in the region surrounding endothelial cells. The extracellular milieu is rich in fibronectin and vitronectin, which indicates that it could serve as a source for these proteins for bacterial interaction. Bacterial–ECM interactions could help the bacteria connect indirectly to integrins through ECM proteins. Fibronectin and vitronectin could also be present on cell surfaces. Collectively, the ECM and surface fibronectin or vitronectin are called cellular ECM. The role of cellular ECM proteins was studied by performing invasion assays in the presence of anti-ECM or control antibodies, with serum-free media. In serum-free conditions, the only proteins the antibodies would recognize would be cellular in nature. Data showed that *B. bacilliformis* uptake was inhibited by 47% in the presence of monoclonal anti-fibronectin antibodies (Figure 1.7, table 1.4). Furthermore, the number of externally bound bacteria was reduced by 52% in the presence of monoclonal fibronectin antibodies. Thus, unavailability of cellular fibronectin decreases *B. bacilliformis* adhesion to and internalization into HMEC-1 cells. Monoclonal vitronectin antibodies caused cell rounding and detachment six hours post infection, for unexplained reasons; therefore, they could not be used in these studies. However, polyclonal vitronectin antibodies also lowered bacterial invasion by 31% (Figure 1.7, table 1.4). Adhesion was also affected by 15% in assays with anti-vitronectin antibodies. Because adhesion was not affected as much as invasion with anti-

vitronectin antibodies, it is possible that a portion of the bacteria that bind, but do not subsequently invade the cells. This would suggest that adhesion does not ensure bacterial uptake, and additional cellular vitronectin–dependent factors may be required for invasion. Finally, fibronectin and vitronectin antibodies do not abolish invasion completely, and therefore, *B. bacilliformis* may bind directly to integrins to establish the invasion of endothelial cells.

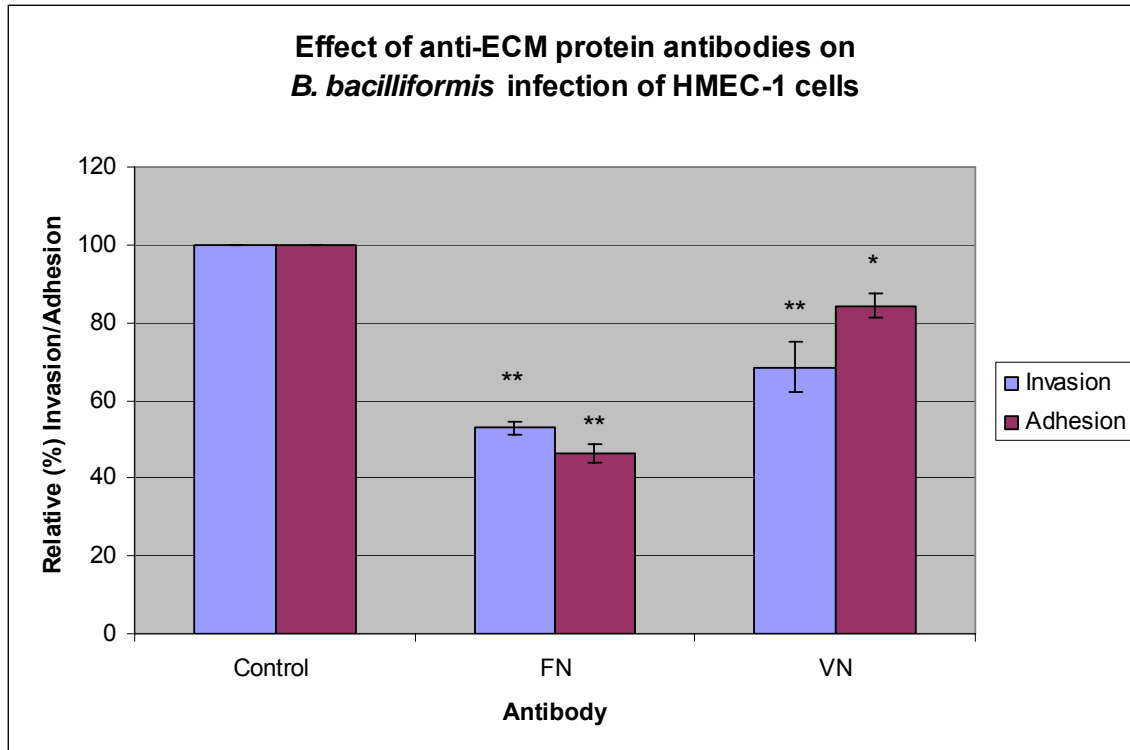


Figure 1.7. Effect of anti-ECM protein antibodies on *B. bacilliformis* infection of HMEC-1 cells.

HMEC-1 cells were grown in 24-well plates and infected with ^{35}S -methionine labeled *B. bacilliformis* at 1:100 m.o.i. in the presence or absence of anti-fibronectin (FN), anti-vitronectin (VN), and control anti-GFP antibodies. Cells were treated with 0.08% trypsin to release extracellular bacteria into the media, six hours post infection. Media containing bacteria and detached cells were centrifuged at 1000xg for 10 minutes to pellet out the host cells. The supernatants were centrifuged again at 2000xg to obtain bacterial pellets. *B. bacilliformis* was resuspended in liquid scintillation fluid to determine the radioactivity incorporated. HMEC-1 cells were lysed with 0.1% Triton-X100 to release intracellular *B. bacilliformis*. Lysed cells were added to liquid scintillation fluid. Percent adhesion/invasion was calculated as $(\text{recovered DPM}/\text{added DPM}) \times 100$, with the control experiments set to 100, and treated samples calculated in relation to 100%. The X-axis denotes the antibody used, and the Y-axis plots the relative percent adhesion/invasion. The numbers reflect the average of three replicates, and error bars represent the SEM. The p-values obtained by Student's t-test were significant at (*) ≤ 0.05 and (**) ≤ 0.01 .

Table 1.4. Effect of anti-ECM antibodies on *B. bacilliformis* invasion of HMEC-1 cells.

HMEC-1 cells were infected with ^{35}S -methionine labeled *B. bacilliformis* for six hours in the presence of $5\mu\text{g/ml}$ of anti-ECM protein antibodies or control antibodies in serum-free M199 media with 1% BSA. Percent adhesion/invasion and percent inhibition values are the means \pm SEM of three experiments. Adhesion/invasion values were calculated as $(\text{recovered DPM}/\text{added DPM})\times 100$ and set to 100 for untreated samples. Percent adhesion/invasion from the treated samples was calculated in relation to 100% adhesion/invasion of control. Percent inhibition was determined by the normalized adhesion/invasion $- 100$. Student's t-test was performed with data from treated and untreated samples; a p-value of <0.05 is considered significant. In the table, NA indicates not applicable.

Antibody Used	Percent Adhesion	Percent Inhibition	p-Value	Percent Invasion	Percent Inhibition	p-Value
Control	100 \pm 0.1	NA	NA	100 \pm 0.1	NA	NA
Anti-fibronectin	46.47 \pm 2.25	52.35 \pm 3.58	0.0003	53.02 \pm 1.70	46.98 \pm 1.69	0.001
Anti-vitronectin	84.36 \pm 3.25	15.70 \pm 3.25	0.001	68.57 \pm 6.38	31.41 \pm 6.39	0.025

Human serum enhances *B. bacilliformis* invasion into HMEC-1 cells

B. bacilliformis is a human pathogen, and humans are the only known reservoir for these bacteria. The bacteria are transmitted via sandflies that feed on the blood of infected patients. Previous data suggest that *B. bacilliformis* interacts with human plasma proteins such as fibronectin and vitronectin. Invasion assays, therefore, were performed in the presence of human serum to determine whether invasion was enhanced under these conditions. Serum was first heated to 56°C to inactivate complement proteins that could be inhibitory to the bacteria. Serum was serially diluted in M199 to determine the most effective concentration for invasion. *B. bacilliformis* invasion was enhanced in the presence of human serum in a concentration dependent manner (Figure 1.8, table 1.5). An increase of 40% in the number of intracellular bacteria was noted in assays performed in the presence of 5% serum. The same number of bacteria was obtained from infections with 7.5% serum, after which the invasion levels diminished with 15% human serum (Table 1.5). It is possible that at high concentrations, human serum proteins prevent *B. bacilliformis* invasion through steric hindrance. Similar experiments with fetal calf serum (FCS) did not affect *B. bacilliformis* infectivity as much as human serum (Figure 1.9, table 1.6). Invasion peaked at 17% when the media contained 7.5–10% FCS, as opposed to a 51% jump with human serum. Use of human serum could provide conditions more similar to those experienced by the bacteria *in vivo*; therefore, future experiments carried out in the presence of human serum would provide results that more closely mimic the infectious process.

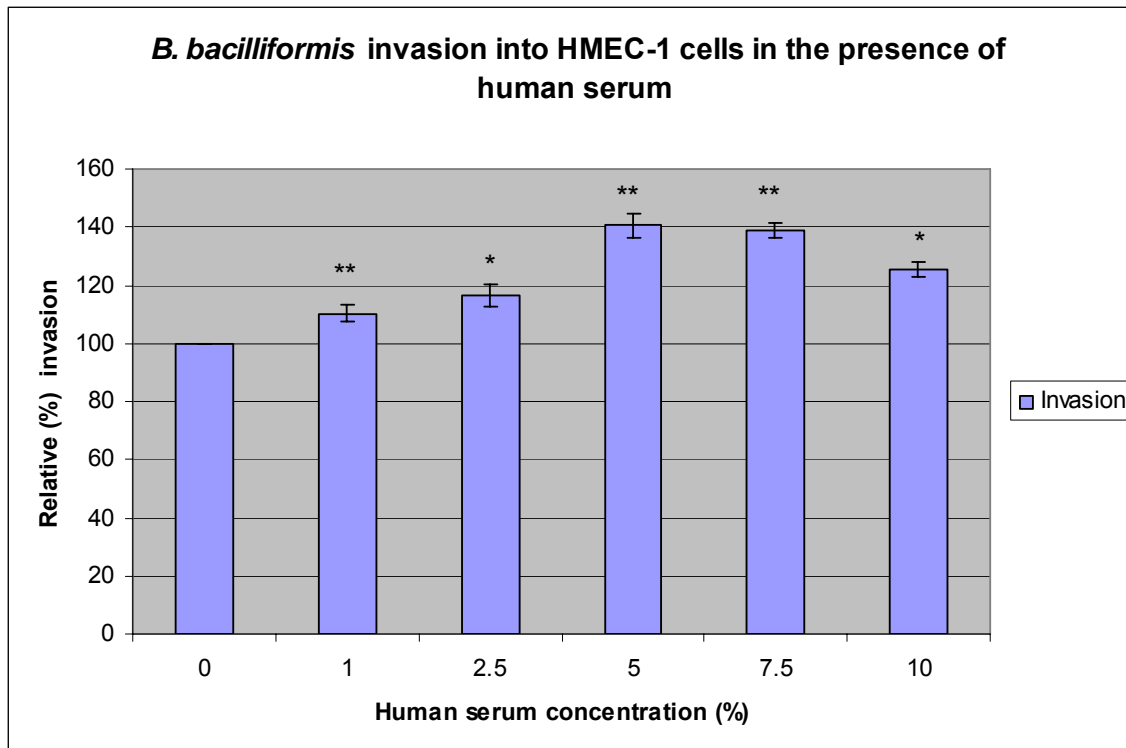


Figure 1.8. Effect of human serum on *B. bacilliformis* invasion into HMEC-1 cells.

HMEC-1 cells were grown in 24-well plates and infected with ^{35}S -methionine labeled *B. bacilliformis* at a m.o.i. of 1:100. In the presence of varying concentrations of human serum. Cell lysates prepared after six hours, were used to determine the number of intracellular bacteria. The radioactivity recovered provided an indicator of the number of internalized bacteria. Percent invasion was calculated as $(\text{recovered DPM}/\text{added DPM}) \times 100$. Percent invasion from the control experiments was set to 100, whereas percent invasion of the treated samples was calculated in relation to 100%. The X-axis denotes the percentage of human serum added to the media, whereas relative percent invasion is plotted on the Y-axis. The numbers are the average of three replicates, and error bars represent the SEM. The p-values obtained by Student's t-test indicate significant p-values of (*) ≤ 0.05 and (**) ≤ 0.01 .

Table 1.5. Effect of human serum on *B. bacilliformis* invasion into HMEC-1 cells.

HMEC-1 cells were infected with ^{35}S -methionine labeled *B. bacilliformis* for six hours in M199 media with increasing concentrations of human serum. Percent invasion and percent increase values are the means \pm SEM of three experiments. Invasion values were calculated as (recovered DPM/added DPM) \times 100, set to 100 for untreated samples; for treated samples, the percent invasion was calculated in relation to 100% control invasion. Percent increase was determined by normalized invasion – 100. Student's t-test was performed with data from treated and untreated samples; a p-value of <0.05 was considered significant.

Human Serum Concentration (%)	Percent Invasion	Percent Increase	p-Value
0	100 \pm 0.40	NA	NA
1	110.12 \pm 2.87	10.12 \pm 2.89	0.088
2.5	116.60 \pm 3.91	16.60 \pm 3.91	0.029
5	140.55 \pm 4.05	40.5 \pm 4.05	0.003
7.5	139.18 \pm 2.57	39.18 \pm 2.57	0.004
10	125.44 \pm 2.36	25.44 \pm 2.36	0.012

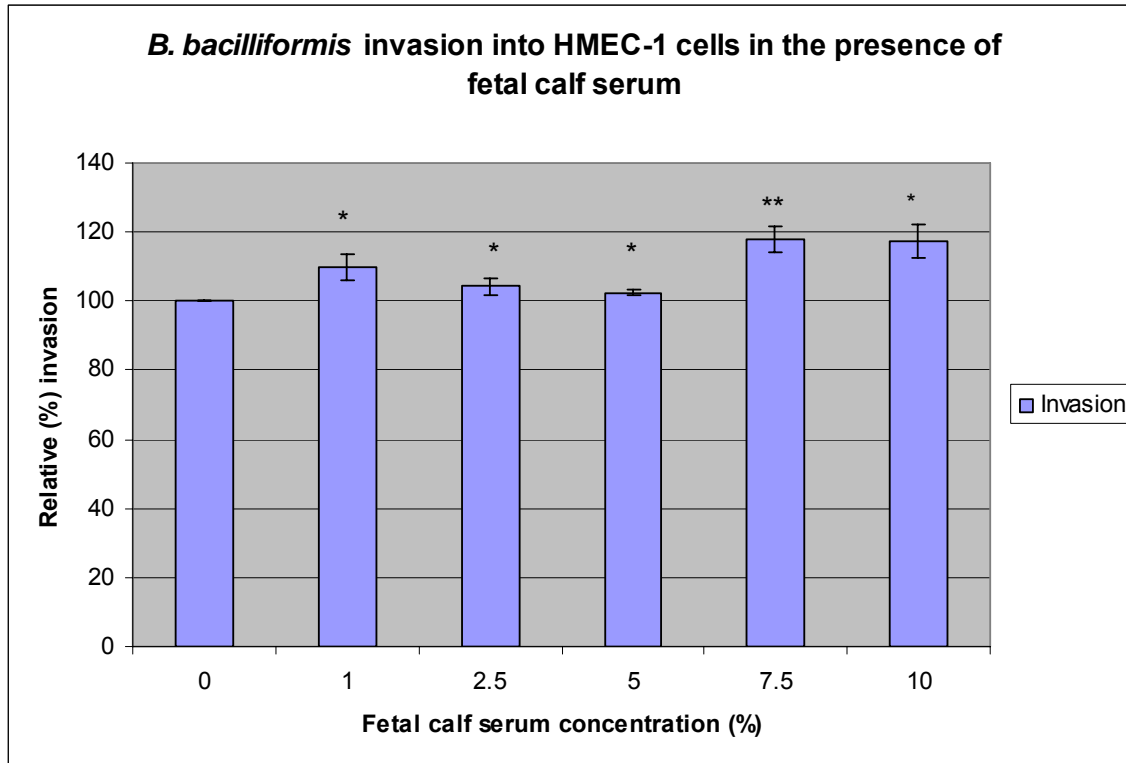


Figure 1.9. Effect of fetal calf serum on *B. bacilliformis* invasion into HMEC-1 cells.

HMEC-1 cells were grown in 24-well plates and infected with ^{35}S -methionine labeled *B. bacilliformis* at a m.o.i. of 1:100 in the presence of varying concentrations of fetal calf serum. Cell lysates prepared after six hours, were used to determine the number of intracellular bacteria. The radioactivity recovered served as an indicator of the number of internalized bacteria. Percent invasion was calculated as $(\text{recovered DPM}/\text{added DPM}) \times 100$. Percent invasion from the control experiments was set to 100, and percent invasion of the treated samples was calculated in relation to that level. The X-axis denotes percentage of human serum added to the media; the Y-axis denotes the relative percent invasion. The numbers represent the average of three replicates, and error bars represent the SEM. The p-values were obtained by Student's t-test, indicating significance at (*) ≤ 0.05 and (**) ≤ 0.01 .

Table 1.6. Effect of fetal calf serum on *B. bacilliformis* invasion into HMEC-1 cells.

HMEC-1 cells were infected with ^{35}S -methionine labeled *B. bacilliformis* for six hours in M199 media with increasing concentrations of fetal calf serum (FCS). Percent invasion and percent increase values are the means \pm SEM of three experiments. Invasion values were calculated as (recovered DPM/added DPM) \times 100 and were set to 100 for untreated samples, whereas percent invasion from the treated samples was calculated in relation to the untreated sample invasion. Percent increase was determined by normalized invasion – 100. Student's t-test was performed with data from treated and untreated samples. A p-value <0.05 is considered significant.

FCS Concentration (%)	Percent Invasion	Percent Increase	p-Value
0	100 \pm 0.4	NA	NA
1	109.95 \pm 3.77	9.95 \pm 3.77	0.023
2.5	104.36 \pm 2.43	4.36 \pm 2.43	0.043
5	102.38 \pm 0.79	2.38 \pm 0.79	0.048
7.5	117.83 \pm 3.86	17.83 \pm 3.86	0.004
10	117.15 \pm 4.84	17.15 \pm 4.84	0.011

NlpD is an outer membrane protein

The highly antigenic *B. bacilliformis* protein NlpD_{Bb} contains RGD, a tripeptide that is commonly found in bacterial adhesions. Sequence analysis of NlpD_{Bb} has shown the presence of a leader peptide that allows the translocation of the protein to the outer membrane. To determine whether this highly antigenic protein is present in the outer membrane, membrane fractions from *B. bacilliformis* and NlpD expressing *E. coli* expressing clones nlpD were prepared and analyzed. Total membrane fractions were isolated by differential ultracentrifugation, and then separated by centrifugation in a sucrose gradient. When separated by this method, the inner membrane appears lighter than the outer membrane at the 20–53% sucrose junction. The heavier outer membrane moves through the gradient to settle at the 53–70% interface. These bands were concentrated, and the separated proteins were analysed with anti-NlpD antibodies. NlpD (43kDa) can be clearly detected in the outer membrane fractions of *E. coli* expressing the *B. bacilliformis* protein (Figure 1.10). The analysis of the *B. bacilliformis* membrane yielded the same results (Figure 1.10). Membranes were also probed with OmpA antibodies to check for outer membrane protein contamination in the inner membrane fractions. The absence of a distinct 35kDa band corresponding to the OmpA band from the inner membrane fractions confirmed the purity of the membrane preparations (data not shown).

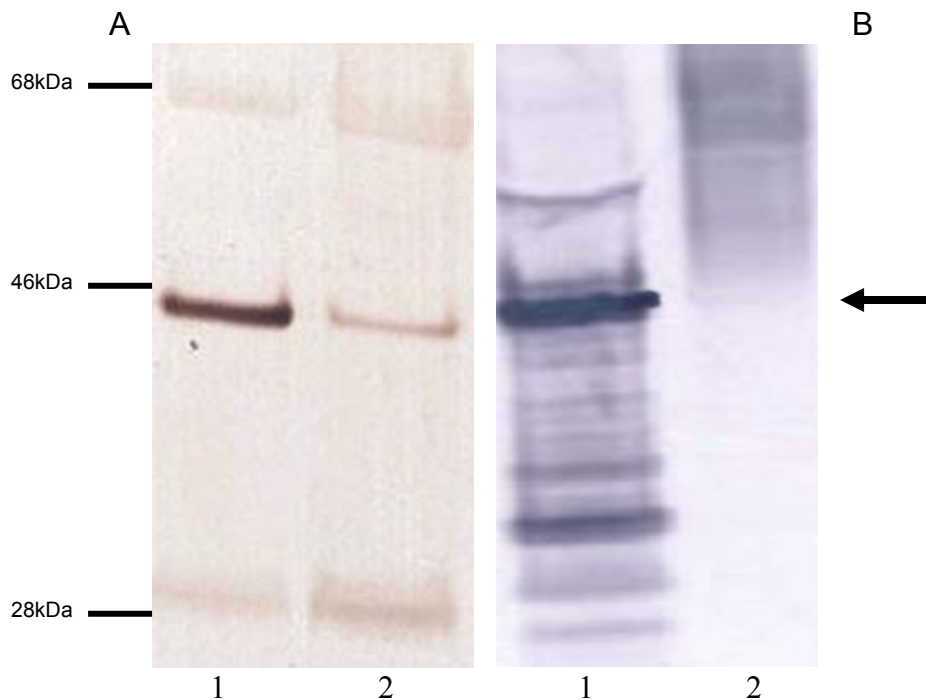


Figure 1.10. Western immunoblot showing the presence of the 43kDa antigen in the outer membrane preparations from *B. bacilliformis* and recombinant *E. coli* expressing *NlpD_{Bb}*.

Outer and inner membrane fractions were isolated from total membrane fractions of *B. bacilliformis* (Panel A) and *E. coli* HMS174 cells expressing *B. bacilliformis nlpD* (Panel B) by the sucrose gradient centrifugation. The individual membrane proteins were separated by SDS-PAGE and then transferred onto PVDF membranes. These membrane were probed with primary anti-NlpD peptide antibodies, followed by AP-conjugated, anti-Rabbit antibodies. The blots were developed with AP- substrate according to the method described in materials and method section. Lane 1 of both panels is the outer membrane proteins and lane 2 the inner membrane proteins. The numbers on the left are the approximate molecular masses in kilodaltons (kDa) and the arrow indicates the NlpD band.

Site-directed mutagenesis and expression of NlpD mutants

The C-terminal domain of the NlpD protein has an arginine-glycine-aspartate (RGD) motif. Various bacterial and viral proteins containing the RGD motif are involved in host cell attachment and invasion. Previously, NlpD was found to be highly immunogenic, and our studies also show that it is an outer membrane protein. These factors make it an attractive adhesion and/or invasion molecule. The aspartate amino acid of the RGD motif was mutated to glutamate through a two-step PCR. The point mutation was confirmed by sequencing; immunoblots with anti-NlpD antibody showed that the level of protein expression by the mutant was comparable to that of the wild type protein (Figure 1.11).

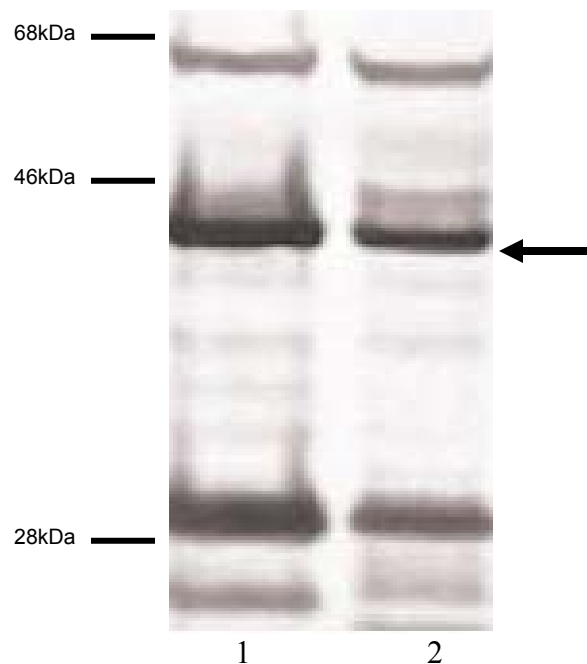


Figure 1.11. Western immunoblot of recombinant E. coli expressing wild type NlpD_{Bb} and mutant NlpD_{Bb}.

Whole cell lysates of recombinant *E. coli* HM174 expressing *B. bacilliformis nlpD* and the *nlpD* gene (lane 1) harboring a point mutation in the RGD motif (lane 2) were separated by SDS-PAGE and then transferred onto PVDF membranes. The membranes were screened with polyclonal rabbit serum against a cocktail of synthetic peptides of NlpD_{Bb}. The position of the wild type and mutant form of NlpD is indicated by the arrow. The numbers on the left are the approximate molecular masses in kilodaltons (kDa).

Adhesion and gentamicin protection assays

Pathogens expressing proteins with the RGD tripeptide often mediate host binding via this motif. *B. bacilliformis* NlpD also has a RGD motif, and therefore, its function in cellular binding and invasion was examined.

Giemsa staining was used to detect adherence to HMEC-1 cells by *E. coli* pNlpD₂₀ (expressing wild type gene) or *E. coli* pNlpD.E₂₀ (expressing mutant gene). *E. coli* with the vector alone was used as a control. The controls and *E. coli* expressing the mutant NlpD did not adhere to the HMEC-1 cells. A few bacteria expressing the wild type NlpD were found attached to the host cells, however, these were not significant enough in number to conclude that NlpD confers an adhesion phenotype to non-adhesive *E. coli* strains.

Gentamicin protection assays were performed to determine whether *B. bacilliformis* NlpD expression results in *E. coli* uptake by HMEC-1 cells. Bacteria were allowed to invade for six hours. Gentamicin (100µg/ml) was then added to kill extracellular *E. coli*. Eukaryotic cells are impermeable to gentamicin, so intracellular bacteria would be protected from the lethal effects of this antibiotic. Host cells were washed extensively to remove unbound bacteria. The cells were then lysed to release intracellular bacteria. Cell lysates were plated on LB-ampicillin plates to allow the growth of viable bacteria. No bacterial colonies were recovered from cell lysates of HMEC-1 cells infected with *E. coli* wild-type NlpD or RGD mutants. Unfortunately, numerous colonies were obtained from HMEC-1 cells infected with control *E. coli* with plasmids alone. Because of the failure of the control experiments, the interpretation of the experimental results remains questionable.

Discussion

Role of Integrins in *B. bacilliformis* Pathogenesis

Bartonella spp invade endothelial cells *in vivo* and stimulate their proliferation. Endothelial cells are also thought to serve as the primary niche for *B. bacilliformis*, where the bacteria reside and possibly multiply before they infect the erythrocytes. In addition, endothelial cell infection could help *B. bacilliformis* disseminate into tissues and protect it from immune response molecules. The first step of a successful cellular infection involves bacterial interaction with the host surface molecules. Endothelial cell receptors that recognize *Bartonella* spp are not known. This study is the first to identify endothelial integrins as *B. bacilliformis* receptors. Antibodies that block integrin function by preventing ligand interactions were used, and *B. bacilliformis* invasion was inhibited significantly by 84.2% by anti- $\alpha_5\beta_1$ antibodies during microvascular endothelial cell infection assays. Furthermore, the blocking antibodies for α_5 and β_1 decreased *B. bacilliformis* invasion into epithelial cells (Hep-2) when used individually or in conjunction with one another (Williams-Bouyer *et al.*, 1999). The level of inhibition reported for epithelial cell invasion was only 33%, significantly lower than the inhibitory effect seen in our studies. The use of polyclonal antibodies against $\alpha_5\beta_1$, coupled with the different cell line used, could explain the variance in the degree of inhibition in these two studies. An analysis of the number of extracellular *B. bacilliformis* showed that not only is *B. bacilliformis* invasion affected in the presence of anti- $\alpha_5\beta_1$, but adherence is also lowered. The other two antibodies tested, anti- β_1 and anti- $\alpha_v\beta_3$, also had an inhibitory effect on *B. bacilliformis* attachment and invasion of 31.62% and 27.82%, respectively. Moreover, these antibodies decreased the attachment of *B. bacilliformis* to cell surfaces.

As mentioned previously, monoclonal antibodies against β_1 decreased *B. bacilliformis* entry into epithelial cells (Williams-Bouyer *et al.*, 1999). Therefore it was not surprising to find an inhibitory effect in endothelial cells as well. The role of β_1 integrin in *B. henselae* infection of host cells also has been suggested. *B. henselae* expresses an adhesin, BadA, that mediates its binding to ECM and endothelial cells (Riess *et al.*, 2004). BadA resembles Yersinia protein YadA, which indirectly interacts with β_1 integrins (Bliska *et al.*, 1993). BadA expressing *B. henselae* showed decreased binding capacity to β_1 -null fibroblasts, suggesting that β_1 functions as a receptor during *B. henselae* infections (Riess *et al.*, 2004).

Various intracellular pathogens alter the host gene expression upon infection. Transcriptional factors in *B. bacilliformis*-infected endothelial cells are activated throughout the infection period (Verma *et al.*, 2002a). Changes in fibronectin and vitronectin integrin gene expression, determined by real time RT-PCR, suggested that the integrin genes were differentially regulated in the *B. bacilliformis* infection (Figure 3a and 3b). Levels of α_5 integrin mRNA were two times higher in infected cells and decreased with time; in addition, expression of the β_1 integrin genes showed a similar trend. *S. pyogenes*-infected epithelial cells also indicated a significant increase in α_5 expression; this integrin was found to be utilized for adhesion and invasion (Halasz *et al.*, 2008). In the studies reported here, the α_V and β_3 genes showed an elevated transcriptional response at 30 minutes post infection, after which they were significantly down regulated (Figure 3b). The data suggest that, transcriptional induction of genes encoding *B. bacilliformis* receptors were beneficial for increased bacterial uptake and enhance infection efficiency. One possibility for the eventual down regulation is that

host responses curtail *B. bacilliformis* ingestion and control the number of intracellular bacteria.

The use of integrins as receptors for invasion may be advantageous, because these molecules are involved in bidirectional cell signaling. One of the most critical functions of integrins is the modulation of the internal actin network through signaling pathways such as phosphatidylinositol 4,5-bisphosphate (PtdIns (4,5)P₂) and Rho family GTPases. Cytoskeletal proteins are regulated by integrin binding to ligands, and bacterial binding to integrins could manipulate the internal signaling environment to facilitate their ingestion. Furthermore, $\alpha_5\beta_1$ is the most commonly expressed integrin for several cell types. The ubiquitous expression also makes $\alpha_5\beta_1$ the most commonly targeted integrin for bacterial attachment and invasion. The definitive role of $\alpha_5\beta_1$ in *Streptococcal* infection of host cells already has been established using non-peptide agonists (Cue *et al.*, 2000). In addition, attachment of the causative agent for lyme disease, *Borrelia burgdorferi*, onto endothelial cells decreases in the presence of anti- $\alpha_5\beta_1$ antibodies (Coburn *et al.*, 1998). Anti- α_5 and anti- β_1 antibodies also inhibit the ingestion of *Mycobacterium avium subsp paratuberculosis* into M cells. Functional blocking of $\alpha_5\beta_1$ has been used to demonstrate the integrin's role in *Neisseria* spps and *Porphyromonas gingivalis* infections of host cells (Unkmeir *et al.*, 2002; Yilmaz *et al.*, 2002). Finally, *Shigella flexneri* attachment to mammalian cells varies with the differential expression of $\alpha_5\beta_1$ integrins on the cell surface (Watarai, M *et al.*, 1996). The role of $\alpha_v\beta_3$ has not been demonstrated in other *Bartonella* spps, although a few bacteria exploit this integrin for effective host colonization. *Borrelia* spps bind to purified $\alpha_v\beta_3$, and mutations in the OMP P66 disrupt bacterial adherence to the $\alpha_v\beta_3$ integrin (Coburn *et al.*, 2003c; Coburn *et al.*, 1998).

Invasion of *Neisseria gonorrhoeae* relies heavily on the Opa protein interactions with $\alpha_V\beta_3$ via vitronectin (Dehio *et al.*, 1998), because anti- $\alpha_V\beta_3$ antibodies minimize the intracellular bacteria recovered.

This study thus demonstrates effects of blocking of integrins with antibodies in *B. bacilliformis* attachment and invasion. Neutralization of $\alpha_5\beta_1$ has the maximum inhibitory effect on *B. bacilliformis* infection. However, the other antibodies also reduced bacterial ingestion, which suggests the involvement of multiple integrins in efficient *B. bacilliformis* infection of endothelial cells. Experiments with cell lines deficient in integrin expression would strengthen these observations and help establish the definitive role of integrins.

Role of ECM proteins in *B. bacilliformis* pathogenesis

The binding of *B. bacilliformis* to the integrin ligands fibronectin and vitronectin was determined by ELISAs. Pretreatment of *B. bacilliformis* with these proteins significantly enhanced their uptake by endothelial cells. ECM proteins are often used by bacteria to form an indirect link between their surface and integrins. Bacterial attachment to host proteins allows the pathogen to target specific cell types that express receptors for the bound proteins. The two well-characterized bacteria that bind host molecules are *S. pyogenes* and *S. aureus*, which express high-affinity fibronectin-binding proteins (Jonsson *et al.*, 1991b; Vercellotti *et al.*, 1984). These bacteria trigger their uptake by interacting with the $\alpha_5\beta_1$ integrin via fibronectin, which leads to integrin-mediated cell signaling changes (Agerer *et al.*, 2005; Purushothaman *et al.*, 2003). Fibronectin coating of *S. pyogenes* enhances its internalization into epithelial cells, and the percentage of cells internalized plateaus when the concentration of fibronectin used to opsonize the bacteria

exceeds 20µg/ml (Ozeri *et al.*, 1998). Pretreatment of *M. avium* subsp paratuberculosis with fibronectin also augments its entry into M-cells (Secott *et al.*, 2004). *B. bacilliformis* invasion increased by a maximum of 51% when the bacteria were pretreated with upto 25 µg/ml of fibronectin. This pattern suggests that the fibronectin binding sites on *B. bacilliformis* achieve saturation at a ligand concentration of 25µg/ml, and therefore, a further addition of fibronectin does not affect its infectivity. However, a saturation effect was not seen in *B. henselae* opsonized with fibronectin, as a dose-dependent inhibition of endothelial cell surface adherence was noted (Dabo *et al.*, 2006). The study reported by Dabo *et al* (2006) did not look at the effect of fibronectin pretreated *B. henselae* on invasion, but it is reasonable to assume that a decrease in invasion would result from reduced *B. henselae* attachment. The discrepancy between the two *Bartonella* species could be explained by analyzing the fibronectin-binding properties of *B. bacilliformis* and *B. henselae*; it seems likely that *B. henselae* binding to fibronectin prevents fibronectin from interacting with integrins by binding to the integrin-binding regions of fibronectin. *B. bacilliformis*, in contrast, may bind to a region of fibronectin that is not involved in integrin adherence. The role of fibronectin in *B. henselae* remains controversial though, because another study of the role of fibronectin-binding protein BadA suggests that *B. henselae* binds to the β_1 integrin via fibronectin (Riess *et al.*, 2004). Fibronectin is present in a soluble form in plasma, cerebral spinal fluid, and inflammatory exudates. The insoluble fibronectin forms a part of the extracellular matrix and cross-links with other fibronectin molecules to form a fibrillar network. Fibronectin is synthesized and secreted by the cells themselves. The fibronectin from the ECM interacts with cellular receptors and coats the cell surface. This fibronectin, called

cellular fibronectin, in the absence of serum is the only source of fibronectin available to maintain cellular functions. Cellular fibronectin neutralized with monoclonal antibodies decreased *B. bacilliformis* entry by 46% and also affected its adhesion. The approach described here has also been used to investigate the function of fibronectin in the attachment of various bacteria, such as *Treponema palladium*, *S. aureus*, and *Pneumocystis carinii* (Peacock *et al.*, 1999; Peterson *et al.*, 1983; Pottratz *et al.*, 1990). The inhibition of invasion by anti-fibronectin antibodies in the absence of serum implies that *B. bacilliformis* uses surface-bound and/or ECM fibronectin as a bridge to interact with endothelial cell integrins.

In 1996, Ihler suggested that *B. bacilliformis* could interact with integrins and vitronectin because a phylogenetically related organism, *Agrobacterium tumefaciens*, can bind to carrot cells via vitronectin (Ihler, 1996; Wagner *et al.*, 1992). Our studies on *B. bacilliformis* binding with vitronectin support this hypothesis. In addition to binding vitronectin ECM protein, plasma vitronectin-coated *B. bacilliformis* invaded endothelial cells with greater efficiency than did untreated bacteria. Like anti-fibronectin antibodies, anti-vitronectin affected *B. bacilliformis* adhesion and internalization, though the inhibitory effects of anti-vitronectin on invasion were slightly lower than those of fibronectin. The absorbance values for *B. bacilliformis* binding to fibronectin were also higher in comparison with vitronectin. Finally, almost complete inhibition of *B. bacilliformis* entry occurred when the $\alpha_v\beta_3$ fibronectin integrin $\alpha_5\beta_1$ was neutralized, though blocking of the vitronectin integrin decreased *B. bacilliformis* ingestion to a much lesser degree than anti- $\alpha_5\beta_1$. Taken together, these results suggest that *B. bacilliformis*

employs both ECM proteins and their receptors for endothelial infection. However, fibronectin and its integrin may play a more significant role than vitronectin and $\alpha_V\beta_3$.

Fibronectin and vitronectin are both available in serum. *B. bacilliformis* is released into the blood stream upon hemolysis, where it can freely interact with human serum proteins that would enhance their recognition by cell receptors. When we compared the effect of human serum and fetal bovine serum on *B. bacilliformis* internalization, we found that human serum improved *B. bacilliformis* translocation into endothelial cells by 40% at a concentration of just 5%. Invasion increased by just 2% in the presence of FCS at this dilution. Of course, human pathogens generally have a higher affinity for human proteins compared with other mammalian proteins. A similar effect of human serum was seen in the *N. meningitides* infection of human brain microvascular endothelial cells (Unkmeir *et al.*, 2002). Additional experiments that use human serum may be required to more effectively mimic *in vivo* conditions and thereby provide a greater understanding of the events surrounding *B. bacilliformis* infection.

We have shown that plasma fibronectin and vitronectin-coated *B. bacilliformis* invade endothelial cells with greater efficiency than uncoated bacteria. The unavailability of cellular ECM proteins and their receptors has a detrimental effect on *B. bacilliformis* attachment and uptake. During host infection, it is possible that the *B. bacilliformis* released from erythrocytes capture plasma fibronectin and vitronectin, which predisposes them to anchor onto integrins (e.g., $\alpha_5\beta_1$ and $\alpha_V\beta_3$, respectively). *B. bacilliformis* also can be found in the interstitial spaces and extracellular matrix. *B. bacilliformis*-bound fibronectin and vitronectin could interact with their ECM counterparts, which would favor bacterial survival in the extracellular spaces. However,

cellular fibronectin and vitronectin also are required for *B. bacilliformis* adherence and invasion; therefore, the bacteria could engage extracellular proteins directly and increase integrin attachment efficiency. Because *B. bacilliformis* infects endothelial cells in the absence of ECM proteins, pathways independent and/or alongside ECM binding pathways maybe involved in *B. bacilliformis* and endothelial interaction.

Analysis of *B. bacilliformis* NlpD as a potential adhesion molecule

B. bacilliformis NlpD/Lpp (Lipoprotein) was identified when the *B. bacilliformis* genomic library was screened with serum from a patient with the verruga phase of Carrion's disease (Padmalayam *et al.*, 2000b). This highly antigenic protein is conserved among the *Bartonella* spp. NlpD/Lpp is homologous to the LppB protein in *Haemophilus somnus*, an outer membrane protein with potential hemin-binding properties. NlpD_{Bb} has an N-terminal signal peptide that allows its transport to the outer membrane. In this study, we show that the protein is present in the outer membrane fractions of *B. bacilliformis* and *E. coli* expressing wild-type NlpD_{Bb}. Bacterial and viral proteins that attach and/or play a role in invasion are generally present on the surface, which provides accessibility to the host cell receptors that allow for optimal interactions in support of subsequent infection events. However, pathogen surface molecules are also great targets for the host immune system, making them excellent antigens. On the basis of the observations that NlpD_{Bb} is an OMP and highly immunogenic, and has the RGD motif, known to be involved in infections, we studied the role of NlpD_{Bb} in infection. *E. coli* expressing wt NlpD_{Bb} and RGD mutants were allowed to adhere to endothelial cells. Bacterial attachment to host cells was observed microscopically. Unfortunately, only 1% of the host cells bound recombinant *E. coli*. The absence of more externally bound

bacteria suggests that NlpD_{Bb} expression may not be involved in host cell attachment. When expressed on the outer member of *E. coli*, no successful assays to determine the functionality of NlpD_{Bb} expressed by *E. coli* have been developed thus far. Therefore, the absence of recombinant *E. coli* on endothelial cells' surface could result from the improper expression of *B. bacilliformis* protein. The recognition of the tripeptide RGD depends on the amino acids that flank the motif. The neighboring sequence determines the optimal RGD conformation that enables it to fit the integrins (Ruoslahti *et al.*, 1987). The amino acids surrounding the RGD motif in NlpD_{Bb} may not allow the tripeptide to be exposed to the protein surface, which would prevent its interaction with the integrin.

Standard gentamicin protection assays were performed to study the function of NlpD_{Bb} in endothelial cell invasion. *E. coli* pNlpD₂₀ or pNlpD.E₂₀ could not invade; we did not recover any colonies from the cell lysate after killing the extracellular bacteria with gentamicin. However, colonies were recovered from the control *E. coli* with just the vector. This result was obtained with different *E. coli* strains, expressing different recombinant plasmids. The *E. coli* used were noninvasive laboratory strains that are sensitive to gentamicin. Therefore, it is unusual to recover colonies from the control experiments. At this point, we do not have an explanation for these results.

Chapter II: Role of cell signal molecules during *B. bacilliformis* infection

Introduction

Intracellular bacteria require the concerted action of several cell signaling molecules for optimal invasion and the subsequent establishment of infection. Invasive pathogens can subvert and control cellular functions to aid their ingestion and dissemination. Cytoplasmic proteins regulating cellular functions also can be altered by bacterial interactions with host cell receptors, the injection of bacterial proteins into the cell, or the internalized bacteria themselves. Cytoskeletal proteins are the most common target for virulent organisms, because cytoskeletal components modify membrane structures involved in bacterial uptake. The cytoskeleton is composed of actin filaments, microtubules, and intermediate filaments. Pathogens manipulate the actin network indirectly by modulating small GTPases (Rho, Cdc42, Rac), and kinases, which control transcription factors and other actin-related proteins. A few cytosolic components have been identified, but existing information has been insufficient to understand in any detail the interactions between the molecules and the role they play during infection. The inhibitory effects of cytochalasin D, an actin inhibitor, on invasion by *B. bacilliformis* demonstrated the need for actin reorganization during the infectious process (Hill *et al.*, 1992). Subsequent studies showed that endothelial cell exposure to *B. bacilliformis* results in actin rearrangement along with Rac and Cdc42 activation (Verma *et al.*, 2002b). Activated Rac and Cdc42 generate the membrane protrusions lamellipodia and filopodia, respectively, which surround and engulf the bacterial aggregates. Inhibition of tyrosine kinases also decreases invasion (Williams-Bouyer *et al.*, 1999). Small GTPases participate in complex signal networks, resulting in the phosphorylation of various

kinases. Downstream kinases engaged by *B. bacilliformis* that control the phosphorylation or actin cytoskeleton for efficient invasion have not been identified. The premise of this study is to identify kinases belonging to mitogen-activated protein kinases (MAPK) that play a role in the infection of endothelial cells by *B. bacilliformis*.

Involvement of Mitogen Activated Protein Kinases in bacterial pathogenesis

Bacteria interfere with phosphorylated state of signaling kinases that promote their internalization. Kinase modulation can be achieved by bacterial effector proteins or by bacterial interaction with host cell receptors. Receptors are linked to intracellular signaling pathways, such as mitogen-activated protein kinase (MAPK) (Pelech *et al.*, 1992). This cascade is initiated by the phosphorylation of MAPKKKs (MAPK kinase kinase), followed by MAPKKs (MAPK kinase) and finally MAPKs. Activated MAPKs are phosphorylated at threonine and tyrosine residues of the activation loop. The MAPKs can be divided into three groups on the basis of the different motifs in the activation loop: the extracellular signal-regulated kinases 1 and 2 (ERK1/2) contain a Thr-Glu-Tyr motif and two groups of stress-activated protein kinases/c-Jun N-terminal kinases (SAPK1, JNK1/2/3) contain Thr-Pro-Tyr motif and four p38 enzymes (α , β , γ , δ , or SAPK2) contain a Thr-Ala-Tyr motif (Johnson *et al.*, 2002; Kyriakis *et al.*, 2001). The MAPK pathway plays a central role in several cell functions, including growth, differentiation, survival, and cytoskeletal rearrangements through interactions of the enzymes with cytoplasmic proteins and modulation of transcriptional factors. Activators of this pathway include cytokines, environmental stress factors, mitogens, and pathogens. Activation of MAPKs by bacteria and their subsequent requirement for successful infection has been reported. *Listeria monocytogenes* activates and requires the MAPKK,

MEK1/2, and the upstream kinase for the ERK1/2 pathway for invasion into epithelial cells (Tang *et al.*, 1994; Tang *et al.*, 1998). MEK1/2 involvement in *Campylobacter jejuni* and *Staphylococcus aureus* for host cell entry also has been established (Ellington *et al.*, 2001; Hu *et al.*, 2006). *Neisseria meningitidis*, *Neisseria gonorrhoeae*, and *Porphyomonas gingivitis* phosphorylate the stress response kinases, JNK, upon host cell infection, which then participate in bacterial internalization (Naumann *et al.*, 1998; Sokolova *et al.*, 2004; Watanabe *et al.*, 2001). *B. bacilliformis* also activates SAPK/JNK1, 2 and p38 kinase during infection of endothelial cells (Verma *et al.*, 2002b). SAPK/JNK 1, 2 is phosphorylated at 1 and 8 hours after infection, and activated p38 is observed until 8 hours post infection. These kinases also activate transcription factor AP-1. The function of stress-activated kinases JNK, p38 kinase, and MEK1/2 in *B. bacilliformis* uptake by endothelial cells is unknown. The present study attempts to elucidate the role of MAPKs in *B. bacilliformis* invasion of endothelial cells.

Involvement of Phosphoinositide 3 Kinase in bacterial pathogenesis

Phosphatidylinositol kinases refer to a group of conserved molecules that orchestrate receptor-mediated signaling. One of the members of this group of kinases, phosphatidylinositol 3 kinase (PI3K), phosphorylates the three-position ring of phosphatidylinositides at the plasma membrane. The resulting secondary messengers modulate actin cytoskeletal functions and recruit effector molecules, which causes changes in the membrane structure (Cantley, 2002). The cytoskeletal functions regulated by PI3K are phagocytosis, migration, adhesion, and macropinocytosis. Due to these functions, PI3K is necessary for the invasion of several pathogens, such as *Pseudomonas aeruginosa*, *Neisseria gonorrhoeae*, and *E. coli* (Booth *et al.*, 2003; Kierbel *et al.*, 2005a;

Sukumaran *et al.*, 2002). The human herpes virus 8 (HHV8), the causative agent of Kaposi's sarcoma; a condition with similar etiology similar to that of verruga peruana, relies on PI3K for efficient cellular entry (Naranatt *et al.*, 2003). However, the role of PI3K in *B. bacilliformis* infection of endothelial cells remains unexplored. Because cytoskeletal regulation is heavily dependent on PI3K and required by several pathogens, we examine the effect of PI3K inhibition on *B. bacilliformis* invasion into endothelial cells.

Materials and Methods

HMEC-1 cell line growth and culturing.

The immortalized human microvascular endothelial cell line (HMEC-1) was a kind gift from Dr. Ades at the CDC, Atlanta (Ades EW *et al.*, 1992). HMEC-1 cells from passages 19–27 were grown in 15ml of growth media, consisting of 50% M199 (Cambrex), 15% FBS (Hyclone), 2% penicillin/streptomycin (Cellgro), and 50% EGM-2 (Cambrex). Cells were grown and maintained in T-75 flasks (Starstedt) at 37°C under 5% CO₂ and humid conditions. The media were changed every 2–3 days until 70-80% confluence was reached. The cells were maintained in 10ml of maintenance media (M199 + 15%FBS + 2% penicillin/streptomycin) between passages. For cell detachment, confluent cells were washed twice with PBS to remove all traces of serum, before adding 10mls/75²mm cell stripper (Cellgro). The cells were incubated at 37°C for 10 minutes and then gently scraped with cell scrapers (Starstedt). Detached cells were collected in 15ml Falcon tubes and centrifuged at 700xg for 10 minutes at 25°C. Cells were resuspended in 1ml maintenance media and enumerated microscopically using the hemocytometer, before seeding the T-25, T-75, and T-150 flasks or 6- or 24-well plates. Cells were allowed to adhere for 1 six hours before use.

To prepare frozen stocks, cell pellets were resuspended in the DMSO freeze medium (Cellgro) to obtain a final concentration of 1×10^5 cells/ml. The vials then were allowed to freeze at -80°C in a cryofreezing container (Nalgene) for 24 hours and transferred to a liquid N₂ tank facility.

Bacterial growth and culturing.

B. bacilliformis KC584 was obtained from ATCC (35686) and grown on brain heart infusion (BHI) plates supplemented with 10% sheep blood (BD Bioscience) at 26°C for 4–7 days. Low-passage bacteria (1–3 passages) were used in all experiments. When confluent colonies became visible, the plates were overlaid with 7mls of PBS. The bacteria were gently scraped off the plate with a loop. The bacterial suspension was centrifuged at 2000xg for 10 minutes at 25°C. Pellets were washed once with PBS and centrifuged again. The final suspension was in 1ml of BHI broth, unless otherwise noted.

Radio-labeling of *B. bacilliformis* with ³⁵S-methionine.

The method for radio-labeling is adapted from Williams-Bouyer et al (Williams-Bouyer *et al.*, 1999). *B. bacilliformis* was harvested and pelleted as described. Bacterial pellets were resuspended in 1ml methionine-free RPMI (Cellgro) containing 2% FBS and 0.2% sheep erythrocyte lysate. Radioactive, ³⁵S-methionine (Perkin-Elmer) was added to a final concentration of 50μCi/ml. *B. bacilliformis* was allowed to incorporate the radioactivity for one hour at 26°C, after which the bacteria were washed twice with PBS to remove unbound radioactivity. *B. bacilliformis* was resuspended in 1ml of PBS containing 10mM glucose. The number of bacteria was determined microscopically using a hemocytometer.

Kinase inhibitors.

The PD98059, SB203580, SP600125, and LY294002 all were purchased from Calbiochem. Wortmannin was supplied by Axxora chemicals and the U0126 by Cell Signaling Technologies. All compounds were dissolved in DMSO and diluted in M199 media containing 5% FCS. The concentrations used were 12.5μM, 25μM and 50μM,

75 μ M, and 100 μ M for PD98059, U0126, SB203580, and SP600125, respectively.

Wortmannin was diluted to 12.5nM, 25nM, 50nM, 100nM, and 250nM. The LY294002 concentrations used were 15 μ M, 30 μ M, 50 μ M, 75 μ M, 150 μ M, and 225 μ M. Dilutions were prepared in such a manner that the final DMSO concentration was less than 0.1%.

Adhesion and invasion assays.

HMEC-1 cells were seeded at a concentration of 1×10^6 cells/ml in 24-well plates containing maintenance media. The media were aspirated after the cells were allowed to adhere for 24 hours. Cells were washed three times with PBS. To the experimental wells, 500 μ l of media containing different concentrations of inhibitor was added. Media with DMSO also was added to control wells. Cells were incubated at 37°C under 5% CO₂ for one hour before the addition of radio-labeled *B. bacilliformis* at a m.o.i. of 1:100 m.o.i. in 100 μ l of PBS. Infection was allowed to proceed for six hours at 37°C with 5% CO₂. Unbound bacteria were removed by washing the cells four times with 1ml of PBS. Surface-bound bacteria and cells were detached with 500 μ l of 0.08% trypsin-EDTA. An equal volume of maintenance media then was added to neutralize the trypsin. The bacterial and cell mixture was collected and centrifuged at 700xg for 10 minutes to pellet the eukaryotic cells. The supernatant was aspirated and centrifuged at 2000xg for 10 minutes to collect *B. bacilliformis*. The HMEC-1 cell pellet was treated with 500 μ l of 1% Triton X100 to release internalized bacteria, then mixed with 5ml of Optima GoldXR scintillation fluid. Bacterial pellets were resuspended in 500 μ l of PBS before being added to the scintillation fluid. The volume of bacteria used to infect the cells also was added to 5ml of scintillation fluid to determine the amount of radioactivity added. Radioactivity was measured in a LS2500 scintillation counter. The percent

adhesion/invasion was calculated as follows: (DPM recovered/DPM added) \times 100. The percent adhesion/invasion results of the control experiments were normalized to 100, and the adhesion/invasion experimental values were calculated in relation to that normalized control. The percent inhibition was calculated as (normalized invasion -100). All experiments were performed in triplicate, and p-values were determined by Student's t-test.

Cell viability assay.

HMEC-1 cells were seeded at a concentration of 1×10^6 cells/ml in 24-well plates in maintenance media. Media were aspirated after the cells were allowed to adhere for 24 hours. Cells were washed three times with PBS. HMEC-1 cells were incubated for one hour with 50 μ M of LY29004 prior to infection with *B. bacilliformis* at a m.o.i. of 1:100. The three sets of controls consist of HMEC-1 cells, HMEC-1 cells with 50 μ M LY294002, and HMEC-1 cells with *B. bacilliformis*. Plates were incubated at 37 $^{\circ}$ C in a 5% CO₂ incubator. The cells were processed for enumeration for two hours, six hours, and 24 hours post infection. The unbound bacteria were removed by washing the cells three times with PBS. Cells were incubated with 0.08% trypsin-EDTA to detach the cells, and the tubes were centrifuged at 700 \times g for 10 minutes to pellet the cells. Cells were resuspended in 50 μ l of PBS and stained with the same volume of trypan blue dye. Cell enumeration was performed microscopically using a hemocytometer. Only viable cells that did not take up trypan blue dye were counted. The percentage of viable cells was calculated as (treated cells/untreated cells) \times 100.

Fluorometric detection of apoptosis.

Cell viability assays were set up as written previously. At two hours, six hours, and 24 hours post infection, the supernatant from all the wells was collected, and adherent cells were subjected to trypsin treatment. The supernatant and detached cells were pooled and spun down at 700xg for 10 minutes. The cell pellets were washed three times with 500 μ l of PBS. The cells were resuspended in 100 μ l of 1X binding buffer from the AnnexinV Apoptosis Kit (BD Biosciences). Cells were incubated with 5 μ l of 7AAD (7-Amino actinomycin D) dye for 15 minutes in the dark at room temperature, then concentrated by centrifugation at 700xg for five minutes. Cells were resuspended in 10 μ l of 1X binding buffer, and the entire volume was placed on glass slides for microscopic examination. The cells were observed under white light, and the same field was examined for apoptosis using fluorescent filters on the Axioplane microscope (Zeiss). Apoptosis was visually observed in cells that were stained red under the fluorescent filters.

Results

Effect of MEK1/2 inhibitors on *B. bacilliformis* invasion into endothelial cells

MEK1/2 is one of many cell signal molecules that are a part of the extracellular signaling pathway. These kinases regulate cell growth and differentiation regulators and can be activated by membrane depolarization, growth factors, cytokines, and calcium influx (Alessi *et al.*, 1994; Crews *et al.*, 1992; Rosen *et al.*, 1994). In addition to the functions mentioned, MEK1/2 is also implicated in bacterial uptake by host cells. The MEK inhibitors PD98059 and U0126 were used to determine whether MEK1/2 is involved in *B. bacilliformis* internalization by endothelial cells. Semi-confluent HMEC-1 cells in 24 wells were treated with different dilutions of MEK inhibitors for one hour of MEK inhibitors. Media with 5% FCS and 0.1% DMSO were used as vehicle controls. Pretreated cells were infected with radio-labeled *B. bacilliformis* at a m.o.i. of 1:100. for six hours. Infected cells were processed to recover externally bound and internalized bacteria. Results presented in figures 2.1a, 2.1b and tables 2.1a and 2.1b show that both the compounds caused a decrease in *B. bacilliformis* uptake in a dose-dependent manner. With PD9805809, the maximal degree of inhibition (41%) was achieved at 100 μ M inhibitor concentration (Figure 2.1a and table 2.1a). However, it took only 50 μ M of inhibitor to obtain this level of reduction when the inhibitor was U0126 (Figure 2.1b and table 2.1b). At higher concentrations of U0126, the uptake was inhibited even more and reached 81% at 100 μ M. *B. bacilliformis* uptake was not affected in assays with DMSO alone (Figure 2.1b and table 2.1b). Bacterial attachment was not compromised by inhibitors or DMSO. All results were statistically significant with p-values of <0.05. On the basis of these studies, we conclude that MEK1/2 is required for optimal entry of *B.*

bacilliformis into host cells. Because internalization was not completely abrogated, additional factors may be required as well.

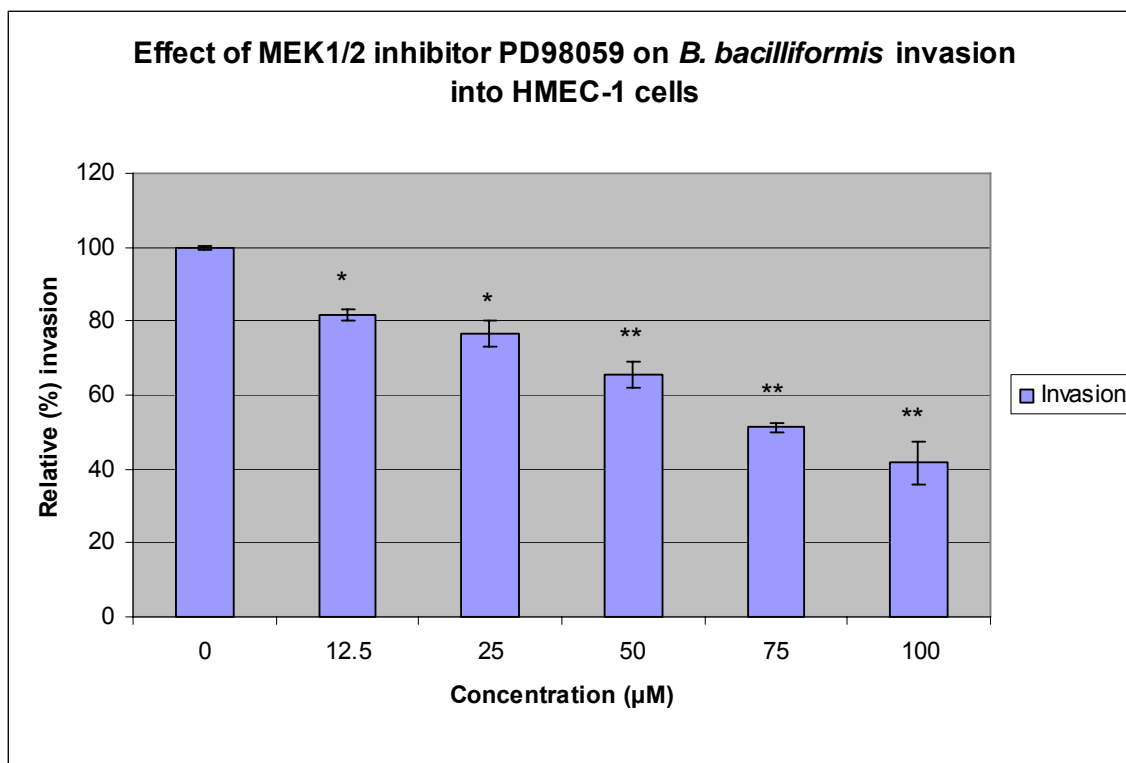


Figure 2.1a. Effect of MEK1/2 inhibitors PD98059 on *B. bacilliformis* invasion into HMEC-1 cells.

HMEC-1 cells were grown in 24-well plates and infected with ^{35}S -methionine labeled *B. bacilliformis* at a m.o.i. of 1:100 in the presence of various PD98059 concentrations. Control infections were performed with DMSO concentrations to dissolve the inhibitor. Cell supernatants were collected six hours post infection, after treatment with 0.08% trypsin. Cell pellets obtained by centrifugation were lysed in 1% Triton X100 and then resuspended in liquid scintillation fluid. The radioactivity recovered indicates the number of externally bound bacteria. Percent invasion was calculated as (recovered DPM/added DPM) \times 100. The percent invasion from the control experiments was set to 100, and percent invasion of the treated samples was calculated in relation to this standard 100%. The X-axis denotes the concentration of inhibitor (μM) used; the Y-axis shows the relative percent invasion. The numbers are the average of three replicates, and error bars represent the SEM. The p-value was obtained by Student's t-test, such that p-values (*) \leq 0.05 and (**) \leq 0.01 are considered significant.

Table 2.1a. Effect of MEK inhibitor PD98059 on *B. bacilliformis* invasion into endothelial cells.

HMEC-1 cells were infected with ^{35}S -methionine labeled *B. bacilliformis* for six hours in the presence of PD98059 or DMSO dissolved in M199 media with 5% serum. Percent invasion and percent inhibition values are the means, \pm SEM, of three experiments. Invasion values were calculated as (recovered DPM/added DPM) \times 100, set to 100 for untreated samples. Percent invasion from treated samples was calculated in relation to 100% invasion in untreated samples. Percent inhibition was calculated as (normalized invasion – 100). Student t-test was performed with data from treated and untreated samples; p-values of <0.05 are considered significant, and NA indicates not applicable.

Concentration (μM)	Percent Invasion	Percent Inhibition	p-Value
0	100 \pm 0.52	NA	NA
12.5	81.50 \pm 1.57	18.58 \pm 1.57	0.035
25	76.56 \pm 3.57	23.04 \pm 3.57	0.026
50	65.49 \pm 3.67	34.33 \pm 3.67	0.004
75	51.23 \pm 1.34	48.18 \pm 1.34	0.002
100	41.63 \pm 5.96	59.00 \pm 5.96	0.002

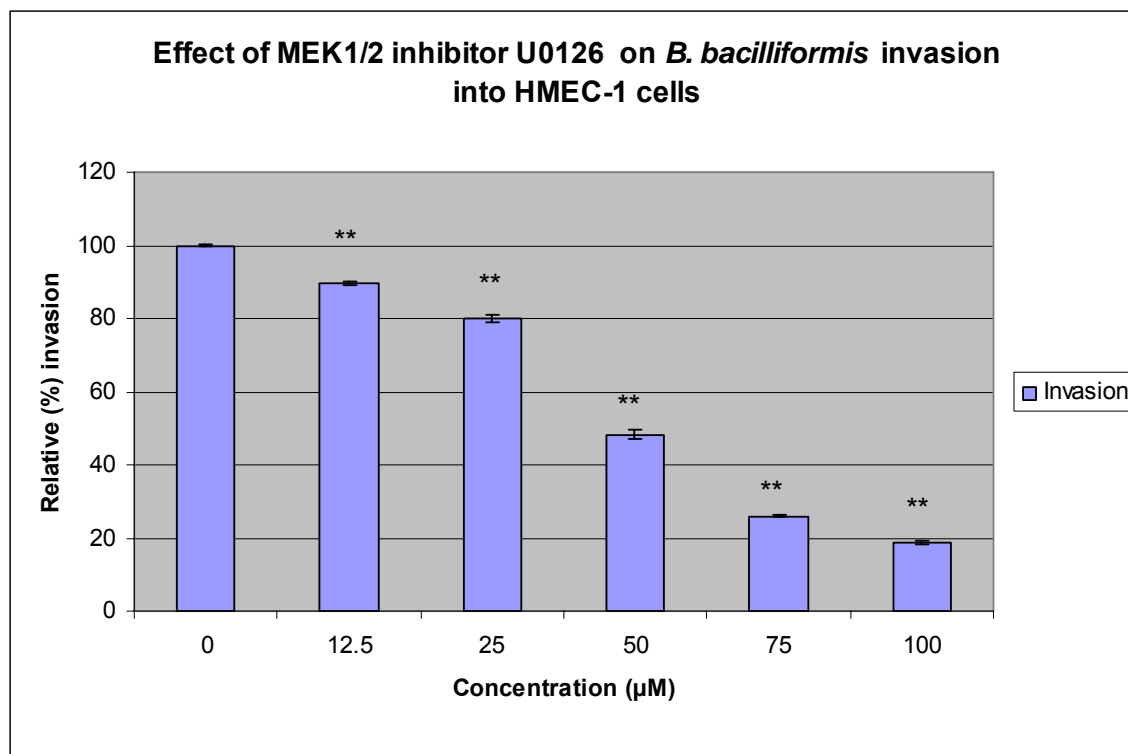


Figure 2.1b. Effect of MEK1/2 inhibitor U0126 on *B. bacilliformis* invasion into HMEC-1 cells.

HMEC-1 cells were grown in 24-well plates and infected with ^{35}S -methionine labeled *B. bacilliformis* at a m.o.i. of 1:100 in the presence of various U0126 concentrations. Control infections were performed with DMSO concentrations used to dissolve the inhibitor. Cell supernatants were collected six hours post infection, after treatment with 0.08% trypsin. Cell pellets obtained by centrifugation were lysed in 1% Triton X100 and then resuspended in liquid scintillation fluid. The radioactivity recovered indicates the number of externally bound bacteria. Percent invasion was calculated as (recovered DPM/added DPM) \times 100. The percent invasion from the control experiments was set to 100, and the percent invasion of the treated samples was calculated in relation to 100%. The X-axis denotes the concentration of U0126 (μM) used, whereas the relative percent invasion is plotted on the Y-axis. The numbers are the average of three replicates, and error bars represent the SEM. The p-value was obtained by Student's t-test, such that p-values (**) \leq 0.01 are considered significant.

Table 2.1b. Effect of MEK inhibitor U0126 on *B. bacilliformis* invasion into HMEC-1 cells.

HMEC-1 cells were infected with ^{35}S -methionine labeled *B. bacilliformis* for six hours in the presence of increasing concentrations of U0126 or 0.1% DMSO in M199 with 5% FCS. Percent invasion and percent inhibition values are the means, \pm SEM, of three experiments. Invasion values were calculated as (recovered DPM/added DPM) \times 100 and set to 100 for untreated samples. Percent invasion from treated samples was calculated in relation to the 100% invasion in untreated samples; percent inhibition is (normalized invasion – 100). Student's t-test, performed with data from treated and untreated samples, provides p-values, and those <0.05 were considered significant. NA indicates not applicable.

Concentration (μM)	Percent Invasion	Percent Inhibition	p-Value
0	100 \pm 0.14	NA	NA
12.5	89.54 \pm 0.59	10.46 \pm 0.59	0.005
25	80.04 \pm 1.06	19.96 \pm 1.06	0.0008
50	48.22 \pm 1.28	51.78 \pm 1.28	0.0007
75	26.06 \pm 0.43	73.94 \pm 0.43	0.0003
100	18.85 \pm 0.62	81.15 \pm 0.62	0.0003

Effect of p38 kinase inhibitor on *B. bacilliformis* invasion into HMEC-1 cells

The p38 kinase belongs to the stress response signaling pathway and is activated by numerous factors, such as LPS, inflammatory cytokines, and growth factors (Han *et al.*, 1994; Raingeaud *et al.*, 1995). Its role in uptake of certain bacteria also has been demonstrated. A highly specific inhibitor of p38 kinase, SB203580 also suppresses MAPKAP kinase-2 (mitogen activated protein kinase-activated protein kinase2) and Hsp-27 activation in response to IL-2, stress factors, and bacterial endotoxin (Cuenda *et al.*, 1995). Concentrations of SB203580 ranging from 12.5 μ M to 100 μ M were used to treat monolayers before the addition of *B. bacilliformis*. Bacterial uptake was determined after six hours of infection by the method previously described. An inhibitor concentration-dependent decrease in *B. bacilliformis* ingestion was observed (Figure 2.2 and table 2.2). Bacterial uptake was significantly inhibited by 26.3% at 50 μ M and 40.7% at 100 μ M (Figure 2.2 and table 2.2). Bacterial adhesion to cell surfaces was not affected at any point. Control experiments with 0.1% DMSO had no effect on *B. bacilliformis* adhesion or invasion. These observations suggest that a p38 kinase pathway is required for optimal *B. bacilliformis* ingestion by HMEC-1 cells.

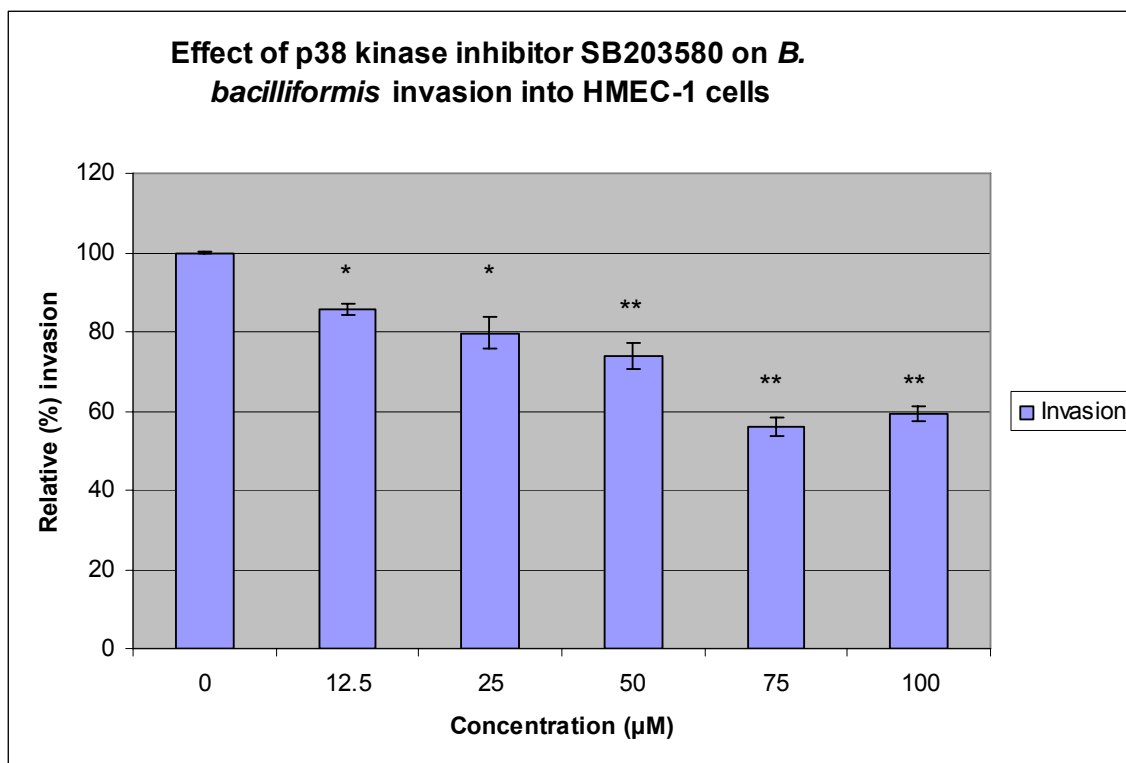


Figure 2.2. Effect of p38 kinase inhibitor SB203580 on *B. bacilliformis* invasion into HMEC-1 cells.

HMEC-1 cells were grown in 24-well plates and infected with ^{35}S -methionine labeled *B. bacilliformis* at a m.o.i. of 1:100 in the presence of various SB203580 concentrations. Control infections were performed with DMSO concentrations, used to dissolve the inhibitor. Cell supernatants were collected six hours post infection, after treatment with 0.08% trypsin. Cell pellets obtained by centrifugation were lysed in 1% Triton X100 and then resuspended in liquid scintillation fluid. The radioactivity recovered indicates the number of externally bound bacteria. Percent invasion was calculated as (recovered DPM/added DPM) \times 100, with percent invasion from the control experiments set to 100 and that of the treated samples calculated in relation to 100%. The X-axis denotes the concentration of SB203580 (μM) used, and the relative percent invasion is plotted on the Y-axis. The numbers reflect the average of three replicates, and error bars represent the SEM. The p-value was obtained by Student's t-test, such that p-values (*) \leq 0.05 and (**) \leq 0.01 are considered significant.

Table 2.2. Effect of p38 kinase inhibitor, SB203580 on *B. bacilliformis* invasion into HMEC-1 cells.

HMEC-1 cells were infected with ^{35}S -methionine labeled *B. bacilliformis* for six hours in the presence of SB203580 or DMSO dissolved in M199 media with 5% serum. Percent invasion and percent inhibition values are the means, \pm SEM, of three experiments. Invasion values were calculated as (recovered DPM/added DPM) \times 100 and set to 100 for untreated samples. The percent invasion from treated samples was calculated in relation to the 100% invasion in untreated samples, whereas percent inhibition equals (normalized invasion – 100). Student's t-tests performed with data from treated and untreated samples suggests p-values <0.05 are significant. NA indicates not applicable.

Concentration (μM)	Percent invasion	Percent inhibition	p-Value
0	100 \pm 0.3	NA	NA
12.5	85.66 \pm 1.58	14.26 \pm 1.58	0.02
25	79.75 \pm 4.02	20.97 \pm 2.20	0.015
50	73.72 \pm 3.28	26.26 \pm 0.37	0.002
75	55.98 \pm 2.41	43.98 \pm 0.71	0.002
100	59.23 \pm 1.88	40.7 \pm 1.24	0.002

Effect of JNK1/2/3 kinase inhibitor on *B. bacilliformis* invasion into HMEC-1 cells

Stress-activated protein kinase/Jun amino terminal kinase (SAPK/JNK) is potently and preferentially stimulated by cellular stress factors. This kinase is activated early during *B. bacilliformis* infection. However, the role of SAPK/JNK during *B. bacilliformis* uptake remains unresolved. A potent yet reversible inhibitor of JNK, SP600125 was used to block JNK phosphorylation. HMEC-1 cells were infected with *B. bacilliformis* for six hours in the presence of various SP600125 dilutions. At the end of the infection, intracellular bacteria were recovered from lysed cells, and radioactivity was measured.

Inhibition of JNK decreased *B. bacilliformis* internalization by HMEC-1 cells, depending on the inhibitor concentration. As seen in figure 2.3 and table 2.3, bacterial invasion decreased from 76.6% at 12.5 μ M to 52.71% at 75 μ M of SP600125. However, the inhibitor did not affect the adhesion of *B. bacilliformis* to the cell surface. No change in invasion or adhesion was recorded in experiments carried out in the presence of 0.1% DMSO, the control drug vehicle used to dissolve SP600125. Therefore, JNK phosphorylation appears to play a role in *B. bacilliformis* penetration into HMEC-1 cells.

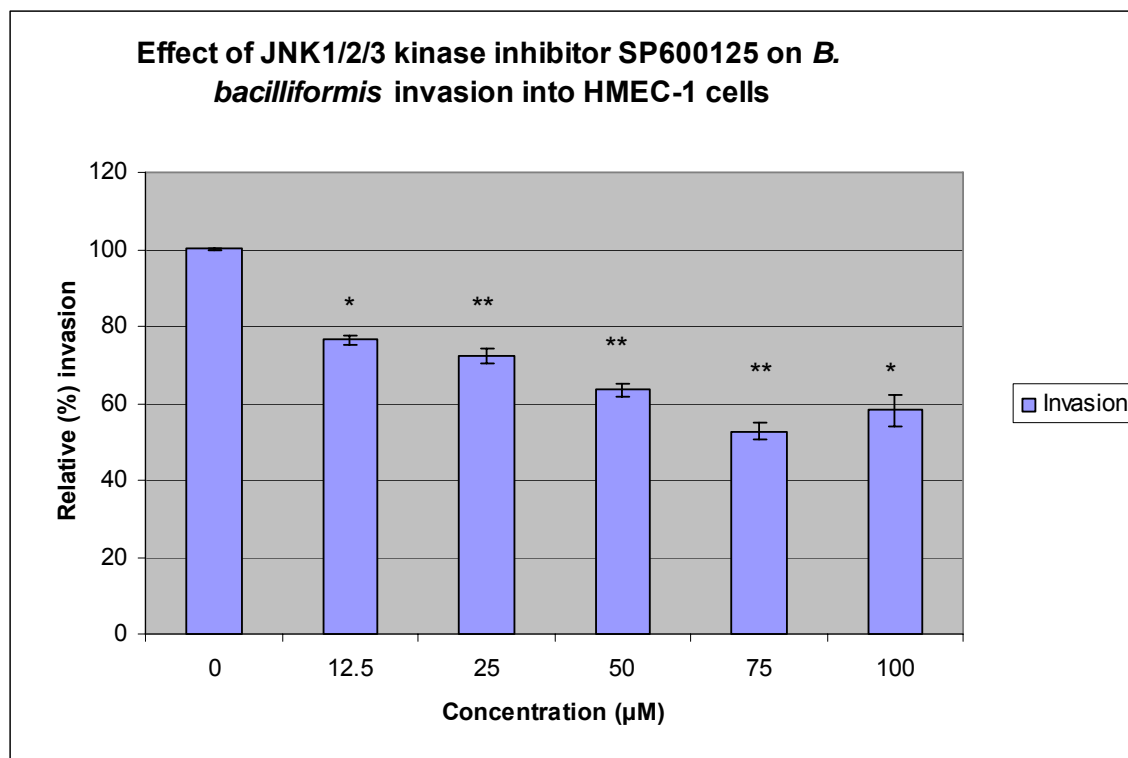


Figure 2.3. Effect of JNK1/2/3 inhibitor SP600125 on *B. bacilliformis* invasion into HMEC-1 cells.

HMEC-1 cells were grown in 24-well plates and infected with ^{35}S -methionine labeled *B. bacilliformis* at a m.o.i. of 1:100 in the presence of various SP00125 concentrations. Control infections were performed with the DMSO concentrations used to dissolve the inhibitor. Cell supernatants were collected six hours post infection, after treatment with 0.08% trypsin. Cell pellets obtained by centrifugation were lysed in 1% Triton X100 and then resuspended in liquid scintillation fluid. The radioactivity recovered indicates the number of externally bound bacteria. Percent invasion, calculated as $(\text{recovered DPM}/\text{added DPM}) \times 100$, is set to 100 for the control experiments; the percent invasion of the treated samples was calculated in relation to this 100% level. Whereas the X-axis denotes the concentration of SP600125 (μM) used, the Y-axis reveals the relative percent invasion. The numbers indicate the average of three replicates; error bars represent the SEM. The p-value was obtained by Student's t-test, such that p-values (*) ≤ 0.05 and (**) ≤ 0.01 are considered significant.

Table 2.3. Effect of JNK inhibitor SP600125 on *B. bacilliformis* invasion into HMEC-1 cells.

HMEC-1 cells were infected with ^{35}S -methionine labeled *B. bacilliformis* for six hours in the presence of SP600125 or DMSO dissolved in M199 media with 5% serum. Percent invasion and percent inhibition values are the means, \pm SEM, of three experiments. Invasion values were calculated as (recovered DPM/added DPM) \times 100 and set to 100 for untreated samples. Percent invasion from treated samples was calculated in relation to the 100% invasion in untreated samples, whereas percent inhibition was calculated as (normalized invasion – 100). The Student's t-test was performed with data from treated and untreated samples. A p-value \leq 0.05 was considered significant, and NA means not applicable.

Concentration (μM)	Percent Invasion	Percent Inhibition	p-Value
0	100 \pm 0.39	NA	NA
12.5	76.6 \pm 1.2	23.31 \pm 1.2	0.012
25	72.41 \pm 1.88	27.44 \pm 1.88	0.007
50	63.42 \pm 1.83	36.46 \pm 1.83	0.003
75	52.71 \pm 2.16	47.09 \pm 2.16	0.005
100	58.15 \pm 4.13	40.05 \pm 4.13	0.05

Effect of PI3K inhibition on *B. bacilliformis* invasion into HMEC-1 cells

Phosphoinositide 3 kinase (PI3K) is an integral part of the signal cascades involved in diverse cellular functions. These functions range from cell growth and survival to intracellular trafficking of molecules. Various pathogens employ PI3K for translocation into host cells. The role of PI3K in *B. bacilliformis* invasion into endothelial cells was determined by using the specific inhibitors wortmannin and LY294002. Both inhibitors are specific for PI3K and have been used in previous studies. The HMEC-1 cells were incubated for one hour with different concentrations of wortmannin or LY294002. *B. bacilliformis* then were allowed to infect the cells in the presence of these compounds. The cells were processed to recover intracellular bacteria after six hours of infection. The radioactivity of the radio-labeled intracellular *B. bacilliformis* was measured with a liquid scintillation counter, which revealed that PI3K inhibition had a dramatic effect on *B. bacilliformis* internalization. Although, no change in invasion was recorded at 12.5 and 25nM of wortmannin a gradual decrease in the number of intracellular bacteria recovered occurred at concentrations greater than 25nM (Figure 2.4a and table 2.4a). The maximal effect on invasion took place at 250nM, at which point only 35% of intracellular bacteria were recovered (Figure 2.4a and table 2.4a). Low concentrations of LY294002—15 μ M and 30 μ M—also inhibited invasion by 41% and 44%, respectively (Figure 2.4b and table 2.4b). *B. bacilliformis* attachment to external cell surfaces was not affected by the inhibitors, whereas invasion and adhesion remained unaffected in the presence of 0.1% DMSO control assays. These studies demonstrate the need for PI3K during *B. bacilliformis* invasion into endothelial cells.

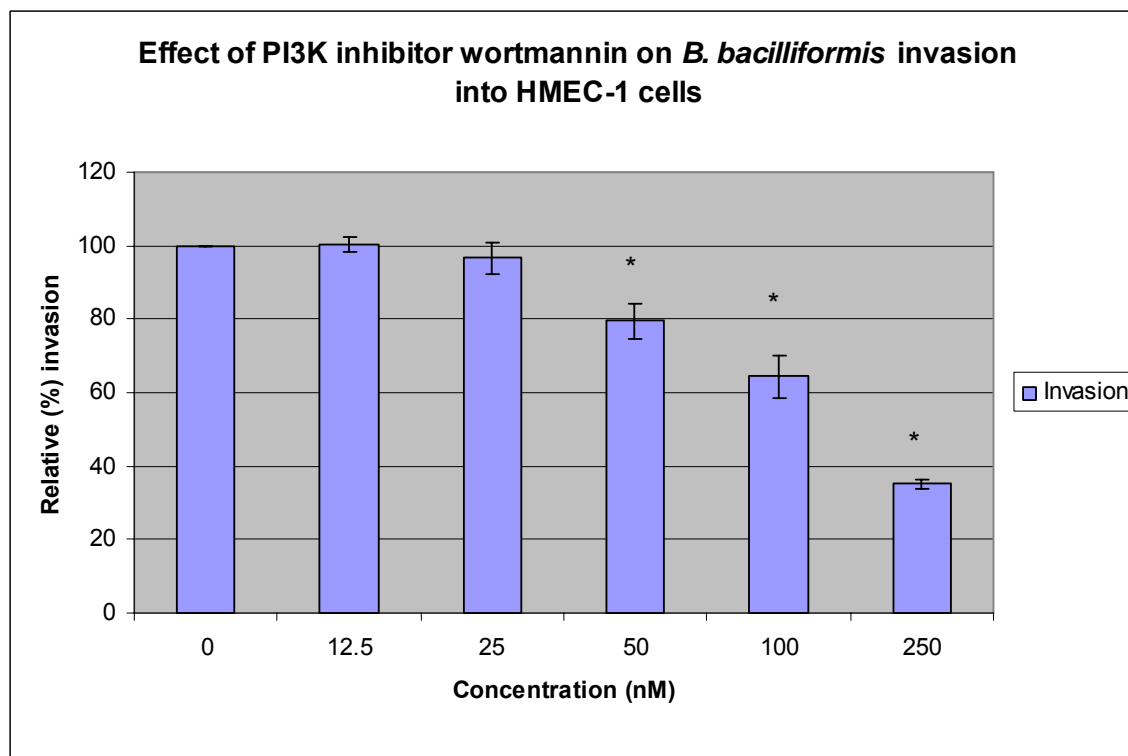


Figure 2.4a. Effect of PI3K inhibitor wortmannin on *B. bacilliformis* invasion into HMEC-1 cells.

HMEC-1 cells were grown in 24-well plates and infected with ^{35}S -methionine labeled *B. bacilliformis* at a m.o.i. of 1:100 in the presence of various wortmannin concentrations. Control infections were performed with DMSO concentrations, used to dissolve the inhibitor. Cell supernatants were collected six hours post infection, after treatment with 0.08% trypsin. Cell pellets obtained by centrifugation were lysed in 1% Triton X100 and then resuspended in liquid scintillation fluid. The radioactivity recovered indicates the number of externally bound bacteria. Percent invasion was calculated as (recovered DPM/added DPM) \times 100. The percent invasion from the control experiments was set to 100, and the percent invasion of the treated samples was calculated in relation to 100%. The X-axis denotes the concentration of wortmannin (nM) used; the Y-axis displays the relative percent invasion. The numbers equal the average of three replicates, and error bars represent the SEM. The p-value was obtained by Student's t-test, such that p-values (*) \leq 0.05 is considered significant.

Table 2.4a. Effect of PI3K inhibitor wortmannin on *B. bacilliformis* invasion into HMEC-1 cells.

HMEC-1 cells were infected with ^{35}S -methionine labeled *B. bacilliformis* for six hours in the presence of wortmannin or DMSO dissolved in M199 media with 5% serum. Percent invasion and percent inhibition values are the means, \pm SEM, of three experiments. Invasion values, calculated as (recovered DPM/added DPM) \times 100, were set to 100 for untreated samples; the percent invasion from treated samples then was calculated in relation to the 100% invasion in untreated samples. Percent inhibition was calculated as (normalized invasion – 100). Student's t-tests were performed with data from treated and untreated samples. The p-value <0.05 was considered significant, and NA indicates not applicable.

Concentration (μM)	Percent Invasion	Percent Inhibition	p-Value
0	100 \pm 0.04	NA	NA
12.5	100.44 \pm 2.10	0.44 \pm 2.10	0.4
25	96.59 \pm 4.10	3.41 \pm 4.10	0.2
50	79.55 \pm 4.77	20.45 \pm 4.77	0.02
100	64.37 \pm 5.90	35.63 \pm 5.90	0.03
250	35.10 \pm 0.03	61.90 \pm 3.75	0.012

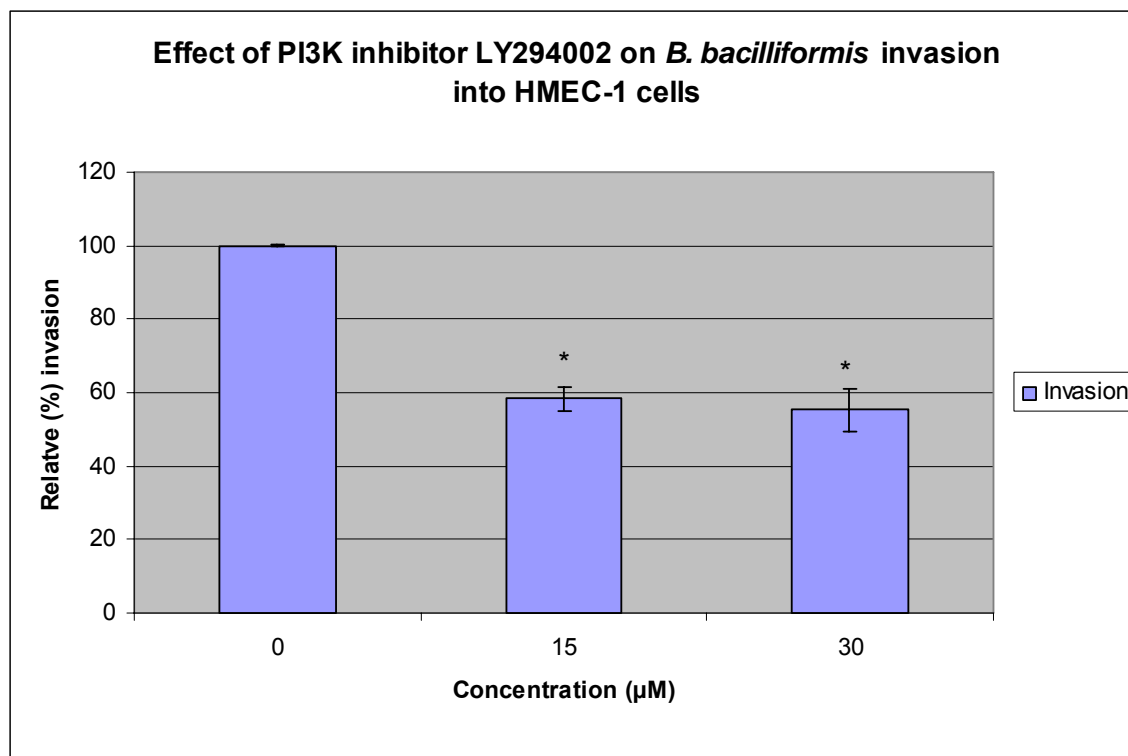


Figure 2.4b. Effect of PI3K inhibitor LY294002 on *B. bacilliformis* invasion into HMEC-1 cells.

HMEC-1 cells were grown in 24-well plates and infected with ^{35}S -methionine labeled *B. bacilliformis* at a m.o.i. of 1:100 in the presence of various LY294002 concentrations. Control infections were performed with DMSO concentrations that dissolve the inhibitor. Cell supernatants were collected six hours post infection, after treatment with 0.08% trypsin. Cell pellets obtained by centrifugation were lysed in 1% Triton X100 and resuspended in liquid scintillation fluid. The radioactivity recovered reveals the number of externally bound bacteria. Percent invasion was calculated as $(\text{recovered DPM}/\text{added DPM}) \times 100$. The percent invasion from the control experiments was set to 100, and the percent invasion of the treated samples was calculated in relation to this 100% level. The X-axis denotes the concentration of LY294002 (μM) used. The relative percent invasion is plotted on the Y-axis. These numbers average three replicates. Error bars represent the SEM. The p-value was obtained by Student's t-test, such that p-values (*) ≤ 0.05 is considered significant.

Table 2.4b. Effect of PI3K inhibitor LY294002 on *B. bacilliformis* invasion into HMEC-1 cells.

HMEC-1 cells were infected with ^{35}S -methionine labeled *B. bacilliformis* for six hours in the presence of LY294002 or DMSO dissolved in M199 media with 5% serum. Percent invasion and percent inhibition values equal the means, \pm SEM, of three experiments. Invasion values were calculated as (recovered DPM/added DPM) \times 100, set to 100 for untreated samples. Percent invasion from treated samples was calculated in relation to the 100% invasion in untreated samples. Percent inhibition was calculated as (normalized invasion – 100). Using data from treated and untreated samples, Student's t-tests demonstrate significance at p-values <0.05 . NA is not applicable.

Concentration (μM)	Percent Invasion	Percent Inhibition	p-Value
0	100 \pm 0.32	NA	NA
15	58.28 \pm 3.0	41.72 \pm 3.20	0.045
30	55.36 \pm 5.86	44.64 \pm 5.86	0.015

Effect of PI3K inhibition on viability of *B. bacilliformis* infected HMEC-1 cells

PI3K plays an extremely important role in cell survival by inactivating pro-apoptotic factors. At concentrations greater than 50 μ M, LY294002 inhibited *B. bacilliformis* invasion by 61% (data not shown). However, this effect was due to cell death that leads to cell detachment. Therefore to understand the function of PI3K in cell attachment and survival, the cell viability of infected cells was examined in the presence of 50 μ M LY294002. HMEC-1 cells were incubated with 50 μ M of LY294002 in the presence or absence (control) of *B. bacilliformis*. Control wells consisted of untreated HMEC-1 cells and *B. bacilliformis*-infected cells without the inhibitor. At two, six, and 24 hours, cells were washed thoroughly and detached with a mild trypsin treatment. Cells were stained with trypan blue to enable differentiation between unstained live cells and blue dead cells. Viable cells were scored microscopically, and the percentage of viable cells was calculated with respect to the appropriate controls as described in the materials and method section. As figure 2.5a shows, inhibition of PI3K affects the viability of both uninfected and infected cells, but the detrimental effects of the PI3K inhibitor are more pronounced in the presence of *B. bacilliformis*. The number of viable LY294002-treated cells decreases by 25% after two hours of bacterial infection, and by 81%, six hours post infection (Figure 2.5a and table 2.5). Control cells that received only LY294002 retained 85% and 79% viable cells after two and six hours of incubation, respectively. By 24 hours, no surviving cells were recovered from wells containing HMEC-1, inhibitor, and *B. bacilliformis*, whereas 58% of uninfected cells remained viable at that point (Figure 2.5a and table 2.5). Cell viability remains unaffected in the absence of the inhibitor.

Cell death was also examined with 7AAD fluorescent dye, a DNA stain that permeates only compromised membranes of dead cells. The stained cells that took up the dye were viewed under a fluorescence microscope, which revealed that the number of fluorescent cells increased with time. At two hour post infection, no apoptotic cells were detected in cell treated with LY294002 in the presence or absence *B. bacilliformis* (Figure 2.5b and 2.5c). The increase in the number of dead cells infected with *B. bacilliformis*, in the presence of inhibitor is much more dramatic at six and 24 hours post infection (Figure 2.5e and 2.5g), whereas uninfected cells (with LY294002) did not undergo cell death at these times points (Figure 2.5d and 2.5f) These results strongly support the hypothesis that *B. bacilliformis*-induced cell survival depends on the PI3K pathway.

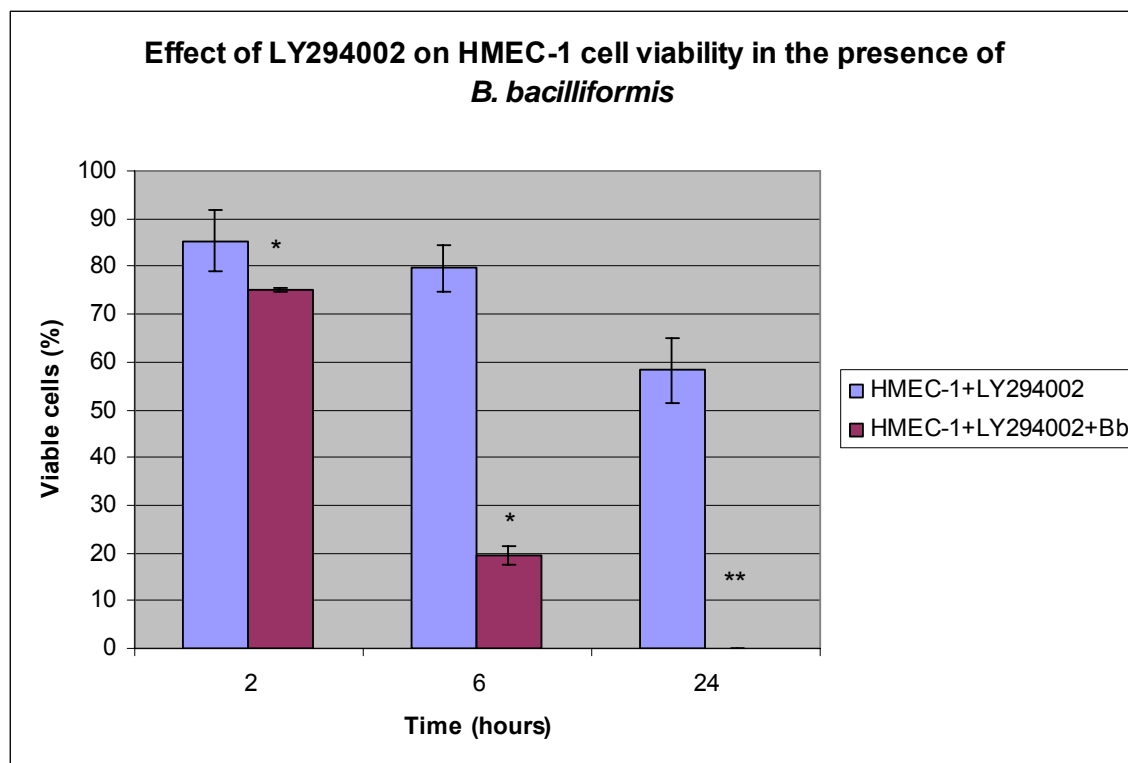


Figure 2.5a. Effect of LY294002 on HMEC-1 cells infected with *B. bacilliformis*.

HMEC-1 cells were infected with *B. bacilliformis* in the presence of 50 μ M of LY294002. Another set of experimental wells contained HMEC-1 and 50 μ M of LY294002. Wells that contained HMEC-1 cells serve as the controls for this set of experiments. At two, six, and 24 hours post infection, the cells were washed to remove unbound bacteria and detached cells. The adherent cells were trypsinized with 0.08% trypsin-EDTA for 10 minutes, then cells were centrifuged at 700xg, and the pellet was resuspended in 50 μ l of PBS and 50 μ l of trypan blue. The tubes were incubated for 10 minutes; cells then were enumerated microscopically using a hemocytometer. The percentage of viable cells was calculated with respect to the controls. The X-axis in the figure denotes the time in hours, whereas the Y-axis plots the percentage of viable cells. The numbers indicate the average of three replicates; error bars represent the SEM. The p-value was obtained by Student's t-test, such that p-values (*) ≤ 0.05 and (**) ≤ 0.01 are considered significant.

Table 2.5. Effect of PI3K inhibitor LY294002 on the viability of infected HMEC-1 cells.

HMEC-1 cells in the presence of M199 media with 5% serum containing 50 μ M LY294002 were infected with *B. bacilliformis* (Bb) for two, six, and 24 hours. Control wells received only bacteria. HMEC-1 alone or with 50 μ M LY294002 were used to determine the effect of the inhibitor on uninfected cells. Viable cell values are the means, \pm SEM, of three experiments. Invasion values were calculated as (untreated cells/treated cells) \times 100.

Condition	Viable Cell (%)			
	Time in hours	2	6	24
HMEC-1+LY294002		85.38 \pm 6.30	79.67 \pm 4.85	58.24 \pm 6.94
HMEC-1+LY294002+Bb		75.15 \pm 0.3	19.48 \pm 1.78	0.00 \pm 0.00

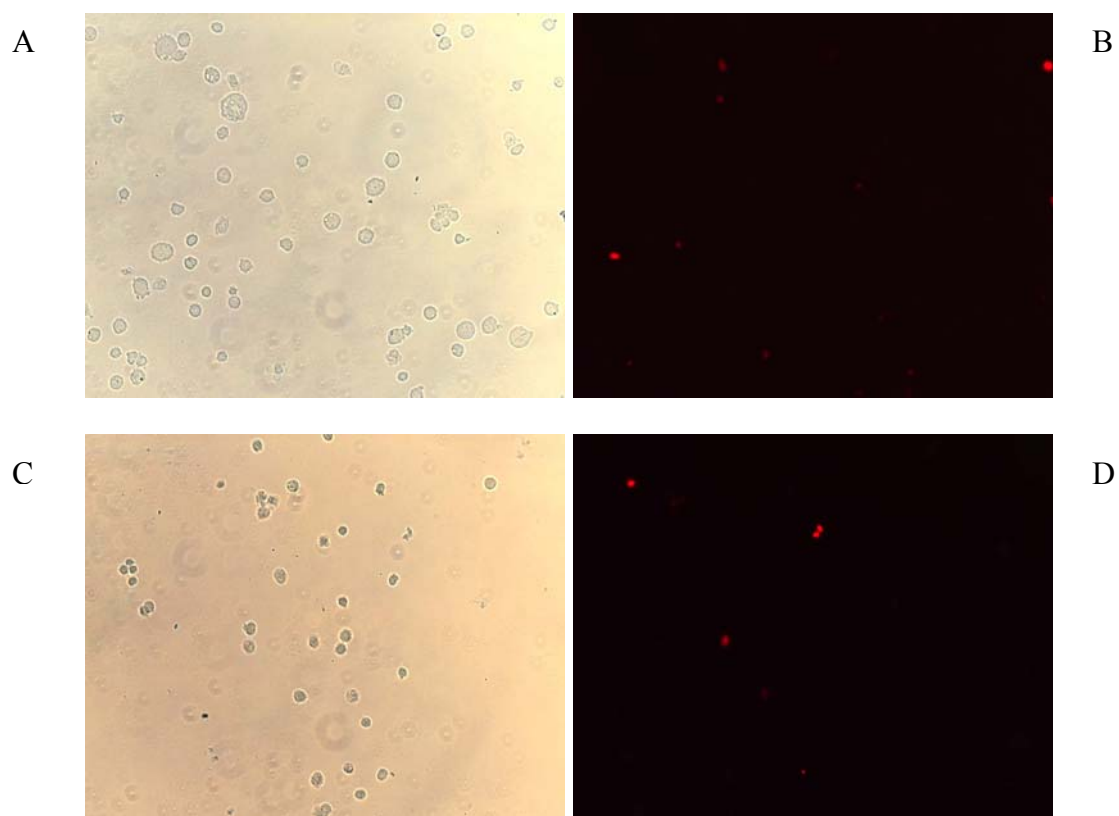


Figure 2.5b. Effect of PI3K inhibitor, LY294002, on endothelial cell viability, two hours post-infection.

HMEC-1 cells were incubated with 50 μ M of LY294002 for two hours. Control cells were left untreated. Cells were washed and detached with 0.08% trypsin-EDTA, then stained with fluorescent dye 7AAD and examined under the microscope. Panels A and B display untreated HMEC-1 cells, as seen under light and fluorescent filters, respectively. Panels C and D depict LY294002-treated HMEC-1 cells, again as seen under light and fluorescent filters, respectively.

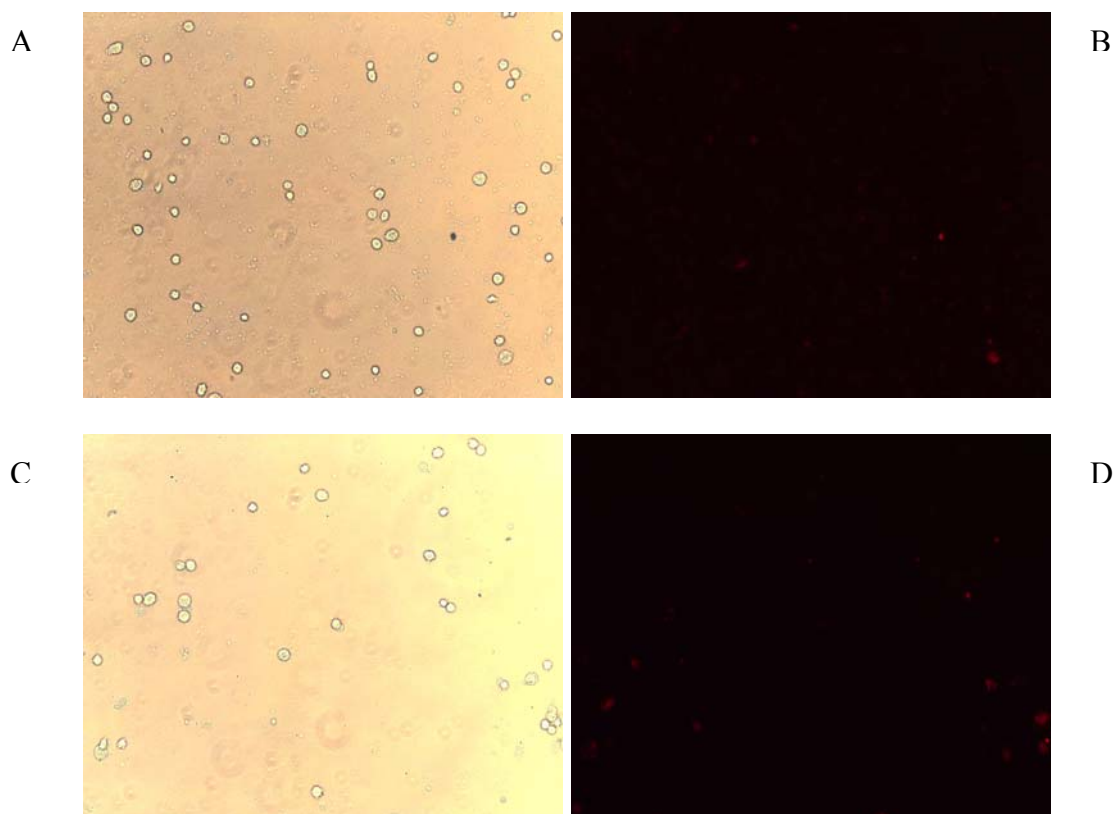


Figure 2.5c. Effect of PI3K inhibitor, LY294002, on B. bacilliformis-infected endothelial cell viability, two hours post-infection.

HMEC-1 cells were incubated with 50 μ M of LY294002 for two hours. Control cells were left untreated. Cells were washed and detached with 0.08% trypsin-EDTA, then stained with fluorescent dye 7AAD and examined under the microscope. Panels A and B reveal *B. bacilliformis*-infected HMEC-1 cells under light and fluorescent filters, respectively. Panels C and D show LY294002-treated, *B. bacilliformis*-infected HMEC-1 cells under light and fluorescent filters, respectively.

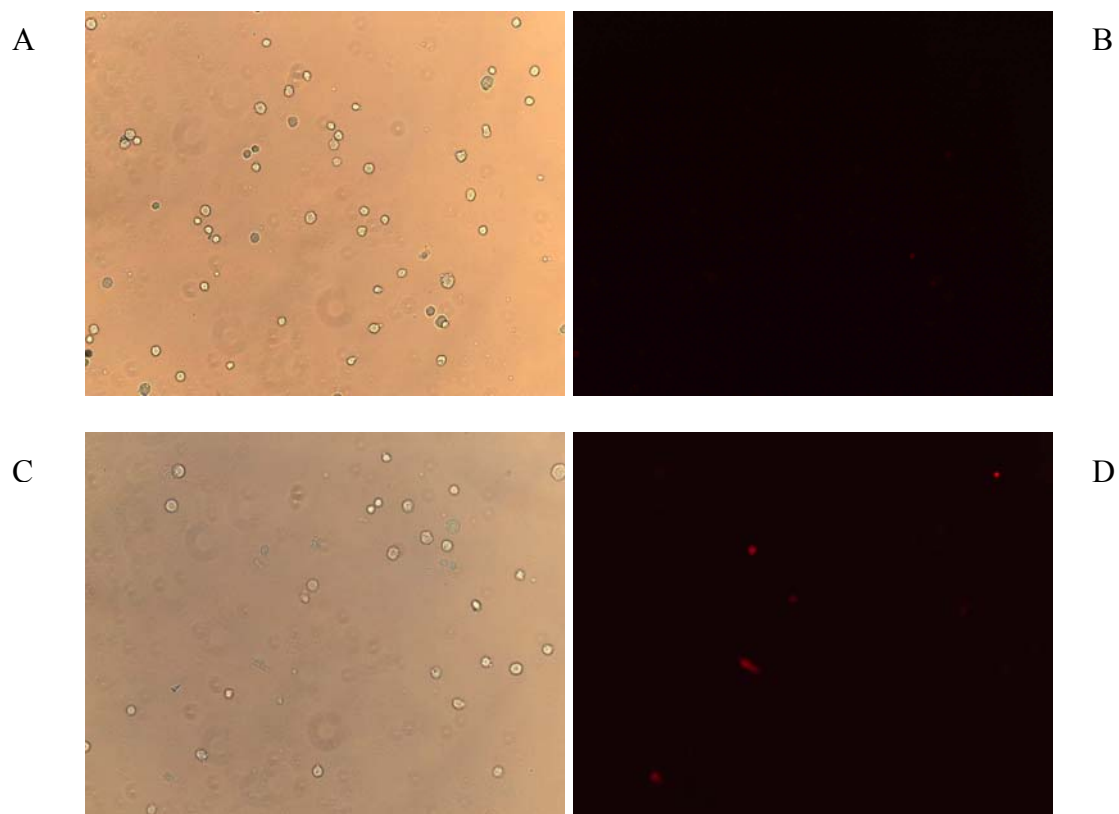


Figure 2.5d. Effect of PI3K inhibitor, LY294002, on endothelial cell viability, six hours post-infection.

HMEC-1 cells were incubated with 50 μ M of LY294002 for six hours. Whereas the control cells were left untreated, other cells were washed and detached with 0.08% trypsin-EDTA, then stained with fluorescent dye 7AAD and examined under the microscope. Panels A and B show untreated HMEC-1 cells under light and fluorescent filters, respectively. Panels C and D depict LY294002-treated HMEC-1 cells, again under light and fluorescent filters.

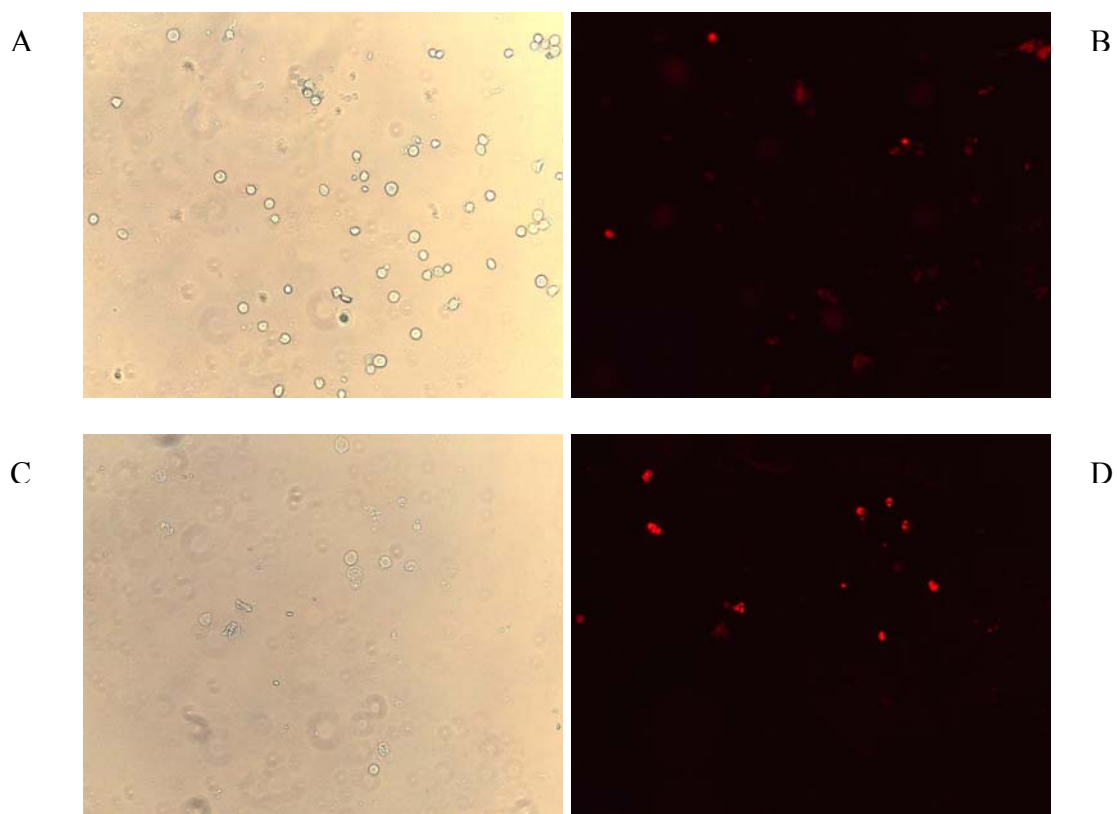


Figure 2.5e. Effect of PI3K inhibitor, LY294002, on B. bacilliformis-infected endothelial cell viability, six hours post-infection.

HMEC-1 cells were incubated with 50 μ M of LY294002 for six hours. Control cells were left untreated. After being washed and detached with 0.08% trypsin-EDTA, cells were stained with fluorescent dye 7AAD and examined under the microscope. Panels A and B display *B. bacilliformis*-infected HMEC-1 cells, as seen under light and fluorescent filters, respectively. Panels C and D are LY294002-treated, *B. bacilliformis*-infected HMEC-1 cells, as seen under light and fluorescent filters.

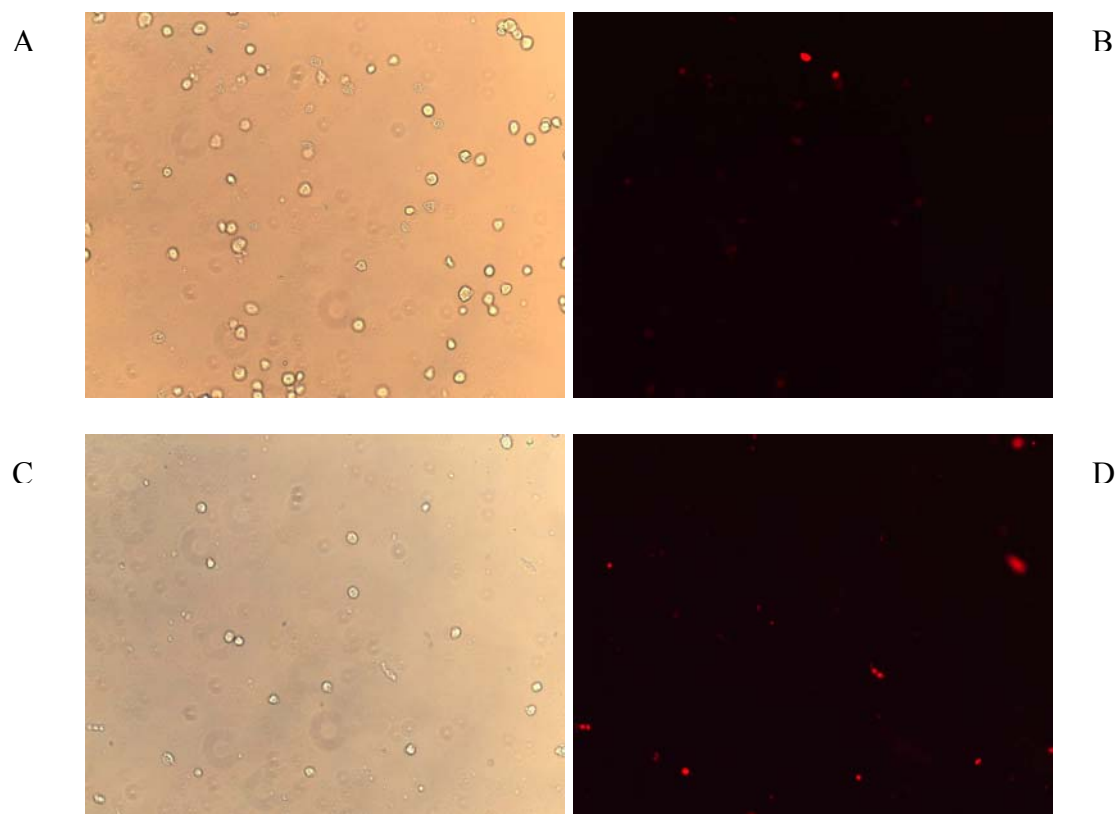


Figure 2.5f. Effect of PI3K inhibitor, LY294002, on endothelial cell viability, 24 hours post-infection.

HMEC-1 cells were incubated with 50 μ M of LY294002 for 24 hours. Control cells were left untreated. Cells were washed and detached with 0.08% trypsin-EDTA, then stained with fluorescent dye 7AAD and examined under the microscope. Untreated HMEC-1 cells appear under light and fluorescent filters in Panels A and B, respectively. The LY294002 treated HMEC-1 cells under light and fluorescent filters appear in Panels C and D, respectively.

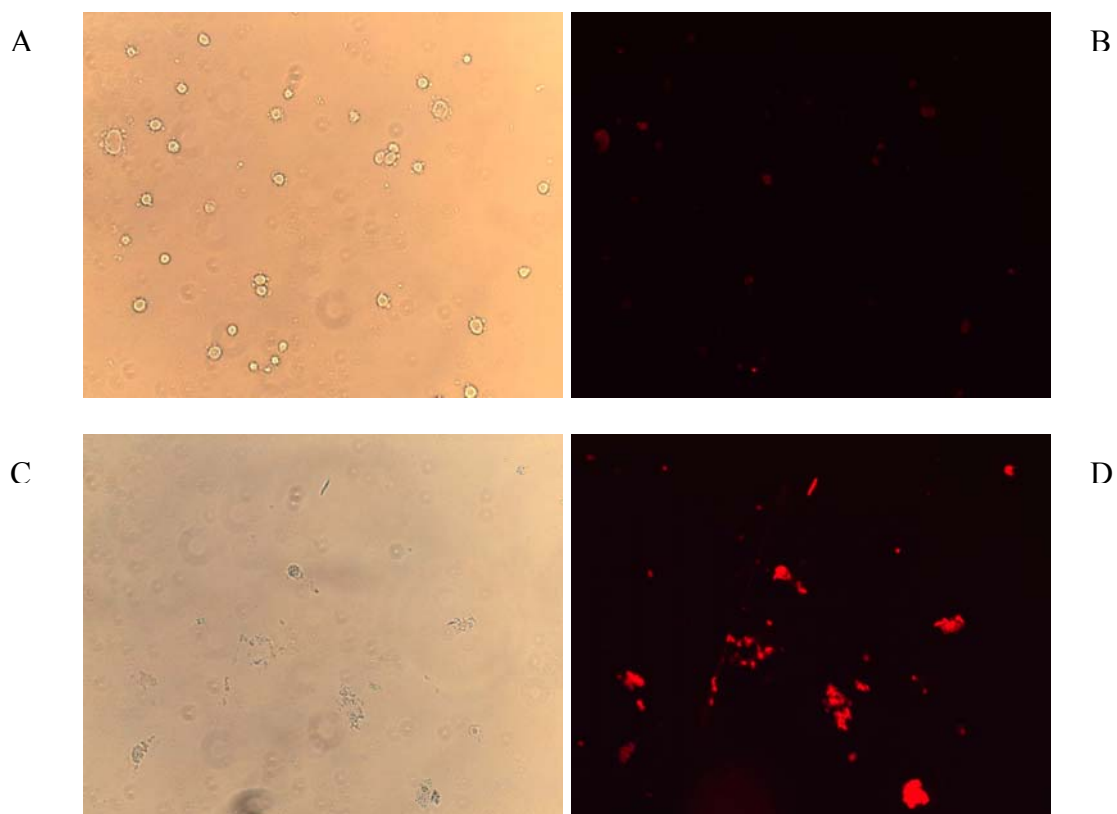


Figure 2.5g. Effect of PI3K inhibitor, LY294002, on B. bacilliformis-infected endothelial cell viability, 24 hours post-infection.

HMEC-1 cells were incubated with 50 μ M of LY294002 for 24 hours. Control cells were left untreated. Cells were washed and detached with 0.08% trypsin-EDTA and then stained with fluorescent dye 7AAD and examined under the microscope. Panels A and B reveal *B. bacilliformis*-infected HMEC-1 cells under light and fluorescent filters, respectively. Panels C and D are LY294002-treated, *B. bacilliformis*-infected HMEC-1 cells under light and fluorescent filters, respectively.

Discussion

Role of MAP kinases in *B. bacilliformis* invasion of endothelial cells

Pathogens commonly hijack cytosolic signaling pathways to establish intracellular infection. After the bacteria attach to cell receptors, they initiate a signaling cascade that results in the modulation of the cytoskeletal network and optimizes bacterial translocation into the cells. The recruitment of signaling molecules by bacteria also ensures their intracellular survival and the prevention of host cell death. Incubation of *B. bacilliformis* with host cells results in ingestion and subsequent host cell proliferation (Garcia, F. *et al.*, 1992; Hill *et al.*, 1992). Electron transmission observations of infected cells show the presence of *B. bacilliformis* both inside and outside endocytotic vesicles, which suggests internalization by phagocytosis (Hill *et al.*, 1992). The same study reveals the incomplete inhibition of *B. bacilliformis* invasion in the presence of cytochalasin D, an actin polymerization inhibitor. Inactivation of small GTPases also impairs *B. bacilliformis* invasion into endothelial cells (Verma *et al.*, 2000; Verma *et al.*, 2002b). Activated MAPKs, SAPK/JNK1 and 2, p38 kinase, and their downstream JNK-dependent transcription factors have been detected in *B. bacilliformis*-infected endothelial cells (Verma *et al.*, 2002b), though the relation between activated MAPKs and *B. bacilliformis* internalization remains unclear. The role of MAPKs in *B. bacilliformis* infection is studied herein by inhibiting the kinases during the course of the invasion assay. All three MAPKs are required for *B. bacilliformis* invasion; furthermore, the percentage of internalized *B. bacilliformis* is reduced but never completely inhibited at the various inhibitor concentrations investigated.

PD98059 and U0126 are highly selective inhibitors of MEK1/2, PD98059 and U0126 and prevent the activation of MAP kinase and their substrates (Alessi *et al.*, 1995; Favata *et al.*, 1998). The suppression of microbial invasion in the presence of MEK1/2 inhibitors already has been reported for several bacteria. For example, *C. jejuni* 81-176 invasion decreased by 75% in the presence of 50 μ M PD98059, and at 100 μ M of PD98059, *L. monocytogenes* invasion was reduced by a factor of 10; similar effects were observed in the context of *S. aureus* infection of osteoblasts (Ellington *et al.*, 2001; Tang *et al.*, 1998). In the study described here, MEK1/2 inhibition has a negative effect on *B. bacilliformis* uptake by endothelial cells. Specifically, invasion was inhibited by 59% and 81% with 100 μ M of the compounds PD98059 and U0126, respectively, without any detrimental effect on bacterial attachment. However, U0126 had a stronger inhibitory effect on *B. bacilliformis* than PD98059, perhaps because U0126 has a significantly greater affinity for MEK1 than PD98059 and the capacity to suppress both MEK1 and 2, unlike PD98059, which inhibits MEK1 more potently than it does MEK2 (Favata *et al.*, 1998). Thus, both MEK1 and 2 may be required for *B. bacilliformis* penetration into host cells. The MAPK substrates for activated MEK1/2 are ERK1/2. When activated, ERK1/2 transmit signals to the migration pathways of various cell types in response to extracellular matrix (ECM) proteins such as fibronectin, vitronectin, and collagen (Anand-Apte *et al.*, 1997). The activation state of ERK1/2 in *B. bacilliformis*-infected cells is not known, but the need for MEK1/2 during *B. bacilliformis* invasion supports the notion that MEK1/2 could be phosphorylated upon *B. bacilliformis* infection. In addition, phosphorylated paxillin can be detected in *B. bacilliformis* infected endothelial cells, which in turn is known to facilitate activation of ERKs (Ishibe *et al.*, 2003; Verma

et al., 2001). Activated ERKs have several cytoskeletal elements that could be required for bacterial internalization. In particular, some activated ERK molecules affect cytoplasmic protein phosphorylation. One of the cytosolic targets modulated by ERK2 is phospholipase A2, an essential regulator of endothelial motility (Sa *et al.*, 1995). In addition, ERK2 appears colocalized in a cytoskeleton signaling complex, targeted by leukocyte-specific protein1 to the peripheral actin filaments (Harrison *et al.*, 2004). ERKs also phosphorylate paxillin, which participates in regulation of adhesion and morphogenesis (Ishibe *et al.*, 2003; Ku *et al.*, 2000). Determination of the ERK1/2 activation state and further elucidation of the receptors that mediate their stimulation during *B. bacilliformis* invasion should help delineate more precisely the events that lead to *B. bacilliformis* uptake accurately.

Phosphorylated JNK acts on a wide range of substrates, including transcription factors, apoptosis-related proteins, signaling molecules, and cytoskeletal associated proteins. As a result of its association with cytoskeletal molecules, JNK plays an important role in cell migration and reorganization (Huang *et al.*, 2004). Previous studies have demonstrated the presence of activated JNK in *B. bacilliformis* infected endothelial cells (Verma *et al.*, 2002b). We show that inhibition of JNK with SP600125 affects *B. bacilliformis* ingestion. In a similar study with *N. meningitidis*, the invasion process has been shown to depend on JNK (Sokolova *et al.*, 2004), and JNK activation may be associated with the internalization of *P. gingivalis* in epithelial cells (Watanabe *et al.*, 2001). Although *B. bacilliformis* invasion was affected by JNK inhibition, adhesion remained unaffected; this indicates that the decrease in invasion actually is a function of JNK inhibition, not inefficient adhesion. Furthermore, *B. bacilliformis* uptake by

endothelial cells was not abrogated completely in the presence of SP600125; therefore, JNK-independent pathways could be involved during the infection process.

Kinase p38 traditionally is involved in cytokine responses, apoptosis, and cell differentiation. The role of p38 kinase in cell migration also is becoming clearer in recent studies. For example, the p38 kinase inhibitor SB203580 impairs growth factors and cytokine-induced cell migration in various cell types. One of the substrates for p38 kinase, heat shock protein 27 (Hsp-27), modulates cell migration through actin dynamics (Rousseau *et al.*, 1997). In addition, SB203580 suppresses not only p38 but also Hsp-27 in response to bacterial endotoxin, IL-1, and cellular stress (Cuenda *et al.*, 1995). The α isoform of p38 kinase specifically is inhibited by SB203580; this isoform is the predominant form of p38 kinase in the endothelial cells we use in our invasion assays (Gum *et al.*, 1998). This inhibitor also has been used effectively to demonstrate a requirement for p38 in *C. jejuni* and *S. typhi* invasions (Hobbie *et al.*, 1997; Hu *et al.*, 2006). *B. bacilliformis* penetration into HMEC-1 cells also is partially inhibited when p38 activation is inhibited. The degree of bacterial attachment remains the same as that observed in control assays; hence, the reduced invasion can be considered due to the effects of p38 kinase inhibition, not decreased adhesion. At the present time, the cytoskeletal proteins affected by p38 kinase in *B. bacilliformis*-infected cells are unknown. One attractive substrate for activated p38 kinase, caldesmon (caD), is an actin, myosin-binding protein. Previous caD mutation studies show that it plays a critical role in endothelial cell cytoskeletal remodeling and its activation depends on p38 kinase (Mirzapoiazova *et al.*, 2005).

Invasive pathogens bind to receptors and trigger host signal cascades. Receptor-mediated signal transduction also recruits various MAPKs that participate in the cytoskeletal modulation required for efficient bacterial ingestion. Our work provides data in support of the hypothesis that *B. bacilliformis* invasion is a complex process involving multiple kinases. The MAPK effector proteins engaged in *B. bacilliformis* have not been previously studied. Most downstream MAPK mediators are transcription factors and cytoskeletal proteins that must be identified to understand the course of cytoskeletal alterations that lead to optimized *B. bacilliformis* uptake and pathogenesis.

Role of PI3K in *B. bacilliformis* endothelial cell invasion and survival

The actin network is regulated by kinases other than those of the MAPK family. Phosphoinositides such as PI3K are short-lived lipid kinases that play a significant role in the modulation of the cytoskeletal scaffold. These lipid kinases also have an established role in cell motility and phagocytosis and can be synthesized at cell membrane sites through carefully orchestrated events that themselves can be altered by pathogens to optimize their cell entry. InlA- and B-mediated *L. monocytogenes* entry, *P. aeruginosa* and *C. pneumoniae* invasion, and FimH-dependent uropathogenic *E. coli* entry into host cells all depend on the activation of PI3K (Coombes *et al.*, 2002; Ireton *et al.*, 1996; Kierbel *et al.*, 2005b; Martinez *et al.*, 2002). Furthermore, small GTPases and PI3K are part of a complex regulation system. Rac activates PI3K, and PI3K inhibition prevents GTP loading of Rac (Kotani *et al.*, 1995). Thus, Rac can act both upstream and downstream of PI3K. In addition to Rac activation, PI3K inhibition can prevent membrane ruffling and actin assembly in PDGF and insulin-stimulated cells (Kotani *et al.*, 1995; Wennstrom *et al.*, 1994). The inhibitory effects of pharmacological PI3K

inhibitors also emerge in *Helicobacter pylori*-infected cells. Specifically, *H. pylori* mediated, activated PI3K molecules accumulate at the leading phagosomes, but this accumulation (along with actin polymerization) is blocked in the presence of nanomolar concentrations of the PI3K inhibitor wortmannin (Allen *et al.*, 2005). Although we did not examine the subcellular location and activation state of PI3K in *B. bacilliformis*-infected cells, we observed that PI3K inhibition by two different compounds, namely, wortmannin and LY294002, markedly reduces the number of intracellular *B.*

bacilliformis recovered from endothelial cells. Wortmannin is an irreversible, non-specific inhibitor that is unstable in aqueous solutions, whereas LY294002 is a stable, specific, but reversible inhibitor. The exact mechanism by which *B. bacilliformis* exploits PI3K to gain entry into host cells remains unclear, but *B. bacilliformis* can be found in small aggregates surrounded by membrane protrusions that eventually engulf the membrane-bound bacteria; furthermore, the requirement for Rho, Rac, and Cdc42 in *B. bacilliformis* infection already has been elucidated. (Arias-Stella *et al.*, 1986a; Verma *et al.*, 2002b). Because small GTPases act both upstream and downstream of PI3K, it is tempting to assume that the PI3K requirement involves both Rac and Cdc42. Additional experiments that link the small GTPases to the PI3K pathway would help expand the knowledge base pertaining to invasion tactics employed by *B. bacilliformis*.

Alternatively, PI3K could also impede *B. bacilliformis* internalization by preventing the Rac stimulated pseudopod extension during bacterial engulfment (Cox, D. *et al.*, 1999).

Beyond its function in regulating cytoskeleton dynamics, PI3K is an essential member of the anti-apoptotic pathway (Kennedy *et al.*, 1997; Qi *et al.*, 1999). Activated PI3K induces the phosphorylation of protein kinase B/Akt (PKB/Akt) through PIP₃,

which in turn contributes to cell survival by inactivating the pro-apoptotic Bcl-2 proteins, such as BAD (Bcl-2 associated death promoter) (Datta *et al.*, 1997). The intracellular survival of *Bartonella* spp and endothelial proliferation requires that anti-apoptotic signals prevent cell death. *B. henselae*-associated endothelial proliferation results from the suppression of caspase activation in the early stages of infection and the prevention of DNA fragmentation in the later stages by unidentified factors (Kirby *et al.*, 2002b). Furthermore, *B. quintana* infected endothelial cells show an interesting pattern of programmed cell death. Initially, *B. quintana* induces apoptosis with peaks at six hours post infection, after which anti-apoptotic factors become activated and mitogenesis occurs. The factors analysed during this process include caspase 8, the APAF-1 gene, and Bcl-2 (Liberto *et al.*, 2003). No information indicates which host cell survival proteins are involved in *B. bacilliformis*-infected endothelial cells. During the course of the invasion assays with the PI3K inhibitor LY294002, we observed that at concentrations at or above 50 μ M, the infected cells underwent detachment. Upon further examination, we found that in the presence of LY294002 (50 μ M), the number of viable, *B. bacilliformis*-infected cells dramatically decreased during the course of the infection, becoming undetectable by 24 hours post infection. We examined the viability using trypan blue and 7AAD stain, both of which permeate cells with compromised plasma membranes. Cells stained with 7 AAD showed distinct nuclear condensation at six hours post infection, a hallmark of cells undergoing apoptosis (Figure 2.5e). LY294002 also influenced the uninfected endothelial cells to a certain degree, though 59% of viable cells still were recovered after 24 hours. Other bacteria also use the PI3K pathway for cell survival, including *P. gingivalis*, *S. enterica* serovar Typhimurium, and *M. tuberculosis*,

which promote cell survival through the PI3K/Akt cascade (Forsberg *et al.*, 2003; Maiti *et al.*, 2001; Yilmaz *et al.*, 2004). In transformed epithelial cells and serum-deprived fibroblasts, small GTPases (Rac and Cdc42) prevent apoptosis by maintaining the actin network (Cheng *et al.*, 2004; Ruggieri *et al.*, 2001). In both these cases, the protective function of Rac and Cdc42 can be inhibited by PI3K inhibitors. Activation of Rac and Cdc42 occurs in *B. bacilliformis*-infected endothelial cells. Further research focused on the function of small GTPases and PI3K during cell survival could provide important information about how *B. bacilliformis* manipulates the host cell pathways for its propagation.

This study provides the first demonstration of the necessity of PI3K for the survival of *B. bacilliformis*-infected endothelial cells. The data provide a platform for further analysis of apoptosis kinetics modulated by *B. bacilliformis* in endothelial cells. The bacterial regulation of cell survival mediators varies during the course of the infection; therefore, it would be interesting to investigate whether *B. bacilliformis* inhibits apoptosis like *B. henselae* or causes early apoptosis, followed by anti-apoptotic signals, as seen with *B. quintana* and to determine how PI3K participates in these events.

Chapter III: Expression patterns of genes involved in *B. bacilliformis* uptake

Introduction

Bartonella bacilliformis is an ancient human pathogen that causes the bi-phasic Carrion's disease. The primary hematic phase results from erythrocytic infection by *B. bacilliformis*, whereas the persistent intracellular colonization of endothelial cells is the hallmark of the second phase. Endothelial cell parasitization induces several morphological changes, including the subversion of apoptosis and the activation of proinflammatory, mitogenic, and angiogenic factors. These changes ultimately culminate in vasoproliferative tumor growth, manifested as blood-filled lesions on bodily extremities.

Bacterial interaction with cell receptors and prolonged colonization results in the modulation of various host cytosolic and nuclear proteins and genes. We have shown that *B. bacilliformis* engages integrins to gain entry into endothelial cells. The integrin-*B. bacilliformis* interaction could be direct or indirect via integrin ligands. Integrins, the dynamic receptors that maintain cell adhesion to the extracellular matrix and thus ensure cell survival, represent anchoring molecules that also function in relaying extracellular signals to the cells and intracellular signals to the outside environment, which enables the cells to adapt to any changes. Additional, critical roles of integrins include cytoskeletal organization and regulation of cell proliferation signaling pathways. Integrin activation has also been known to alter the activation state of various transcription factors.

Some endothelial cytoplasmic proteins required for the establishment of *B. bacilliformis* have been studied in our laboratory and documented by other researchers, including the small GTPases Rac, Cdc42, and Rho, which are activated upon infection

and alter the actin network to facilitate *B. bacilliformis* internalization (Verma *et al.*, 2000; Verma *et al.*, 2002b). The protein kinases with multiple functions that participate in *B. bacilliformis* infection are mitogen activated protein kinases (MAPKs), protein tyrosine kinases (PTKs) such as focal adhesion kinase, p21-activated kinase and lipid kinase phosphatidylinositol 3 kinase (PI3K) (Verma *et al.*, 2002b; Williams-Bouyer *et al.*, 1999). The activation of these proteins can be controlled by integrin-mediated pathways and then the activated MAPKs can regulate DNA transcription factors. Inhibition of MAPKs, PTKs, and PI3K impairs *B. bacilliformis* invasion into endothelial cells, possibly by disrupting the optimal organization of actin scaffold for bacterial invasion (Williams-Bouyer *et al.*, 1999). Activation of the transcription factor AP-1 also has been recorded in endothelial cells infected with *B. bacilliformis* (Verma *et al.*, 2002b), though the implications of this activation are unclear.

B. bacilliformis invades a variety of cell types *in vitro* but induces mitogenesis only in endothelial cells (Garcia *et al.*, 1990). Effective proliferation requires direct contact between *B. bacilliformis* and host cells and can occur within 30 minutes of bacterial contact (Garcia, F. U. *et al.*, 1992). Infected endothelial cells also form tubules indicative of angiogenesis on the appropriate substrate. The activation of AP-1 and the proliferative effect of *B. bacilliformis* on endothelial cells thus suggest several unidentified changes in the host transcriptome. As the first step in characterizing these changes, the Affymetrix GeneChip microarray technology was used to investigate the transcriptional response of human microvascular endothelial cells to *B. bacilliformis*. This powerful method profiles changes in the gene expression in response to stimuli such as infection by a pathogen and previously has monitored cellular responses to bacteria,

including *B. henselae*, *S. typhimurium*, *H. pylori*, and *S. aureus* (Bryant *et al.*, 2004; Dehio *et al.*, 2005).

The GeneChip consists of cDNA probes of known identity immobilized on a nylon surface by robotics. The probe size varies from 500 to 5000 base pairs. The added target, fluorescently labeled cDNA, obtained from sample RNA, is hybridized onto the chip. A fluorescent signal, digitized by a fluorescent scanner, detects the complementary binding of sample cDNA to the probes. The signal intensity represents the expression level of that gene, and gene profiling relates to the reference. The biggest advantage of DNA microarray analysis is that it enables investigation of the behavior of multiple genes simultaneously. However, this information pertains to the gene transcription level, whereas post-translational modifications provide the next level of cell function regulation. Therefore, DNA microarray studies should be supplemented with high-throughput proteomics to obtain accurate information about factors affecting cellular responses.

We report here our analysis of some of the genes that become highly differentiated during the course of the infection by *B. bacilliformis* and a few that are a part of the integrin-signaling pathways. Almost all of the genes related to the cytoskeletal networks and integrin signaling have increased transcript levels by 30 minutes after the infection. The up-regulation persists for one hour, after which a decrease in gene expression is noted, which may indicate host response to counteract bacterial infection. Other potential defense factors, such as the expression of cytokine and inflammation responsive genes, are enhanced at later points in time, after the initial down-regulation.

Materials and Methods

HMEC-1 cell line growth and culturing.

The immortalized human microvascular endothelial cell line (HMEC-1) was a kind gift from Dr. Ades of the Centers for Disease Control (CDC), Atlanta (Ades EW *et al.*, 1992). The HMEC-1 cells from passages 19-27 were grown in 15ml of growth media consisting of 50% M199 (Cambrex), 15% FBS (Hyclone), 2% Penicillin/Streptomycin (Cellgro), and 50% EGM-2 (Cambrex). Cells were grown and maintained in T-75 flasks (Starstedt) at 37°C under 5% CO₂ and humid conditions. This medium was changed every 2–3 days until 70–80% confluence was reached. The cells were maintained in 10ml maintenance media (M199 +15%FBS+2% Penicillin-Streptomycin) between passages. For cell detachment, confluent cells were washed twice with PBS to remove all traces of serum before the addition of 10mls/ 75²mm Cell stripper (Cellgro). Cells were incubated at 37°C for 10 minutes and then gently scraped with cell scrapers (Starstedt). Detached cells were collected in 15-ml Falcon tubes and centrifuged at 700xg for 10 minutes at 25°C. Cells were resuspended in 1 ml maintenance media and enumerated microscopically using the hemocytometer before seeding the T-25, T-75, or T-150 flasks or 6- or 24-well plates. Cells were allowed to adhere for 16 hours before use.

To prepare frozen stocks, cell pellets were resuspended in DMSO freeze medium (Cellgro) to obtain a final concentration of 1×10^5 cells/ml. The vials were allowed to freeze at -80°C in a cryofreezing container (Nalgene) for 24 hours and then transferred to the liquid N₂ tank facility.

Bacterial growth and culturing.

B. bacilliformis KC584 was obtained from ATCC (35686) and grown on brain heart infusion (BHI) plates with 10% sheep blood (BD Bioscience) at 26°C for 4–7 days. Low-passaged bacteria (1–3 passages) were used for all experiments. After the confluent colonies were visible, plates were overlaid with 7ml of PBS. The bacteria were gently scraped off the plate with a loop. The bacterial suspension was centrifuged at 2000xg for 10 minutes at 25°C. Pellets were washed once with PBS and centrifuged as previously described. Final suspension was in 1ml of BHI broth, unless otherwise noted.

Infection of HMEC-1 cells with *B. bacilliformis* for RT-PCR and microarray studies.

HMEC-1 cells were grown in T150 flasks containing 30ml of growth media, were incubated at 37°C and 5% CO₂, under humid conditions. The HMEC-1 cells were allowed to reach 90% confluence, after which the media were replaced with 30ml of M199 with 5% FBS, and the cells were incubated for 24 hours. Cells from a single flask were counted to give an approximation of the growth in the remaining flasks. *B. bacilliformis*, at a m.o.i. of 100:1 in 100 µl of PBS, was added to each experimental flask, and 100µl of sterile PBS was added to each control flask. The media were aspirated for 30 minutes and one, three, and six hours post infection, and washed three times to remove detached cells and unbound bacteria. The cells were detached from the flasks, as described previously, and centrifuged at 700 xg for 10 minutes at 25°C. The cells were immediately processed to prepare total RNA.

Preparation of HMEC-1 total RNA.

Total RNA from HMEC-1 cells was extracted using the Qiagen RNeasy column (Qiagen). Briefly, the harvested HMEC-1 cells were resuspended gently in 600µl of lysis

buffer with β -mercaptoethanol. The lysate was pipetted into a QIAshredder spin column (Qiagen) for homogenization and centrifuged at 14,000xg for two minutes. The spin columns were washed with 700 μ l of 70% ethanol and mixed well with a pipette. Next, 700 μ l of the lysate-ethanol mixture was added, and the column was centrifuged at 14,000xg for 24 seconds, after which the flow-through was discarded. Into the spin column, 700 μ l of wash buffer was added, and the spin column was again centrifuged at 14,000xg for 24 seconds. This flow-through also was discarded and the bound RNA was then washed twice with 500 μ l of wash buffer. The first wash required centrifugation at 14,000xg for 24 seconds, and the second needed two minutes. The RNA was eluted with 30 μ l of RNase-free water into a fresh 1.5-ml RNase-free microcentrifuge tube (USA Scientific). To increase the elution efficiency, the tubes were incubated at room temperature for five minutes, then centrifuged at 14,000xg for one minute. The eluate was pipetted back into the spin column and allowed to incubate for 30 minutes at room temperature, after which the tubes were centrifuged again at 14,000xg for one minute. The RNA concentrations were determined by BioPhotometer (Eppendorf), and the total HMEC-1 RNA was stored at -80°C until needed.

Microarray analysis of *B. bacilliformis*-infected HMEC.

For microarray studies, the HG-U133 Chip Sets (Affymetrix) that contain two Gene Chip[®] arrays, representing approximately 33,000 human genes, were used. Experiments were performed on two different biological replicates, according to the manufacturer's instructions. Double-stranded cDNA was synthesized using total HMEC-1 RNA, as prepared previously, employing the Affymetrix-supplied SuperScript II first-strand synthesis kit for each sample. Second-strand cDNA was synthesized from the first

cDNA, which had been cleaned using Phase-lock gel tubes (Eppendorf) with a ratio of 25:24:1 phenol:chloroform:isoamyl alcohol (Boehringer Mannheim) and used to synthesize biotin-labeled RNA according to the Enzo BioArray High Yield RNA Transcription Labeling Kit. The labeled RNA was cleaned using Qiagen RNeasy columns, and the required concentration of cRNA was fragmented using the supplied fragmentation buffer. The supplied Affymetrix controls, including the B2 Oligonucleotide and Eukaryotic Hybridization Controls, were mixed with the fragmented cRNA as specified; this mixture then was hybridized onto the HG-U133A chip for 16 hours at 45°C, rotating 60 rpm. After HG-U133A hybridization, the same cRNA mixture was removed and allowed to hybridize onto the HG-U133B chip. The hybridized chips were then developed using the GeneChip Fluidics Station for automated washing and staining. Finally, the chips were scanned using the GeneArray scanner, operating with GeneChip Operating System (GCOS) 5.0. The cell intensity files (CEL) generated from the GCOS analysis, contain information about probe intensity. Each probe intensity for is normalized against the spiked in endogenous controls to give normalized values for each gene. This data was then analyzed further by GeneSpring v7.3 (Agilent).

GeneSpring analysis of human microarray data.

Data were preprocessed using GCOS and then analyzed with GeneSpringv7.3 (Agilent). To normalize the data, the following rules were applied. Raw signal values below 0.01 were set to 0.01. The 50.0th percentile of all measurements in that sample serves as the dividing line for each measurement. Each gene was divided by the median of its measurements in all samples. If the median of the raw values was below 10, each measurement for that gene was divided by 10, assuming the numerator was greater than

10; otherwise, the measurement was discarded. Genes selected for pathway and further analysis were those determined as significantly differentially expressed genes by a Volcano plot, built by comparing "Timed Control" with "Timed Experimental" using all normalized genes. To complete the statistical analysis, a parametric test assumes unequal variances. Genes that were differentially expressed passed this testing method, defined by a fold difference of 2 and a p-value of 0.1.

Real-time RT-PCR.

cDNA was synthesized from 500ng of cellular RNA using the High-Capacity cDNA reverse transcription kit (Applied Biosystems). The reverse transcriptase (RT) Master Mix (2X) was prepared with 2.0 μ l of 10XRT buffer, 0.8 μ l of 25XdNTP mix (100mM), 2 μ l of 10XRT random primers, 1 μ l of MultiScribeTM reverse transcriptase, 1.0 μ l of RNase inhibitor, and 3.2 μ l of nuclease-free DEPC-treated water (Ambion). The Master Mix was kept on ice after gentle mixing. Individual reactions for cellular RNA from each time point were prepared by mixing 10 μ l of RNA with 10 μ l of 2X Master Mix. The reverse transcription was performed in an Eppendorf thermal cycler under the following conditions: 25°C for 10 minutes, 37°C for 120 minutes, and 85°C for five seconds. cDNA was stored at -20°C until further use. Real-time quantitative PCR (RT-qPCR) was performed with the synthesized cDNA using the TaqMan Universal PCR Master Mix (Applied Biosystems) protocol. In short, 1 μ l of cDNA was diluted with 8 μ l of DEPC-treated water, followed by the addition of 10 μ l of Master Mix and 1 μ l of the assay primer (TaqMan Gene Expression Assay, Applied Biosystem). The catalog numbers of the assay primer used for the genes (in parenthesis) were Hs002337443_m1 (integrin α_5), Hs00236976_m1 (integrin β_1), Hs00233808_m1 (integrin α_v), and

Hs01001469_m1 (integrin β_3). The RNA was quantified in an Applied Biosystems 7500 using the following cycling settings: 48°C for 30 minutes, AmpliTaq activation at 95°C for 10 minutes, denaturation at 95°C for 15 seconds, and, finally, annealing/extension at 60°C for one minute (40 cycles). Cyclophin A (PPIA, Hs99999904_m1) was used as the endogenous control. All reactions were performed in triplicates, and the comparative threshold values ($\Delta\Delta C_T$) were calculated in Microsoft Excel. All threshold values (C_T) were first normalized to the endogenous reference (PPIA). The $\Delta\Delta C_T$ was calculated by subtracting the control (uninfected) C_T from the experimental (infected) C_T . Relative quantification (RQ) for mRNA for each sample was determined by $2^{(-\Delta\Delta C_T)}$. The p-value was then calculated using Student's t-test for unequal variances; a value of ≤ 0.1 was considered significant.

Fold-change calculations

The relative quantification for the normalized values for control (uninfected) and experimental (infected) data from microarray data was obtained by dividing the experimental data to the control data. The fold-change for this normalized ratio (NR) was calculated using the formula: IF(NR<1,-1/NR) (Ingenuity™). According to this formula if the normalized ratio is less than one, then the values are divided by -1 to give a negative integer representative of gene down-regulation. If the normalized ratio value is more than 1, then this value represents a positive fold-change or gene up-regulation. If normalized ratio is 1, then this value represents no change in gene expression. The same parameters were used to calculate the fold-change for the RQ values IF(RQ<1,-1/RQ) obtained from real time RT-PCR experiments described above.

Results

Scatter plot analysis of HG-U133A Microarray chips

HG-U133A chips were hybridized with HMEC-1 cDNA from the control and *B. bacilliformis*-infected cells. The results of a scatter plot analysis conducted on the control and experimental gene profiles appear in Figure 3.1a. The blue dots represent a down-regulation of the genes in the experimental sample relative to the control, whereas the orange/red dots indicate an up-regulation of the genes relative to the control compared with the experiment. With the exception of the 30-minute post infection reading, the microarray results show the expected expression variability at most time points in terms of *B. bacilliformis* infection of the HMEC-1 cells. As Panel A shows, there is an upward shift in overall gene expression, such that 8.6% of the genes present are up-regulated and 6.3% of the genes present are down-regulated at the 30-minute post infection point. Wider variability marks Panel A, 30 minutes post-infection, compared with the other panels. Panels B and C show the one hour and three hour post infection time points. As expected, the majority of gene expression levels were altered by a less than twofold-change, as indicated by the yellow dots within the green bars. A 3.5% up-regulation appears at both the one hour and three hour points, though this up-regulation is slight compared with the down-regulation of these genes at the same times (22.2% and 13.4%, respectively).

The scatter plot generated from the host cell gene expression levels six hours after *B. bacilliformis* infection appears in Panel D. The blue dots that indicate that 2.3% of the host genes are up-regulated, and 6.7% are down-regulated.

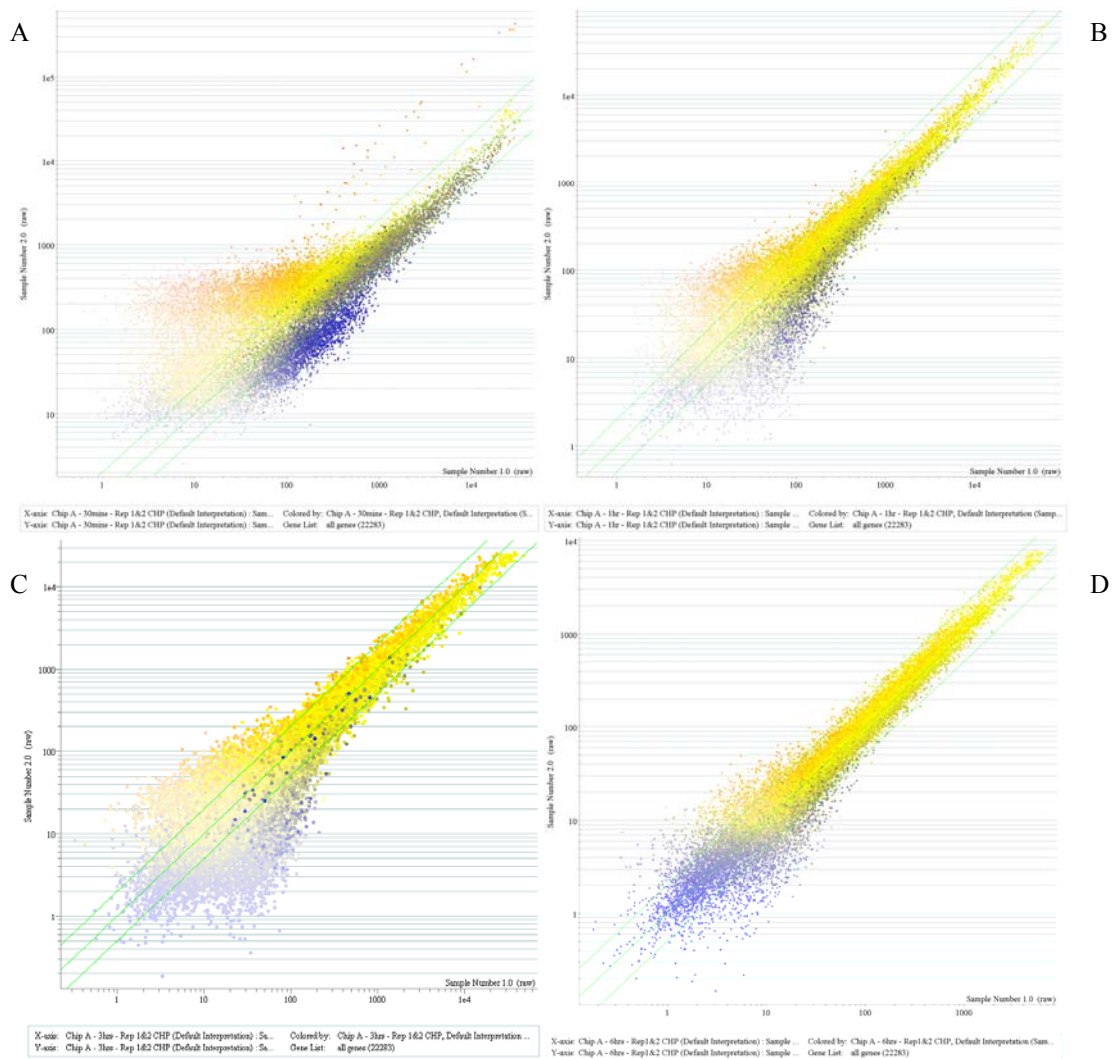


Figure 3.1a. Endothelial gene expression at various time points.

Total mRNA isolated from *B. bacilliformis*-infected HMEC-1 cells and from, uninfected HMEC-1 control cells was hybridized to Affymetrix HG-U133A microarray chips. The five scatter plots represent gene expression profiles comparing the infected to the uninfected endothelial cells at different time points after infection: (A) 30 minutes, (B) one hour, (C) three hours, and (D) six hours. The relative mean hybridization intensity of one of the transcripts represents the Y-axis, and the PBS-mock infected control appears on the X-axis. Yellow dots represent unchanged gene expression, blue dots indicate down-regulated genes, and orange/red dots symbolize up-regulated genes compared with the control. Green bars represent twofold-change range for each chip hybridized. Each point depicts an individual element of the microarray.

Scatter plot analysis of HG-U133B microarray chips

The HG-U133B microarray chip scatter plot analysis shows a higher variability than that of the HG-U133A microarray chips. Figure 3.1b, Panel A displays the gene variation 30 minutes after *B. bacilliformis* infection. The blue dots indicate that approximately 35.0% of the genes have been down-regulated, while only 5.3% of them have been up-regulated. This large number of down-regulated cells could be due to the direct interaction of HMEC-1 cells from *B. bacilliformis*, corresponding to the mRNA transcripts found on the HG-U133B chip.

At the one hour post infection time point, shown in Panel B, 5.4% of all genes are down-regulated, and 3.7% are up-regulated relative to the control samples. This downward trend continues in Panel C, where 12.2% of the genes are down-regulated and 3.8% is up-regulated at the three hour point. Finally, Panels D, which represents the time point six hours post infection reveals a more characteristic pattern of gene expression. As the data show, at this time point 6.8% genes are down-regulated, and a 2.0% are up-regulated, as indicated by their position within the twofold parameter change.

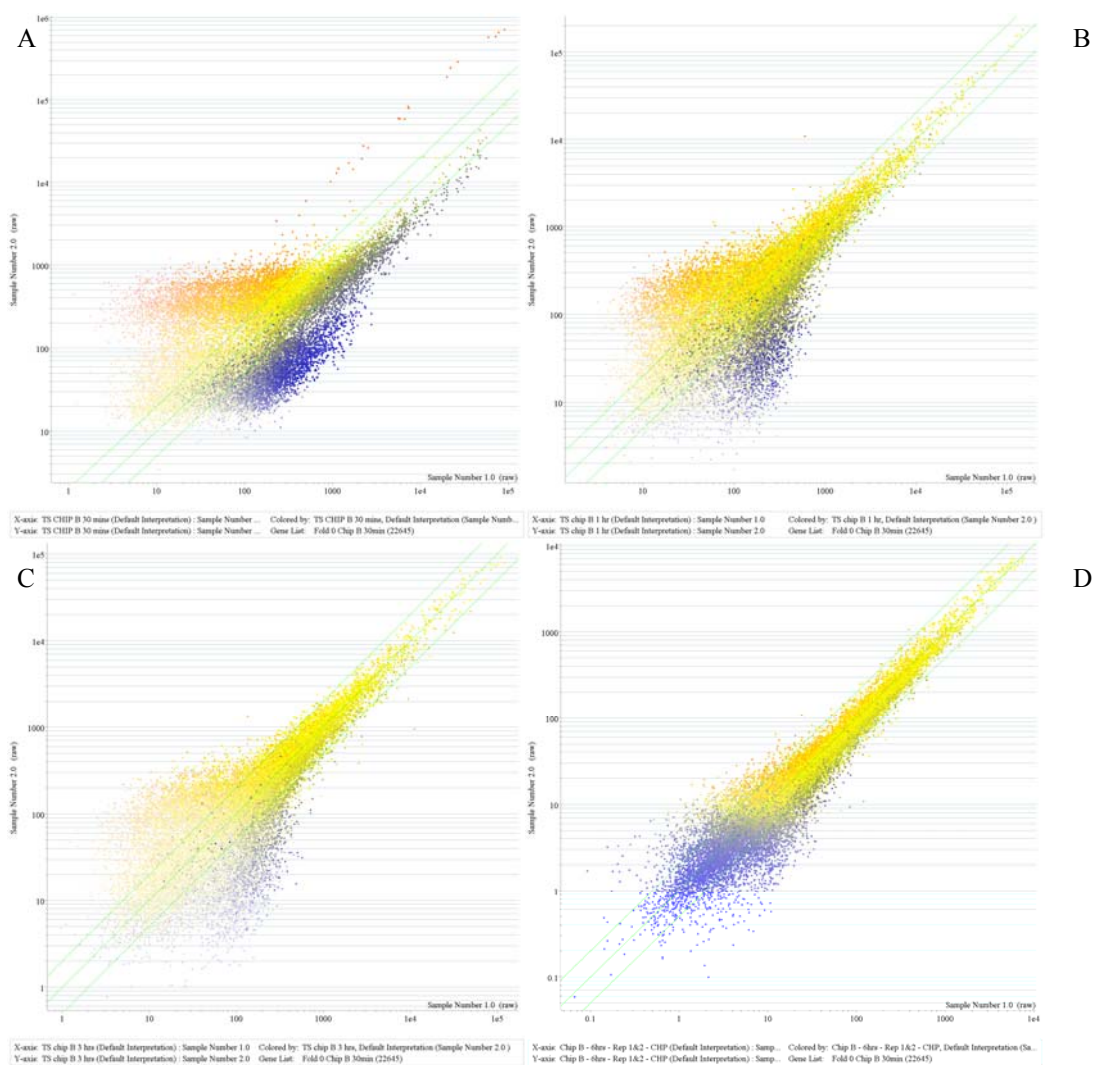


Figure 3.1b. Endothelial gene expression at various time points.

Total mRNA isolated from *B. bacilliformis*-infected HMEC-1 cells and from, uninfected HMEC-1 control cells was hybridized to Affymetrix HG-U133B microarray chips. The five scatter plots represent gene expression profiles comparing the infected to the uninfected endothelial cells at different time points after infection: (A) 30 minutes, (B) one hour, (C) three hours, and (D) six hours. The relative mean hybridization intensity of one of the transcripts represents the Y-axis, and the PBS-mock infected control appears on the X-axis. Yellow dots represent unchanged gene expression, blue dots indicate down-regulated genes, and orange/red dots symbolize up-regulated genes compared with the control. Green bars represent twofold-change range for each chip hybridized. Each point depicts an individual element of the microarray.

Analysis of highly differentially expressed gene transcripts

GeneSprin software was used to determine the fold-change ratio of the gene expression in *B. bacilliformis*-infected endothelial cells. From these data, 20 genes showing maximum and minimal gene expression were identified. These code for proteins involved in various cellular functions, such as JunD proto-oncogene, a component of the transcriptional factor AP1 complex, which exhibits a 23-fold-change at 30 minutes and then decreases to 9-fold by six hours. RNA levels of other transcription factors also show significant decreases and include the POU transcription factor (-21.93 at 30 minutes), transcription factor EC isoform A and B (-58.48 at one hour), and iron-responsive element binding protein 2 (-21.18 at one hour) (Tables 3.1a and 3.1b).

Several cell surface receptor genes show a positive regulation in this analysis. For example, transcripts coding for the toll-like receptor 7 and calcitonin show a 13.47-fold and 9.76-fold increase, respectively, at 30 minutes (Table 3.1a); the CD69 antigen exhibits a 10.74-fold increase at one hour; cadherin is up-regulated by 17.43-fold at three hours; and the fibroblast growth factor receptor 4 increases by 6.28-fold at six hours (Tables 3.1b, 3.1c, and 3.1d). With the exception of the integrin β_1 isoform, no cell surface receptor genes with a negative fold-change were detected in this study (Table3.1a).

A down-regulation of growth factor receptors, including FGF (fibroblast growth factor) receptor substrate 2 and TRAF3 (TNF receptor-associated factor 3) modulator, occurs at three hours after infection, which suggests a decreased role for the selected FGF modulators and the TNF pathways (Table3.1c). The cell growth regulators, the Ras-like p21 activator 3, and the Ras-like estrogen-regulated growth inhibitor each exhibit

significant up-regulation relative to mock cell transcript levels at three and six hours post infection (Tables 3.1c and 3.1d). Significant changes in immune response genes occur in TNF ligand super-family member 8 (8.98 at 30 minutes) and in interleukin 17 (-19.76), interleukin 24 (-7.09), and interleukin 26 (-8.55) at six hours after infection (Tables 3.1a and 3.1d).

Finally, cell morphology modulators exhibiting differential expression in this study include A disintegrin and metalloproteinase domain 7 and tubulin β 8. At 30 minutes after infection, transcriptosomes of these two genes show a negative change of 23.20 fold and 17.36 fold, respectively. Collagen -type XXIV α_1 is also down-regulated, decreasing by 17.06 fold at one hour post infection (Tables 3.1a and 3.1b). Another collagen type, XI isoform A, pre-protein exhibits a positive change with a 8.96-fold increase over the control cells at six hours (Table 3.1d). Finally, the actin-related protein 2/3 complex subunit A shows a 9.28-fold increase at six hours post infection (Table 3.1d).

Table 3.1a. Highly differentially expressed functional HMEC-1 transcriptomes, 30 minutes after *B. bacilliformis* infection.

GeneSpring analysis of microarray data from uninfected control HMEC-1 cells, compared with data of *B. bacilliformis*-infected HMEC-1 cells was performed to determine the fold-change of the highly differentially expressed HMEC-1 genes. Up-regulated and down-regulated genes referred in text are highlighted in red and blue, respectively.

Gene Product	Accession No.	Fold-change	Gene Product	Accession No.	Fold-change
Up-Regulated Gene Products			Down-Regulated Gene Products		
Jun D proto-oncogene	AI339541	23.55	Coiled-coil domain containing 102B	NM_024781	-61.728
Cystic fibrosis transmembrane conductance regulator, ATP-binding cassette (sub-family C, member 7)	W60595	14.72	Centrosome protein 4	NM_025009	-39.841
A-kinase anchor protein 13 isoform 1,2&3	NM_006738	14.32	Zinc finger protein 711	NM_021998	-35.971
Toll-like receptor 7	NM_016562	13.47	Msh homeobox 2	NM_002449	-33.333
Guanine nucleotide binding protein (G protein), beta polypeptide 2-like 1	AA443762	12.61	Xylulokinase homolog	AA777793	-32.258
DNA-damage-inducible transcript 3	BC003637	12.38	Urotensin 2 preproprotein, isoform A&B	NM_021995	-30.581
Lymphocyte cytosolic protein 2	AI123251	11.98	H3 histone family, member I	NM_021018	-26.596
X-linked eukaryotic translation initiation factor 1A	BE542684	11.29	Integrin beta 1 isoform 1A-E	AA215854	-25.189
Delta-sarcoglycan isoform 1; delta-sarcoglycan isoform 2	U58331	11.27	A disintegrin and metalloproteinase domain 7	AF215824	-23.202
NADH dehydrogenase (ubiquinone) Fe-S protein 1, 75kda precursor	NM_005006	10.99	EBV-induced G protein-coupled receptor 2	NM_004951	-22.779
Basic helix-loop-helix domain containing, class B, 2	NM_003670	10.8	POU transcription factor	AI686582	-21.93
Cathepsin S preproprotein	BC002642	10.8	Chemokine (C-X-C motif) ligand 5 precursor	NM_002994	-21.834
Translocase of inner mitochondrial membrane 50 homolog	BE378994	10.71	UDP glucuronosyltransferase 2 family, polypeptide A3	NM_024743	-19.96
Clpx caseinolytic protease X homolog	NM_006660	10.67	Paternally expressed 3	AF208967	-19.724

Gene Product	Accession No.	Fold-change	Gene Product	Accession No.	Fold-change
<i>Up-Regulated Gene Products</i>			<i>Down-Regulated Gene Products</i>		
N-acetylated alpha-linked acidic dipeptidase 2	AJ012370	10.5	C-K-ras2 protein isoform b; c-K-ras2 protein isoform a	NM_004985	-19.493
Tripartite motif-containing 58	AL080170	10.49	Tubulin, beta 8	AI433261	-17.361
Sidekick homolog 1	R38712	10.46	Calcium channel, voltage-dependent, L type, alpha 1D subunit	BE550599	-17.182
Epsilon globin	NM_005330	10.27	Myelin-associated oligodendrocyte basic protein	D28114	-17.094
Karyopherin alpha 1	BF575685	10.11	Transporter 2, ATP-binding cassette, sub-family B isoform 1&2	NM_018833	-16.949
Ubiquitin-conjugating enzyme E2O	NM_022066	10.06	Plasma kallikrein B1 precursor	NM_000892	-16.779
Glutathione synthetase	NM_000178	9.923	Aspartate beta-hydroxylase isoform A-D	NM_020164	-16.502
Calcitonin receptor	AB022177	9.763	Phenylalanine hydroxylase	BG433489	-15.748
ATM/ATR-Substrate Chk2-Interacting Zn ²⁺ -finger protein	AI744148	9.578	RAB27B, member RAS oncogene family	NM_004163	-15.649
Sodium potassium chloride cotransporter 2	AI632015	9.537	Transferrin	NM_014111	-15.267
Phosphoinositide-3-kinase, regulatory subunit 4, p150	AK025026	9.411	Coagulation factor II (thrombin) receptor-like 3 precursor	NM_003950	-15.083
Similar to FERM domain-containing protein 4B (GRP1-binding protein GRSP1) isoform 1	AK000244	9.164	Triadin	AW969675	-15.06
Tropomyosin 1 alpha chain isoform 1-7	NM_000366	9.058	Biliverdin reductase A	U34877	-15.015
Tumor necrosis factor (ligand) superfamily, member 8	NM_001244	8.981	Solute carrier family 25 (mitochondrial carrier; adenine nucleotide translocator), member 31	NM_031291	-14.771
Paired box 5	BF510692	8.968	PDZ and LIM domain 3	BC001017	-14.347
Similar to Ig kappa chain V-I region Walker precursor	Z00008	8.908	Fibroblast growth factor 18 precursor	AB007422	-14.327

Table 3.1b. Highly differentially expressed functional HMEC-1 transcriptomes, one hour after *B. bacilliformis* infection.

GeneSpring analysis of microarray data from uninfected control HMEC-1 cells, compared with data of *B. bacilliformis*-infected HMEC-1 cells was performed to determine the fold-change of the highly differentially expressed HMEC-1 genes. Up-regulated and down-regulated genes referred in text are highlighted in red and blue, respectively.

Gene Product	Accession No.	Fold-change	Gene Product	Accession No.	Fold-change
<i>Up-Regulated Gene Products</i>			<i>Down-Regulated Gene Products</i>		
Solute carrier family 4, sodium bicarbonate cotransporter, member 4	AF011390	20.92	Transcription factor EC isoform A&B	AI830469	-58.480
Ubiquitin specific protease 49	NM_018540	15.95	Itchy homolog E3 ubiquitin protein ligase	AI732502	-36.364
Spectrin repeat containing, nuclear envelope 2 isoform A,B,C,D&E	AW965040	15.61	ADAM metallopeptidase domain 12 isoform 1&2 preproprotein	AU158643	-32.895
Resistin	NM_020415	15.35	Carboxypeptidase M precursor	AI469884	-30.488
Rab3 GTPase-activating protein, non-catalytic subunit	AK021928	15.15	Potassium voltage-gated channel, Shab-related subfamily, member 2	AA017045	-29.851
ATPase, aminophospholipid transporter (APLT), class I, type 8A, member 1	AB013452	14.38	Similar to SMC hinge domain containing 1	AA873021	-28.986
RAS p21 protein activator 3	NM_007368	14.04	Hypothetical protein LOC167691	AI742190	-28.329
CD1E antigen isoform b precursor	AA309511	12.34	Mitogen-activated protein kinase kinase kinase 7 interacting protein 2	AA769450	-26.385
Phosphodiesterase 4D interacting protein isoform 1,2,3,4&5	AU157078	11.43	Phosphatidic acid phosphatase type 2 domain containing 2	H15396	-26.247
IQ motif containing GTPase activating protein 2	NM_006633	11.06	Tudor domain containing 6	AA404231	-24.038
Small inducible cytokine A18 precursor	Y13710	11.05	Transforming growth factor, beta receptor I precursor	AI743727	-23.474
CD69 antigen (p60, early T-cell activation antigen)	BF439675	10.74	ATPase, (Na ⁺)/K ⁺ transporting, beta 4 polypeptide	NM_012069	-23.364
Chromosome 22 open reading frame 16	AI814909	10.57	Zinc finger protein 585B	AW130096	-22.371

Gene Product	Accession No.	Fold-change	Gene Product	Accession No.	Fold-change
<i>Up-Regulated Gene Products</i>			<i>Down-Regulated Gene Products</i>		
Serine (or cysteine) proteinase inhibitor, clade B (ovalbumin), member 3	BC005224	10.25	Ring finger and WD repeat domain 2 isoform d24; ring finger and WD repeat domain 2 isoform a	BF725688	-21.552
Protease, serine, 16	NM_005865	10.17	Methionyl Aminopeptidase 2	AI733395	-21.459
Epsin 1	AK022454	10.06	Sprouty-related protein 1 with EVH-1 domain	AK021887	-21.231
RUN and FYVE domain-containing 1 isoform b	AK025118	9.969	Iron-responsive element binding protein 2	AW470799	-21.186
Similar to trinucleotide repeat containing 9 isoform 1	U80736	9.946	Phospholipid scramblase 1	BE066040	-20.833
Estrogen-related receptor gamma isoform 1; estrogen-related receptor gamma isoform 2	AF094518	9.943	Nance-Horan syndrome protein	AI680913	-20.704
Coiled-coil domain containing 102B	NM_024781	9.896	Zinc finger protein 407	NM_017757	-20.534
RAN binding protein 9	AI476722	9.701	GPI deacylase	AW084937	-19.685
Two AAA domain containing protein	AI656807	9.697	Protein kinase D3	AW008270	-19.380
Sine oculis homeobox homolog 1	N79004	9.673	SEC15-like 1 isoform b; SEC15-like 1 isoform a	AI346849	-18.587
Mitogen-activated protein kinase kinase 7	AI090153	9.405	Solute carrier family 6 (neurotransmitter transporter, GABA), member 1	AI003579	-18.182
Zinc finger protein 496	AA191336	9.295	MORF-related gene X	BE886165	-17.391
			Kinesin family member 13A	AJ291579	-17.094
			Collagen, type XXIV, alpha 1	AI631241	-17.065

Table 3.1c. Highly differentially expressed functional HMEC-1 transcriptomes, three hours after *B. bacilliformis* infection.

GeneSpring analysis of microarray data from uninfected control HMEC-1 cells, compared with data of *B. bacilliformis*-infected HMEC-1 cells was performed to determine the fold-change of the highly differentially expressed HMEC-1 genes. Up-regulated and down-regulated genes referred in text are highlighted in red and blue, respectively.

Gene Product	Accession No.	Fold-change	Gene Product	Accession No.	Fold-change
Up-Regulated Gene Products			Down-Regulated Gene Products		
Sciellin isoform a; sciellin isoform b	AW470178	24.9	ATPase, (Na ⁺)/K ⁺ transporting, beta 4 polypeptide	NM_012069	-23.364
Olfactory receptor, family 51, subfamily E, member 2	AF311306	21.13	Syntrophin, gamma 1	AI939541	-21.598
Solute carrier family 4, sodium bicarbonate cotransporter, member 4	AF011390	20.92	Pleckstrin homology domain containing, family K member 1	AW665138	-21.142
Zinc finger protein 218	AW953679	19.55	Zinc finger protein 407	NM_017757	-20.534
Holocarboxylase synthetase	AJ001863	18.15	Zinc finger protein 518	H57111	-20.243
Sestrin 3	BF685808	17.49	Neurexin 1 isoform alpha & beta precursor	AU146874	-18.692
Cadherin 2, type 1 preproprotein	AW450381	17.43	Solute carrier family 6 (neurotransmitter transporter, GABA), member 1	AI003579	-18.182
Ubiquitin specific protease 49	NM_018540	15.95	Phosphatase and tensin homolog	AK021487	-18.116
Checkpoint suppressor 1	AF138861	15.85	Ubiquitin specific protease 3	AU148154	-16.722
Tachykinin receptor 1 isoform long	AI492860	15.61	Pancreatic lipase precursor	NM_000936	-16.313
Resistin	NM_020415	15.35	5-hydroxytryptamine (serotonin) receptor 2B	NM_000867	-16.287
Rab3 GTPase-activating protein, non-catalytic subunit	AK021928	15.15	Developmental pluripotency associated 2	AI204212	-15.267

Gene Product	Accession No.	Fold-change	Gene Product	Accession No.	Fold-change
<i>Up-Regulated Gene Products</i>			<i>Down-Regulated Gene Products</i>		
ATPase, aminophospholipid transporter (APLT), class I, type 8A, member 1	AB013452	14.38	Numb homolog isoform 1,2,3&4	AW167424	-14.641
Tyrosyl-DNA phosphodiesterase 1	BE222041	14.24	Eukaryotic translation initiation factor 3, subunit 9 eta, 116kda	AA628539	-14.514
RAS p21 protein activator 3	NM_007368	14.04	Nuclear factor of kappa light polypeptide gene enhancer in B-cells inhibitor, zeta isoform a&b	AB037925	-13.928
Transketolase-like 2	AL136779	13.95	Choline phosphotransferase 1	BF940025	-13.755
Zinc finger protein 407	AA012924	13.85	Heterogeneous nuclear ribonucleoprotein M isoform A&B	BF003018	-13.736
Glutamate receptor, ionotropic, AMPA 2	BE219628	13.82	TRAF3-interacting JNK-activating modulator	AI214464	-13.717
Spectrin repeat containing, nuclear envelope 2 isoform A,B,C,D&E	AL035992	12.95	Contactin 3	BE221817	-13.569
Ectonucleotide pyrophosphatase/phosphodiesterase 5 (putative function)	AA609053	12.79	PEST-containing nuclear protein	BE465316	-13.495
ATP-binding cassette, sub-family C, member 6	AW300488	12.52	Filensin	NM_001195	-13.333
CD1E antigen isoform b precursor	AA309511	12.34	Similar to Ubinuclein (Ubiquitously expressed nuclear protein) (VT4)	AW967956	-13.280
Rearranged L-myc fusion sequence	AI742686	12.25	Gamma-aminobutyric acid (GABA) A receptor, alpha 5 precursor	BF966183	-12.920
Solute carrier family 16, member 11	AI802877	12.19	Gp130-like monocyte receptor	AI123586	-12.920
Similar to zinc finger protein 91	AI092709	12.12	Zinc finger RNA binding protein	AA629668	-12.920
			Periostin, osteoblast specific factor	AW137148	-12.788
			Myelodysplasia syndrome protein 1	AW452823	-12.642

Gene Product	Accession No.	Fold-change	Gene Product	Accession No.	Fold-change
<i>Up-Regulated Gene Products</i>			<i>Down-Regulated Gene Products</i>		
			Fibroblast growth factor receptor substrate 2	NM_006654	-12.484
			Transient receptor potential cation channel, subfamily M, member 1	AI277662	-12.453

Table 3.1d. Highly differentially expressed functional HMEC-1 transcriptomes, six hours after B. bacilliformis infection. GeneSpring analysis of microarray data from uninfected control HMEC-1 cells, compared with data of *B. bacilliformis*-infected HMEC-1 cells was performed to determine the fold-change of the highly differentially expressed HMEC-1 genes. Up-regulated and down-regulated genes referred in text are highlighted in red and blue, respectively.

Gene Product	Accession No.	Fold-change	Gene Product	Accession No.	Fold-change
<i>Up-Regulated Gene Products</i>			<i>Down-Regulated Gene Products</i>		
SET and MYND domain containing 3	AW074336	16.04	Interleukin 17	Z58820	-19.76
Polycystic kidney disease 2-like 2	AF182034	14.69	Potassium inwardly-rectifying channel, subfamily J, member 15	BG542347	-14.53
RAD23 homolog B	T93562	14.26	RAP2B, member of RAS oncogene family	NM_002886	-12.89
F-box only protein 3	AL162053	13.68	Cardiomyopathy associated 4 isoform 2	AI800785	-12.84
Basic helix-loop-helix domain containing, class B, 3	R93946	13.65	Myeloid/lymphoid or mixed-lineage leukemia translocated to 10	N64035	-12.84
InaD-like protein	AB044807	11.47	N-methyl-D-aspartate receptor subunit 2A precursor	T65537	-11.20
Glutamate receptor, ionotropic, AMPA1	AF007137	11.19	Mitochondrial ribosomal protein S31	AW007410	-10.63
CD24 molecule	BG327863	11.03	Hepatocyte nuclear factor 4, gamma	AI916600	-10.59
Regulator of G-protein signaling 1	NM_002922	10.88	Ras homolog gene family, member A	AW173151	-10.19
Cerebellar degeneration-related protein 1	NM_004065	10.67	Nuclear distribution gene E homolog like 1	AI963104	-10.17
mutS homolog 6	D89646	10.05	Replication protein A3, 14kDa	AI022132	-9.90
Mohawk homeobox	R59304	10.04	Jun D proto-oncogene	AI339541	-9.52
Golgi autoantigen, golgin subfamily a, 8A	AI829170	9.98	CDC42 small effector 2	AL122039	-9.35

Gene Product	Accession No.	Fold-change	Gene Product	Accession No.	Fold-change
<i>Up-Regulated Gene Products</i>			<i>Down-Regulated Gene Products</i>		
Cholinergic receptor, nicotinic, beta 4	NM_000750	9.63	Protocadherin gamma subfamily A, 3	AF152509	-9.26
Actin related protein 2/3 complex, subunit 1A, 41kDa	AF070647	9.28	Adaptor-related protein complex 1 sigma 2 subunit	N74507	-9.26
Neuropeptide Y receptor Y2	U32500	9.22	Polymerase (DNA directed), beta	S69873	-9.01
Catalase	AU147084	10.5	Epidermal retinal dehydrogenase 2	AI440266	-8.85
Alpha 1 type XI collagen isoform A preproprotein	BG028597	8.967	Retinoic acid receptor, beta	NM_015854	-8.70
RAS-like, estrogen-regulated, growth inhibitor	AW668616	8.679	Interleukin 26	NM_018402	-8.55
Protocadherin beta 14 precursor	NM_018934	8.332	Interleukin 24	NM_006850	-7.092
Interleukin 6 receptor isoform 1 precursor	AV700030	6.469	L1 cell adhesion molecule ras-related GTP-binding protein	AI653981	-6.494
Harakiri, BCL2 interacting protein	NM_003806	6.339	RAB10	AU146686	-6.173
Fibroblast growth factor receptor 4	NM_002011	6.283			

Fold-change analysis of integrin and integrin-signaling pathway-related gene transcripts

The fold-change ratios of integrins and integrin-signaling pathway-related genes were computed from the signal intensity data derived from RNA hybridized cDNA chips. The gene expression values depict the changes in the *B. bacilliformis*-infected HMEC-1 cells compared with mock infected cells during a total infection period of six hours. Many integrin subunit genes are positively induced at 30 minutes and one hour post infection (Table 3.2). Transcript levels decrease after that time with 57% and 42% of the subunits exhibiting significantly lower expression as compared with the mock infected culture by three and six hours, respectively. Genes encoding proteins that are affected by integrin ligation also show an up-regulation at 30 minutes. These include those coding for cytoskeletal proteins like tenascin 1, which have a 4.081-fold-change, and for members of the small GTPase pathway, such as Cdc42 and p21-activating kinase (PAK), which are increased by more than two-fold at 30 minutes and one hour post infection. Several small GTPase genes such as cofilin1, Rac, Cdc42, and PAK exhibit a modest increase at 30 minutes after which their relative level of expression steadily decreases. Certain kinase genes show significant up-regulation at 30 minutes post infection. Focal adhesion kinase is an integral part of integrin signaling, and its expression is enhanced by fivefold and twofold at 30 minutes and three hours, respectively. In contrast, some dual-specificity kinases that regulate MAPKs (such as dual-specificity kinase 1) are down-regulated, whereas two MAPKs (e.g. MAPK-9 and MAPK-14) show the reverse pattern at the same time points. Anti-apoptotic genes, such as the Bcl2 antagonist of death (BAD), insulin-like growth factors (IGFs), and survivin (BRIC5) show a positive change at various time

points; at the same time, some pro-apoptotic factors and caspases 3 and 9 are also up-regulated.

Other cell surface receptors, including Toll-like receptors 2 and 4, PECAM (platelet/endothelial cell association molecules), CEACAM (carcioembryonic antigen-related cell adhesion molecule), Selectin E, and ICAM1 (intracellular adhesion molecule 1), which may play an important roles in the inflammatory response, also were included in this study. Selectin E, a cell adhesion protein expressed on cytokine-activated cells that mediates leukocyte adhesion shows the most dramatic variation. It is maximally down-regulated (-4.167) at 30 minutes, with down-regulation continuing until three hours post infection, after which it is up-regulated almost fourfold. With its multiple functions, CEACAM experiences a twofold increase at 30 minutes and six hours. A few genes that regulate angiogenesis are positively expressed: angiopoietin 1 at three hours and angiopoietin 2 at six hours (after showing a negative fold-change at 30 minutes), and vascular endothelial growth factor (VEGF), which exhibits two-fold or greater up-regulation at one and six hours.

Table 3.2. Integrin subunits and integrin signaling component HMEC-1 transcriptomes. GeneSpring analysis of microarray data from uninfected control HMEC-1 cells, compared with data of *B. bacilliformis*-infected HMEC-1 cells, performed to determine the fold-change at various times points of differentially expressed HMEC-1 genes. Genes exceeding the two-fold cutoff for up- and down-regulation are highlighted in red and blue, respectively.

Gene Name	Accession No.	Fold-change at Times			
		30mins	1hour	3hour	6hour
Integrin receptor subunits					
Integrin alpha 2	AI733222	2.454	1.430	-1.227	-1.127
Integrin alpha IIB	NM_000419	2.832	3.317	2.929	1.070
Integrin alpha 3	NM_002204	1.646	1.180	-1.517	1.359
Integrin alpha 4	NM_000885	2.898	-1.845	1.261	1.339
Integrin alpha 5	NM_002205	1.724	1.130	1.051	1.473
Integrin alpha 6	NM_000210	1.517	1.305	-1.297	-1.151
Integrin alpha 7	AF072132	-2.865	1.006	-1.071	1.281
Integrin alpha 8	BF939224	2.311	1.957	-3.356	3.934
Integrin alpha 9	BF510694	2.299	-1.441	-1.032	-1.119
Integrin alpha 10	AF112345	1.139	-1.117	-1.475	1.444
Integrin alpha11	AF109681	1.149	1.528	1.005	-1.168
Integrin alpha V	AI093579	1.635	1.046	-1.193	1.112
Integrin beta 1	AA215854	1.898	-1.264	-1.451	-1.325
Integrin beta 2	NM_000211	-1.125	1.661	2.248	-1.715
Integrin beta 4	AA808063	1.000	1.091	-2.976	-1.178
Integrin beta 5	AL048423	3.873	1.083	-1.305	1.247
Integrin beta 6	NM_000888	5.671	-2.882	11.010	1.413
Integrin beta 7	NM_000889	1.678	-1.529	1.701	-1.471
Integrin beta 8	NM_002214	1.735	3.165	-1.733	1.859
Cytoskeletal associated proteins					
Myosin light chain 9	NM_006097	1.276	1.249	-1.010	-1.040
Actin related protein complex subunit1A	NM_006409	1.329	1.120	-1.183	-1.110
Actin, alpha 1	NM_001100	1.130	1.853	1.130	-1.433
Paxillin	NM_002859	1.339	1.162	1.066	1.153
Vinculin	NM_014000	1.793	1.028	1.033	-1.001
Zyxin	NM_003461	1.677	1.634	1.173	1.002
Talin	AI345601	1.130	-1.859	1.892	3.405
Tensin 1	AF116610	4.081	-1.572	1.454	1.098
Small GTPase pathway					
Cofilin 1	NM_005507	1.484	1.165	-1.033	1.115
Ras-related C3 botulinum toxin substrate 1	BG292367	1.724	1.114	-1.002	1.149
Cell division cycle 42	BC002711	2.456	1.507	-2.119	-1.397
p21 activated kinase	U51120	2.215	1.551	-1.004	2.079
ADP-ribosylation factor-interacting protein 2	NM_012402	2.075	1.136	1.134	-1.183

Gene Name	Accession No.	Fold-change at Times			
		30mins	1hour	3hour	6hour
Ras homolog gene family, member A (RhoA)	AA011598	-1.001	-2.347	1.377	-1.346
Integrin-related cell signaling kinases					
Focal adhesion kinase	AA912743	5.11	1.933	2.066	-1.572
Integrin linked kinase	BE617348	1.123	3.140	-1.692	-1.041
MAPK signaling					
Mitogen activated kinase 1	AA195999	1.350	1.124	-1.147	1.034
Mitogen activated kinase 2	X60188	1.885	-1.451	1.398	1.076
Mitogen activated kinase 8	AI379407	1.736	1.244	-1.205	1.060
Mitogen activated kinase 9	W37431	2.456	-1.280	1.180	1.035
Mitogen activated kinase 14	AF100544	2.687	1.106	-1.048	-1.280
Dual Specificity kinase 1	AW024420	-6.329	-5.263	-1.057	-2.681
Dual Specificity kinase 5	U16996	2.579	-1.224	-1.013	1.111
Dual Specificity kinase14	NM_007026	2.015	-1.171	1.028	-1.147
Dual Specificity kinase 3	NM_004090	-1.239	-1.508	1.184	-1.508
PI3K/Akt signaling pathway					
Phosphoinositide 3-kinase, catalytic subunit	AA767763	2.394	2.268	-2.155	-1.157
Phosphoinositide 3-kinase, regulatory subunit	AA018968	2.479	3.780	-1.033	1.671
Bcl2 antagonist of cell death	U66879	3.624	-1.037	-1.416	1.046
Caspase 3	NM_004346	3.360	-1.208	-1.300	-1.152
Caspase 9	AB015653	5.161	-1.156	1.130	1.202
v-akt murine thymoma viral oncogene homolog 1	NM_005163	2.318	1.299	1.228	1.030
Insulin like growth factor1	M37484	1.858	4.893	2.548	-1.776
Survivin	AA648913	1.839	1.932	-1.522	-1.107
Transcriptional factors					
Activating transcription factor 2	BE786164	3.483	1.082	-1.110	-1.192
cAMP responsive element binding protein 1	AI655737	3.774	-1.037	-1.412	-1.890
vian sarcoma virus 17 oncogene homolog	BC002646	3.819	1.054	-1.323	-1.045
v-myc myelocytomatosis viral oncogene homolog (avian)	NM_002467	1.480	-1.473	-1.323	-1.041
Nuclear factor of kappa light polypeptide gene enhancer in B cells	M55643	1.056	-1.458	1.018	1.184
Elk1	NM_005229	1.091	1.133	-1.022	-1.305
c-Jun	BC002646	3.819	1.054	-1.323	-1.045

Gene Name	Accession No.	Fold-change at Times			
		30mins	1hour	3hour	6hour
Other receptors					
Toll like receptor 2	NM_003264	-1.297	1.014	-4.219	1.260
Toll like receptor 4	NM_003266	1.226	1.251	-1.395	-1.149
Lymphocyte antigen 96	NM_015364	1.295	1.106	1.052	-1.479
Platelet/endothelial cell adhesion molecule CD98	M37780	3.069	1.221	-1.181	-1.054
NM_002394	NM_002394	2.662	-1.175	-1.742	-1.044
Carcinoembryonic antigen- related cell adhesion molecule 1	NM_001712	2.633	-1.272	1.061	2.106
Selectin E	NM_000450	-4.167	-2.591	-2.660	3.997
Intercellular adhesion molecule 1	NM_000201	2.591	2.631	1.074	1.113
Apoptosis					
Bcl2 associated X protein (BAX)	U19599	4.368	-1.261	-1.328	-1.142
ANGPT1	NM_001146	-1.183	-1.587	1.157	1.306
ANGPT2	NM_001147	-1.092	3.391	1.313	2.292
VEGF	NM_003377	1.388	2.610	-1.101	2.167

Real Time PCR validation of microarray data

GeneSpring analysis of the gene expression in *B. bacilliformis* cells gave the fold-change ratio between the experimental and control samples. The mRNA sample used for microarray hybridization was also used in real time RT-PCR experiments that were designed to analyze the expression of selected genes. The fold-change ratio from the relative quantification values derived from RT-PCR studies was determined and compared with the values obtained from the microarray analysis (Table 3.3). The correlation between the seven genes compared at defined time points is variable. The degree of integrin α_5 gene expression is the same in RT-PCR and microarray studies at all times points, except at six hours post infection. In contrast integrin β_1 fold-change data from microarray analysis correlates with the RT-PCR data only at 30 minutes. Integrin α_v fold-change is similar in both sets of experiments at 30 minutes and three hours and integrin β_3 at one, three and six hours. The three MAPKs fall within the defined range of a 2.5-fold of each other at 30 minutes. At one hour only MAPK1 and MAPK3 show a similar gene expression. According to the results from microarray analysis, MAPK1 and MAPK8 have a negative fold-change at three hours, whereas the RT-PCR data suggests their up-regulation. Lastly at six hours only MAPK8 fold-change was in agreement, while discordance was noted with MAPK1 and MAPK3 gene expression.

Table 3.3. Validation of gene expression data obtained from microarray studies.

The fold-change data of the gene expression obtained by GeneSpring analysis was compared to the fold-change data obtained by real time PCR. The data from the two experiments correlate when the difference between two readings is within ± 2.5 fold-change. The data that does not correlate is indicated by (*).

Gene Name	Accession no.	30'		1hr		3hr		6hr	
		RT-PCR fold-change	Microarray fold-change	RT-PCR fold-change	Microarray fold-change	RT-PCR fold-change	Microarray fold-change	RT-PCR fold-change	Microarray fold-change
Integrin alpha 5	NM_002205	2.18	1.72	1.39	1.13	1.11	1.05	-1.99	1.47
Integrin beta 1	AA215854	1.80	1.90	1.33	-1.26	1.11	-1.45	1.09	-1.33
Integrin alpha V	AI093579	1.49	1.64	-1.22	1.05	-2.02	-1.19	-1.56	1.11
Integrin beta 3	NM_000212	1.79	-1.44	-2.04	-2.3	-2.05	-1.52	-1.56	-1.3
Mitogen activated protein kinase 1	AA195999	1.10	1.35	1.32	1.12	1.28	-1.15	-1.09	1.03
Mitogen activated protein kinase 3	X60188	1.11	1.89	-1.47	-1.45	1.17	1.40	-1.28	1.08
Mitogen activated protein kinase 8	AI379407	1.62	1.74	-1.00	1.24	1.16	-1.21	1.19	1.06

Discussion

With the advent of cDNA microarray technology, it is now possible to characterize the global transcriptional responses in host cells infected with pathogens. In this study, we profiled the endothelial cell genes involved in *B. bacilliformis* invasion. Microvascular endothelial cells line the blood vessels of the body and provide a selective barrier to the translocation of various molecules into the surrounding tissues. These cells are the primary targets for *B. bacilliformis*, and undergo proliferation following infection, both *in vivo* and *in vitro* (Garcia, F. U. *et al.*, 1992). The presence of *B. bacilliformis* also induces pro-angiogenic signals and forces the infected endothelial cells to form angiogenic blood vessels that culminate in the formation of blood-filled nodules, described as verruga peruana. In previous chapters, we have demonstrated the function of integrins and their ligands for establishing *B. bacilliformis* infection. Of the integrins studied, the fibronectin receptor $\alpha_5\beta_1$ reveals the most significant effect on bacterial uptake. Integrin activation by extracellular signals results in hierarchical protein interactions that affect cytoskeletal reorganization, the activation of signaling pathways, and eventually the regulation of gene expression. An important component of integrin signaling is the mitogen-activated protein kinase (MAPK) pathway, components of which also regulate transcription. In our experiments with MAPK inhibitors, we found that MEK1/2, JNK, and p38 kinase are involved in *B. bacilliformis* invasion. In addition to MAPKs, the lipid kinase PI3K plays a critical role in bacterial uptake and cell survival. In this section, we analyze some of the gene transcripts that are part of the integrin-signaling pathway, linking events that may occur in endothelial cells after *B. bacilliformis* infection.

Total RNA isolated from *B. bacilliformis*-infected and mock infected microvascular endothelial cells was hybridized onto Affymetrix GeneChips, which have human gene transcript oligomers spotted on two sets of chips. The analyses of hybridization intensity signals were processed by GCOS and then by GeneSpring (Agilent) as a means to determine the changes in the gene transcriptomes from infected cells in comparison with control cells.

Highly differentially expressed transcripts

GeneSpring analyses of the raw microarray data indicated which genes have the highest and lowest fold-change ratios at various time points. All these genes could play significant roles in determining the fate of *B. bacilliformis*-infected endothelial cells. Discussion of all of these genes is beyond the scope of this study, but a few genes were selected for discussion to provide a better understanding of some of the cellular changes that occur during *B. bacilliformis* infection.

One gene that is significantly up-regulated by 30 minutes post infection codes for the toll-like receptor (TLR7). TLR7 traditionally is responsive to small synthetic compounds and single-stranded RNA. However, it also functions in bacterial infections; for instance, dendritic cells exhibit increased TLR7 expression after exposure to lipopolysaccharide (LPS), a primary component of the outer membrane of Gram negative bacteria (Severa *et al.*, 2007). *Haemophilus influenzae* also stimulates epithelial cell TLR7 expression through a NF κ B-dependent pathway, which enhances the host cell's antiviral response (Sakai *et al.*, 2007). Although the implications of the TLR7 up-regulation are unknown, it could lead to TLR7-specific responses, such as NF κ B activation and cytokine secretion.

The Jun D proto-oncogene, which shows more than a 23-fold positive change at 30 minutes, is a member of the Jun family and a component of the Activation Protein 1 (AP1) factor complex. Its induction is significant because Jun D protects cells from p53-dependent apoptosis brought on by stress signals and the cytotoxic effects of TNF α (Weitzman *et al.*, 2000).

Another factor that contributes to anti-apoptotic signals is phosphoinositide 3 kinase (PI3K). The regulatory component of this complex, p150, shows a 9.4-fold positive change over the controls. Because *B. bacilliformis* is an intracellular pathogen, it can benefit from the activation of cell survival genes early during the infection, which enables it to establish the infection. Furthermore, the inflammatory cytokine CXC5 precursor is strongly suppressed. This cytokine is a potent activator of neutrophils which, if recruited, could prevent *B. bacilliformis* from colonizing the endothelial cells. Thus the down-regulation of CXC5 would be expected to be beneficial to the infecting bacteria (Strieter *et al.*, 1992).

At one hour post infection, the expression of two genes, one coding for the A disintegrin and metalloprotease (ADAM12), and one coding for the TGF beta growth factor, is reduced. ADAM12 and TGF-beta growth factor regulate cell spreading and growth, respectively. The Ras p21 protein activator a negative regulator of the Ras-MAPK pathway required for growth, differentiation, and proliferation in response to receptor tyrosine kinase-mediated stimuli reveals significantly enhanced expression (Gibbs *et al.*, 1990). Together, these signals would repress cell proliferation, which could be a protective measure mounted by the host to balance the mitogenic signals from *B. bacilliformis*. One such bacterial mediated mitogenic stimulus could be MAPK7 (also

called ERK5), which is activated at the one hour time point. This kinase is required for endothelial cell survival and functions by decreasing caspase 3 activity (Pi *et al.*, 2004). The proliferative effects of growth factors, epidermal growth factors, and granulocyte colony-stimulating factors, as well as the oncogenic effect of Ras, are all mediated by ERK5 (English *et al.*, 1999; Kato *et al.*, 1998). In addition, ERK5 is required for VEGF- and FGF-induced angiogenesis (Hayashi *et al.*, 2005). These contradictory signal responses to *B. bacilliformis* appear unique and require detailed exploration to understand how the host cell machinery provokes proliferation while also battling simultaneous apoptotic signals.

The positive expression of some of the pro-angiogenic genes occurs at three hours as well. One of them, cadherin 2, or N-cadherin, is involved in cell–cell contact, and in endothelial cells it regulates angiogenesis by controlling VE-cadherin expression (Luo *et al.*, 2005). The transcription of the NFκB inhibitor zeta (IKBζ) isoform is reduced. This protein has latent transcriptional activity required to inhibit NFκB (Yamazaki *et al.*, 2001). Down-regulation of IKBζ could activate NFκB, and thus mediate proliferative effects and regulate inflammatory responses. Another gene worth mentioning is the TRAF3-interacting JNK-activating modulator, which is down-regulated at three hours. This protein interacts specifically with TRAF3 to activate JNK (Dadgostar *et al.*, 2003). Thus, JNK regulation in *B. bacilliformis* could be a TRAF-dependent event.

At six hours post infection, a pro-apoptosis gene, harakiri Bcl2-interacting protein (HRK), shows a six-fold increase in expression. The HRK gene product physically interacts selectively with Bcl2 and BAX to activate the cell death cycle (Inohara *et al.*, 1997). Interestingly, the JunD proto-oncogene, which displays a dramatic increase in

expression at 30 minutes, shows a nine-fold decrease in expression by six hours post infection. As mentioned previously, JunD is anti-apoptotic, and its down-regulation, together with an increase in HRK expression, could favor cell death at this time point. However, apoptosis is a complex process with multiple protein interactions that must be taken into consideration before drawing any final conclusions. The fibroblast growth factor receptor 4 (FGFR4), which recognizes FGF19, is up-regulated. The receptor may be involved in cell proliferation, differentiation, and angiogenesis. Because *B. bacilliformis*-infected cells eventually undergo angiogenesis, the high expression of genes that contribute to cell growth and blood vessel formation may be advantageous.

Integrins

B. bacilliformis is internalized by endothelial cells within the first hour of coinubation, and endothelial proliferation requires as little as 30 minutes of infection (Garcia *et al.*, 1990). These observations suggest that the function of *B. bacilliformis*-infected cell components changes within a short period after of bacterial incubation. *B. bacilliformis* aggregates also can be found on cell membranes, and integrins have been identified as potential receptors. The inhibition of $\alpha_5\beta_1$ receptor leads to a maximum decrease in invasion, and RT-PCR analyses of the individual subunits show an increase in their gene expression. Microarray data are consistent with these findings (Table 3.3). Furthermore, other alpha and beta subunits are up-regulated at early times after infection. Enhanced integrin gene expression over the course of the infection could ensure efficient and continuous *B. bacilliformis* internalization. The subunit β_6 has the highest fold-change among the β subunits at both 30 minutes and three hours. In addition, β_6 can pair with α_5 subunits that recognize both fibronectin and vitronectin (Huang *et al.*, 1995).

This integrin subunit pairing also serves as a receptor for foot-and-mouth disease virus and coxsackievirus A9 (Jackson *et al.*, 2000; Williams *et al.*, 2004). Fibronectin-bound *B. bacilliformis* are internalized more efficiently than uncoated bacteria and can use $\alpha_v\beta_6$, along with other fibronectin integrins for adherence. Some integrin genes exhibit decreased expression after three hours post infection, which could suggest a host defense mechanism against the uptake of surface-bound bacteria.

The differential regulation of selected genes, such as those involved with integrin binding was also investigated by real-time RT-PCR. To be considered comparable, the RT-PCR and microarray data must have a minimum 80% correlation, with no more than a 2.5-fold-change difference between the sets of data (Draghici, 2002; Gao *et al.*, 2004). With regard to integrin expression, our RT-PCR fold-change data provided a general validation of the data from the microarray experiments with most time points showing similar degrees of up- or down-regulation. However, less consistent results were obtained with other genes such as the MAP kinases. Differences in the immobilized array oligonucleotide and RT-PCR primer binding sites for the specific gene being measured could account for the fold-change variations between the two methods. The fold-change in microarray experiments also is a measure of the hybridization intensity levels, as analyzed by the GCOS software. These signals were normalized as much as possible, yet the fold-change data are extremely sensitive to the computational accuracy of the software. Our microarray data for some of the genes selected does not correlate very well with the RT-PCR data, but we cannot rule out the significance of the microarray data.

Integrin interaction with its ligand leads to conformational changes, resulting in clustering or cross-linking, which constitutes the active form of the integrins and promotes the formation of cell structures, called focal adhesions, at the base of the cytosolic region of the integrins. Focal adhesions or contacts entail a complex of various proteins through which integrins integrate into the outside matrix to the cytoskeleton. The proteins concentrated within focal contacts are tyrosine phosphorylating kinases, signaling kinases, and cytoskeleton components. Actin-binding components in the focal plaques include talin, tensilin, vinculin, paxillin, and zyxin, and some of the protein kinases are focal adhesion kinase (FAK), integrin-linked kinase (ILK), and protein kinase C. Focal plaques can be detected in *B. bacilliformis*-infected cells as well, though the receptors associated with the focal contacts detected in *B. bacilliformis*-infected cells have not been studied (Verma *et al.*, 2001). An integrin-mediated event seems highly likely, as supported by two observations: *B. bacilliformis* interaction with endothelial cells is an integrin-mediated event, and focal contact formation is always associated with the beta integrin subunit.

Focal adhesion kinase (FAK)

Integrins lack intrinsic enzyme activity and depend on adaptor proteins for their downstream signal propagation. As a critical adaptor protein for the mediation of integrin signaling, the FAK protein tyrosine kinase is evolutionarily conserved and activated upon integrin activation. The major phosphorylation site is the tyrosine residue at position 397, which can be autophosphorylated (Eide *et al.*, 1995). Furthermore, FAK activity relies on direct or indirect interaction (via talin) with the beta subunit of the integrin complex (Schaller *et al.*, 1995). The ability of FAK to associate with structural

and signaling proteins is essential for the regulation of cell motility and control of apoptosis. The importance of tyrosine phosphorylation in *B. bacilliformis* infection of host cells also has been demonstrated. Initial evidence was obtained when protein tyrosine kinase inhibitors reduced *B. bacilliformis* uptake into epithelial cells (Williams-Bouyer *et al.*, 1999). In the same study, phosphorylated tyrosine kinases were detected after one hour of epithelial cell infection. A band of approximately 110kDa appeared in infected cells, which could be the similarly sized FAK protein. A time-dependent increase in FAK activity was noted in endothelial cells as well (Verma *et al.*, 2001). *B. bacilliformis* endothelial cells undergo morphological changes due to the formation of stress fibers; at 24 hours, prominent focal contacts occur at the distal ends of these fibers. These focal plaques are rich in FAK, paxillin, and phosphorylated tyrosine kinases. At 30 minutes, FAK is up-regulated by five fold, a change in expression that coincides with the increased integrin gene transcription. In addition to integrin-mediated activation, FAK induction can occur by bFGF- (basic fibroblastic growth factor) or VEGF- (vascular endothelial growth factor) mediated receptor phosphorylation (Abedi *et al.*, 1997). The VEGF mRNA up-regulation has been reported *in vitro* and occurs in our microarray studies; however, the protein has not been detected in culture (Verma *et al.*, 2001). *In situ*, though, VEGF of epithelial origin has been detected in verruga lesions and is believed to be synthesized in the presence of intracellular and/or extracellular *B. bacilliformis* (Cerimele *et al.*, 2003). Elucidation of the receptors involved in the stimulation of FAK and examination of its activity during the course of *B. bacilliformis* infection thus would represent important advances in the understanding of *B. bacilliformis* pathogenesis.

Actin-binding components

The focal plaques previously described are rich in talin, tensilin, vinculin, paxillin, and zyxin, all of which associate with actin and modulate the cytoskeletal network. Talin may recruit FAK to activate integrins by binding the carboxy terminal of FAK; it also interacts with vinculin and paxillin (Chen *et al.*, 1995). The FAK interaction with talin, and thus integrin, then causes a conformational change, a prerequisite for its autophosphorylation. The cytoskeletal protein substrates for activated FAK are paxillin and tensin, which together form an active focal adhesion complex, as required for downstream signaling. The expression of talin, vinculin, tensin, and another cytoskeletal protein, zyxin, are enhanced slightly in *B. bacilliformis*-infected HMEC-1 cells, and tensin is increased over four-fold. This finding supports the possibility of focal plaque formation early in infected cells.

Rho family GTPases and MAPKs

Rapid development of filopodia and lamellipodia occurs in cells plated on extracellular matrix (ECM), which indicates mechanisms that involve integrins and small GTPases Cdc42 and Rac. These protrusions contain cytoskeletal and signaling molecules coupled with integrin clusters. Ligand-bound integrins trigger Rac and Cdc42 activation by allowing GTP loading and membrane targeting of these molecules, which in turn leads to the phosphorylation of the downstream effector kinase, or p21-activating kinase (del Pozo *et al.*, 2000). *B. bacilliformis* infection of endothelial cells elicits the same response as ECM-mediated signaling. Filopodia formation occurs first at 30 minutes, followed by lamellipodia production at one hour. These membrane alterations are synchronized with their respective small GTPase proteins, Cdc42 and Rac (Verma *et al.*, 2002b). The

transcription analysis of Cdc42 and Rac genes in our microarray experiments shows a slight increase in Rac and a significant increase in Cdc42 gene expression, suggesting that *B. bacilliformis* infection affects these proteins at the genetic level as well. Increases in Cdc42 and Rac gene expression occur up to one hour, followed by a subsequent decrease. Enhanced gene expression should result in the production of more Rac and Cdc42 molecules, which, when activated, increase membrane ruffling and augment *B. bacilliformis* invasion. Activated Rac recruits high-affinity integrins to the leading lamellipodia, which again would be expected to facilitate *B. bacilliformis* invasion, since entry is an integrin-mediated event. The Rac in cells grown on fibronectin is induced by $\alpha_5\beta_1$, and the signals generated by activated Rac are mitogenic. Our invasion assays demonstrate that *B. bacilliformis* can bind to $\alpha_5\beta_1$ through fibronectin. Thus, in these cells, Rac may be activated by $\alpha_5\beta_1$ engagement with fibronectin-bound *B. bacilliformis*, which then leads to host cell proliferation—a hallmark of *B. bacilliformis* infections.

The other small GTPase affected by integrins is RhoA, a component of the Rho family proteins. RhoA promotes and maintains the formation of stress fibers. Surprisingly, the RhoA activation in *B. bacilliformis*-infected endothelial cells is exactly like the integrin-mediated RhoA activation pattern. The absence of activated Rho marks the first 16 hours of infection (Verma *et al.*, 2001). According to our data, the bacteria suppress the transcription of Rho early in infection which could allow for membrane modifications. Rho activity subsequently peaks with the assembly of stress fibers and focal contacts (Verma *et al.*, 2001). The initial decrease in RhoA is linked to the activation of FAK in integrin-mediated events through a bidirectional regulation (Ren *et al.*, 2000). Even though a positive expression of this gene takes place at three hours,

activated forms are not detected, so the mechanisms that repress RhoA activity may prevent its phosphorylation in the cytosol.

The downstream substrate for activated small GTPase is p21-activating kinase (PAK). Activated PAK and its genetic up-regulation appears in *B. bacilliformis*-infected endothelial cells (Verma *et al.*, 2002b). Moreover, activated PAK targets MAPK /ERK indirectly through Raf1 and MEK1, as well as JNK (MAPK8) and p38 (MAPK14) through intermediate kinases (Frost *et al.*, 1997). Thus, PAK can contribute to *B. bacilliformis* infection by acting on various cytoskeletal modulators and maintaining cell survival via the MAPK pathway.

Bacterial attachment to cell surface receptors induces a variety of signaling pathways. In the case of *B. bacilliformis*-infected endothelial cells, activated MAPKs have been detected. Of the three MAPKs, the activated forms of JNK1/2 and p38 kinase occur in infected endothelial cells, whereas ERK1/2 phosphorylation has not been studied (Verma *et al.*, 2002b). Our research with MAPK inhibitors demonstrates their necessity for *B. bacilliformis* infection. Integrin engagement by *B. bacilliformis* likely causes integrin aggregation, an event that leads to the activation of MEK1, ERK1/2, and SAPK/JNK at differing times (Miyamoto *et al.*, 1995). The analysis of MAPK gene expression indicates a two-fold or higher up-regulation of MAPK, with JNK2 (MAPK9) and p38 kinase (MAPK14) showing a twofold or greater increase after just 30 minutes of *B. bacilliformis* incubation. At six hours, all the MAPKs with the exception of p38 kinase are positively regulated. The gene expression patterns of these MAPKs compare well with the activation timeline reported in previous research (Verma *et al.*, 2002b). *B. quintana*-infected endothelial cells undergo apoptosis during the first six hours of

infection. This may be mediated by JNK and p38 kinase, since their activation coincides with increased cell death (Liberto *et al.*, 2004). The effect of JNK up-regulation and activation on *B. bacilliformis*-infected endothelial cell survival has not been examined, and its role in apoptosis remains controversial because it functions in cell survival processes as well (Salameh *et al.*, 2005). Thus, the function of JNK as a pro- or anti-apoptotic agent depends on the cell type, external stimuli, and other signaling pathways (Yu *et al.*, 2004). In turn, the effect of activated JNK and its up-regulation on *B. bacilliformis*-infected apoptosis pathways requires further elucidation before any conclusions about its role in cell survival are possible. However, JNK activation leads to the stimulation of transcription factors such as AP1, which is composed of fos and c-Jun. The gene expression of c-Jun is significantly enhanced at 30 minutes, and c-Jun continues to be up-regulated at one hour. Along with an increase in c-Jun gene expression, the protein itself is phosphorylated between one and 16 hours in *B. bacilliformis*-infected cells (Verma *et al.*, 2002b). The activity of these transcription factors is important for the regulation of various cellular functions that may be required for the successful establishment of a *B. bacilliformis* infection.

Integrin-mediated PI3K signaling

Phosphoinositide 3 kinase (PI3K) belongs to the phosphoinositide family of short-lived lipid kinases. An important downstream effector of integrin signaling, it can be activated by FAK and integrin-linked kinase (ILK). The role of FAK has been discussed in detail, whereas the function of ILK, the other kinase involved in PI3K signaling, has not been studied in relation to *B. bacilliformis* infection. Increased expression of the ILK transcript is observed in endothelial cells at one hour post infection. Initial up-regulation

would enhance *B. bacilliformis* invasion because ILK can recruit adaptor proteins for actin modulation. Integrin-dependent invasion of *Staphylococcus aureus* and *Yersinia pseudotuberculosis* also requires proper ILK expression (Wang *et al.*, 2006). It appears that ILK activation should lead to PI3K activation, which also plays a role in bacterial invasion by activating small GTPases and pseudopod formation (Qian *et al.*, 2005).

The phosphorylation state of PI3K kinase in *B. bacilliformis* remains undetermined, but invasion appears impaired in the presence of PI3K inhibitors. The PI3K enzyme consists of both regulatory and catalytic units, whose genes expressions are positively regulated up to one hour post infection. PI3K regulates certain aspects of phagocytosis including pseudopod extension and phagosome closure and actin polymerization (Allen *et al.*, 2005; Cox, Dianne *et al.*, 1999). Therefore, PI3K can act at multiple steps that are involved in *B. bacilliformis* uptake. Additionally, PI3K-dependent pathways are crucial for cell survival, and the survival of *B. bacilliformis*-infected cells also depends on PI3K, as determined by the effects of the PI3K inhibitor, LY294002. The viability of infected cells decreases dramatically in the presence of this inhibitor: by 24 hours post infection, no live cells are present. Protein kinase B (PKB) and v-akt murine thymoma viral oncogene homolog 1 (Akt) depend on PI3K for activation, after which they arrest the apoptotic cycle. Endothelial cells have high Akt-1 expression, which inhibits the pro-apoptotic molecule Bcl2, an antagonist of cell death, the Bcl2-associated X protein (BAX), and caspase 9. Akt-1 also stimulates the expression of survivin, an anti-apoptotic protein. By profiling these genes, our studies show that apoptogenic genes BAD, CASP9, and the anti-apoptotic gene BRIC5 are all up-regulated at 30 minutes. Other anti-apoptotic genes that are part of the PI3K signaling pathway

showing a sustained up-regulation include the insulin-like growth factor 1 (IGF1), which induces cell survival by activating Akt1/2, and the gene for B cell lymphoma 2 (Bcl2), which inhibits caspase activity. These mixed signals are not surprising, because one of the first lines of defense against bacterial infection is apoptosis. However, *B. bacilliformis* coinubation with endothelial cells has a mitogenic effect within just 30 minutes (Garcia, F. U. *et al.*, 1992), which means that as the cells sense invading bacteria, they “turn on” the apoptotic genes and proteins, while *B. bacilliformis* simultaneously manipulates the signaling pathways to express anti-apoptotic factors.

Induction of the gene coding for the angiogenic factor, Angiopoetin-2 has been recorded in *B. bacilliformis*-infected endothelium has been recorded both *in vivo* and *in vitro* (Cerimele *et al.*, 2003). The work of Cerimele *et al* (2003) also reveals that the VEGF in verruga lesions has an epidermal source, and that the angiogenic endothelial cells express high levels of VEGF receptors. Our microarray analysis confirms the up-regulation of angiopoetin-2. Ligation of angiopoetin and VEGF receptors activates the PI3K signal cascade; such activation gets greatly amplified when the integrin couples with its ligands (Gerber *et al.*, 1998; Kim *et al.*, 2000). A likely scenario in *B. bacilliformis*-infected cells thus depicts bacterial attachment to integrins, with additional signals from VEGFR and angiopoetin receptors triggering the activation of PI3K, which then suppresses the apoptotic proteins and maintains cell survival. These signals, coupled with other mitogenic and angiogenic signals, eventually propel the cell cycle toward cell proliferation, followed by angiogenesis. Additional studies involving the elucidation of receptors that induce PI3K activation and PI3K pathway-associated proteins could shed

more light on the mechanisms that lead to cell proliferation and angiogenesis in *B. bacilliformis* endothelial cells.

The microarray analysis of gene transcripts from *B. bacilliformis* infected endothelial cells performed here offers the first glimpse into cellular changes inflicted by these bacteria. Although all of the data could not be analyzed in this study, the alterations in gene expression levels provides us with a foundation for future research to understand the complex cellular reactions that occur during *B. bacilliformis* infection.

Summary and conclusions

B. bacilliformis can attach to and invade vascular endothelial cells; according to our observations and these interactions depend on cell surface integrins. The integrin with the most significant role in endothelial cell infection is $\alpha_5\beta_1$, an integrin known to be essential for cell adhesion to the extracellular matrix as well as cell proliferation, spreading, and survival. Functional blocking of $\alpha_5\beta_1$ inhibits internalization of bacteria by 80% and severely decreases *B. bacilliformis* attachment. Expression of the α_5 and β_1 genes increases after infection for up to six and one hour, respectively, and this increased expression would be expected to enhance the efficiency of *B. bacilliformis* uptake. The other integrins possibly involved are $\alpha_V\beta_3$ and integrins containing β_1 , since antibodies against these molecules also decrease the invasion by 30% on average. Pathogenic engagement of integrins could be direct or through their ligands. The extracellular matrix proteins fibronectin and vitronectin are the natural ligands for $\alpha_5\beta_1$ and $\alpha_V\beta_3$, respectively. These proteins are present in a soluble plasma form and an insoluble cellular form as a part of the extracellular matrix. According to our data, plasma and cellular protein association with *B. bacilliformis* enhances internalization, but endothelial cell infection can occur even in its absence (Figure 3.2a)

Loading of integrins leads to their clustering and transforms them into an activated conformation, which results in cytoplasmic signal transduction that regulates various cellular processes. We propose a hypothetical working model that describes the integrin-mediated cell signaling events that may take place after *B. bacilliformis* infection (Figure 3.2b). According to this model, integrin clustering gives way to the formation of a focal adhesion plaque, which consists of a group of proteins that interact to facilitate

signal transduction. In this respect, phosphorylated tyrosine kinases (PTKs) play central roles, because integrins lack intrinsic enzymatic activity. All integrins with β_1 and α_v phosphorylate focal adhesion kinase, a PTK, which is followed by the formation of stress fibers and focal adhesion plaques at the base of the cytoplasmic domain of integrins. *B. bacilliformis* infection of endothelial cells results in the formation of stress fibers of F-actin bundles (Verma *et al.*, 2001). Focal adhesion structures, which appear at the base of these stress fibers, consist of paxillin, FAK, and PTKs, and the non-specific inhibition of PTKs decreases *B. bacilliformis* invasion (Williams-Bouyer *et al.*, 1999). Based on our microarray data and studies by Verma *et al.* (2000), we propose that *B. bacilliformis* binding to integrins induces the formation of actin polymerization and focal adhesion complexes upon binding. The activated kinases of the focal plaque could trigger the downstream activation of various kinases, including p21-activating kinase (PAK), Ras, and PI3K. Phosphorylated PI3K and Ras then could mediate the stimulation of small GTPases, Rac1, and Cdc42, as seen in *B. bacilliformis* infected cells as early as 30 minutes post infection until as late as eight hours into the infection (Verma *et al.*, 2002b). The membrane alterations brought on by activated Rac1 and Cdc42 thus are proposed as the leading cause of *B. bacilliformis* internalization.

The next step of the cascade involves the stimulation of PAK, a substrate for both FAK and Rac1. The activated form of PAK and PAK gene up-regulation can be detected in *B. bacilliformis*-infected cells at two hours after infection (Verma *et al.*, 2002b). Phosphorylated PAK is an upstream modulator of MAPKs, ERK1/2, JNK, and p38. Phosphorylated ERK1/2 proteins are involved in cell structure remodeling, and the stress-activated kinase JNK is known to induce transcription factors, which promote cell

survival and actin rearrangements. Lastly, p38 can also be activated by PAK and is involved in *C. jejuni* and *S.typhi* invasion of epithelial cells. Therefore, on the basis of previous studies that detect activated JNK and p38, as well as our microarray data and inhibitor studies, we can assume that the initial entry of *B. bacilliformis* is a MAPK-dependent event. The fold-change analysis of FAK, PAK, Rac1, and Cdc42 shows that their gene expression is down-regulated three hours post-infection, although the down-regulation is not significant. Proteomic studies would be required to confirm their suppression at the protein level, but it seems likely that these proteins would be inactivated by the host cell machinery to inhibit parasitization. *B. bacilliformis* invasion is a continuous process, and the up-regulation of FAK and PAK at three and six hours, respectively, suggests that *B. bacilliformis* has the potential to overcome the host cell defenses and induced conditions that could favor its uptake.

Like all intracellular pathogens, *B. bacilliformis* depends on host cell survival to propagate its intracellular lifestyle. Our model proposes the integrin-dependent activation of PI3K, a kinase with multiple functions including cytoskeletal rearrangement and suppression of apoptogenic proteins. The inhibitors of PI3K kinase prevent the internalization of *B. bacilliformis* and induce apoptosis within two hours of infection. Therefore, PI3K could play an important role throughout the course of the infection by sustaining cell survival and abetting *B. bacilliformis* invasion.

In conclusion, this study, the first to demonstrate the role of endothelial cell integrins as *B. bacilliformis* receptors, also clarifies the role of ECM proteins in *B. bacilliformis* infection. Furthermore, our invasion assay data suggest that both plasma and cellular ECM proteins assist *B. bacilliformis* invasion. Cellular signaling pathway

activation is required for cytoskeletal remodeling, proliferation, and the prevention of apoptosis. Although *B. bacilliformis* invasion is not completely dependent on one particular kinase, we note the requirement of MEK1/2, JNK, and p38 kinases. Finally, experiments with PI3K inhibitors strongly support the hypothesis that *B. bacilliformis*-infected endothelial cells transduce anti-apoptotic signals through the PI3K-Pkb/Akt pathway. We have not determined the effect of integrin blocking on the various members of the integrin signaling pathway, yet we provide necessary data for further research into this aspect of *B. bacilliformis* pathogenesis. With further studies on the role of integrin signaling during *B. bacilliformis* infection, it should be possible to compare the gene expression pattern and the protein activation states of infected wild type cells with infected integrin negative cell lines. This study would definitively establish the role of these proteins in the infection process.

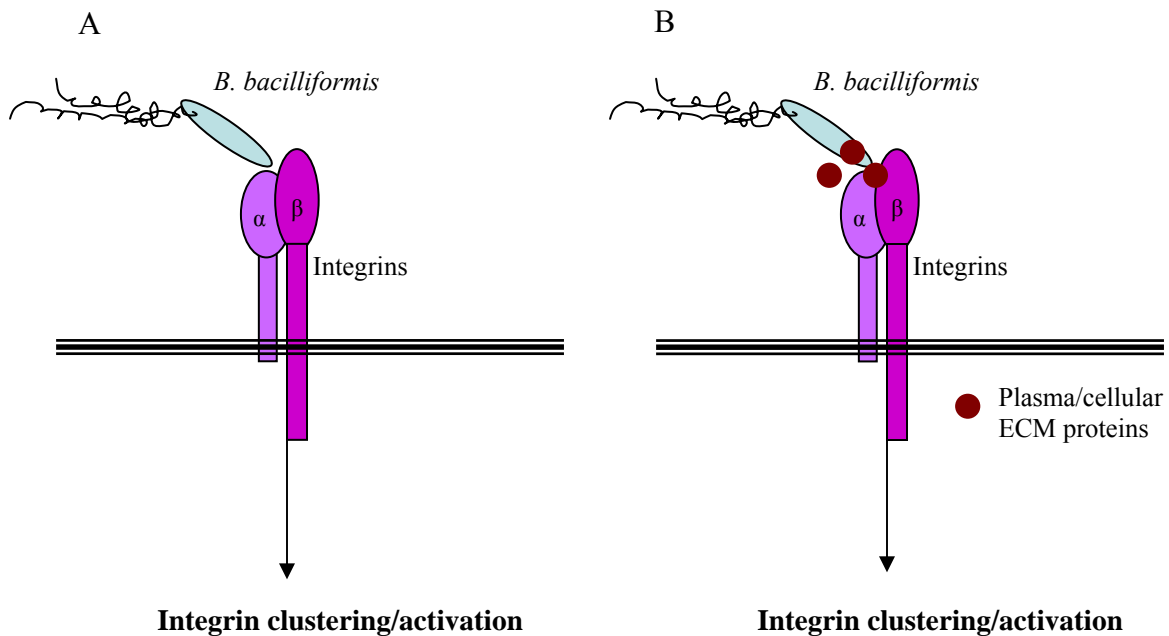


Figure 3.2a. *Bartonella bacilliformis* binding to integrins.

B. bacilliformis attachment to integrins can be a direct event (A) or the bacteria can interact with integrin ligands that bridge bacterial binding to integrins (B). The integrin ligands fibronectin and/or vitronectin can be of the plasma or cellular origin. *B. bacilliformis* binding to integrins then leads to their clustering, a conformational change resulting in integrin activation.

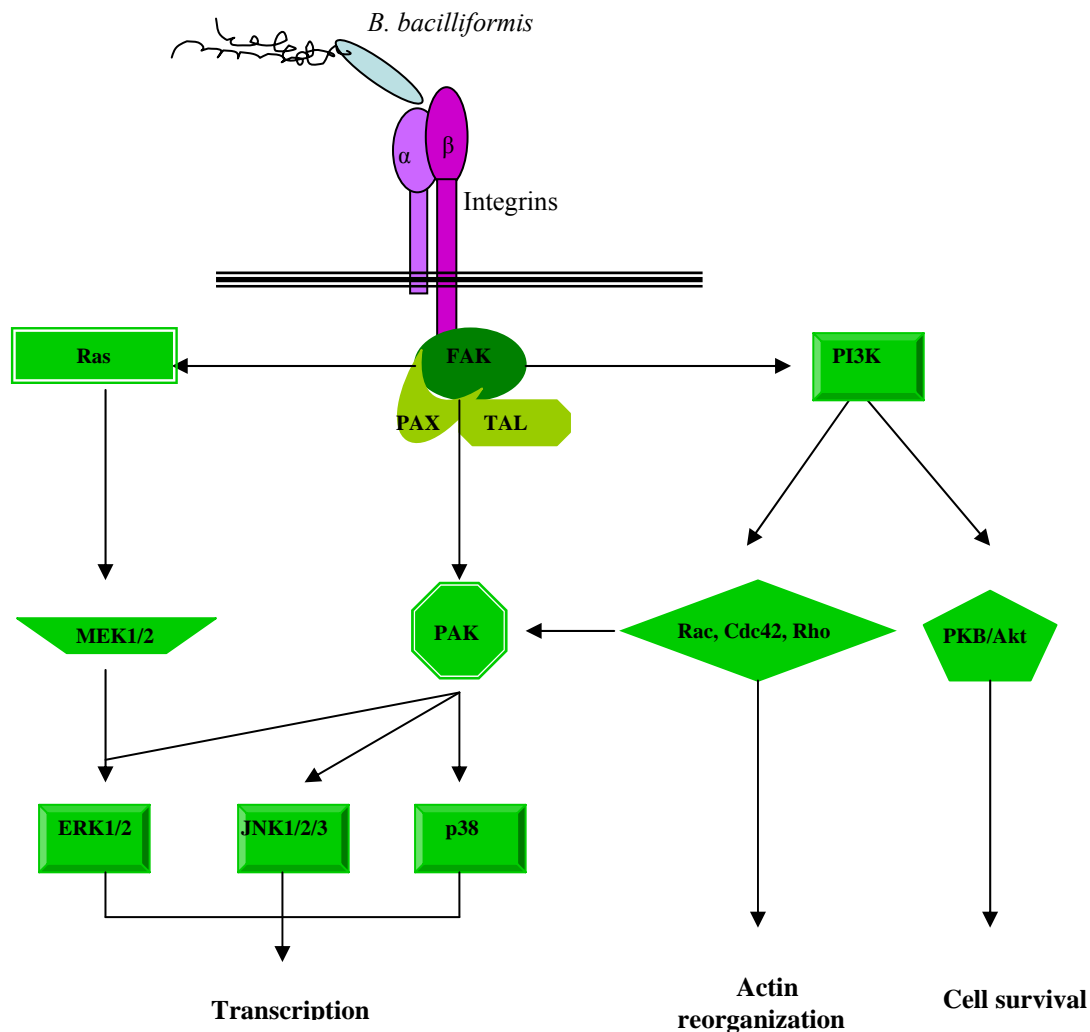


Figure 3.2b. Integrin mediated signaling events occurring after *B. bacilliformis* attachment to integrins.

B. bacilliformis binding to integrins triggers a signaling cascade involving the protein tyrosine kinase focal adhesion kinase (FAK) that forms a focal adhesion plaque with paxillin (PAX) and talin (TAL). Activated FAK then activates Ras, p21 activating kinase (PAK) and phosphatidylinositol 3 kinase (PI3K), which eventually results in the phosphorylation of mitogen activated kinases (MAPKs): extracellular receptor kinase 1/2 (ERK1/2), Jun N-terminal kinase (JNK) and p38 kinase. These MAPKs regulate cellular transcriptional events that account for the changes that occur in response to *B. bacilliformis* infections. Activation of the small GTPases, Rac, Cdc42 and Rho by PI3K results in alterations of the actin network symbolized by formation of lamellipodia and filopodia that aide *B. bacilliformis* internalization. The activation of protein kinase B (PKB) and v-akt murine thymoma viral oncogene homolog 1 (Akt) by PI3K is proposed to be involved in generation of anti-apoptotic signals that allow the *B. bacilliformis* infected cell to survive.

Bibliography

- Abedi, H. and I. Zachary** (1997). "Vascular Endothelial Growth Factor Stimulates Tyrosine Phosphorylation and Recruitment to New Focal Adhesions of Focal Adhesion Kinase and Paxillin in Endothelial Cells." J. Biol. Chem. **272**(24): 15442-15451.
- Ades EW, Candal FJ, Swerlick RA, George VG, Summers S, Bosse DC and L. TJ.** (1992). "HMEC-1: establishment of an immortalized human microvascular endothelial cell line." The Journal of investigative dermatology **99**(6): 683-90.
- Agerer, F., S. Lux, A. Michel, M. Rohde, K. Ohlsen and C. R. Hauck** (2005). "Cellular invasion by Staphylococcus aureus reveals a functional link between focal adhesion kinase and cortactin in integrin-mediated internalisation." J Cell Sci **118**(10): 2189-2200.
- Alessi, D. R., A. Cuenda, P. Cohen, D. T. Dudley and A. R. Saltiel** (1995). "PD 098059 Is a Specific Inhibitor of the Activation of Mitogen-activated Protein Kinase Kinase *in vitro* and *in vivo*." J. Biol. Chem. **270**(46): 27489-27494.
- Alessi, D. R., Y. Saito, D. G. Campbell, P. Cohen, G. Sithanandam, U. Rapp, A. Ashworth, C. J. Marshall and S. Cowley** (1994). "Identification of sites in MAPkinase kinase-1 phosphorylated by p74raf-1." EMBO J. **13**(7): 1610-9.
- Alexander, B.** (1995). "A Review of Bartonellosis in Ecuador and Colombia." Am J Trop Med Hyg **52**(4): 354-359.
- Allen, L.-A. H., J. A. Allgood, X. Han and L. M. Wittine** (2005). "Phosphoinositide3-kinase regulates actin polymerization during delayed phagocytosis of Helicobacter pylori." J Leukoc Biol **78**(1): 220-230.
- Alsmark, C. M., A. C. Frank, E. O. Karlberg, B.-A. Legault, D. H. Ardell, B. Canback, A.-S. Eriksson, A. K. Naslund, S. A. Handley, M. Huvet, B. La Scola, M. Holmberg and S. G. E. Andersson** (2004). "The louse-borne human pathogen Bartonella quintana is a genomic derivative of the zoonotic agent Bartonella henselae." Proceedings of the National Academy of Sciences **101**(26): 9716-9721.
- Anand-Apte, B., B. R. Zetter, A. Viswanathan, R.-G. Qiu, J. Chen, R. Ruggieri and M. Symons** (1997). "Platelet-derived Growth Factor and Fibronectin-stimulated Migration Are Differentially Regulated by the Rac and Extracellular Signal-regulated Kinase Pathways." J. Biol. Chem. **272**(49): 30688-30692.
- Arias-Stella, J., P. H. Lieberman, R. A. Erlandson and J. Arias-Stella, Jr.** (1986a). "Histology, immunohistochemistry, and ultrastructure of the verruga in Carrion's disease." Am J Surg Pathol **10**(9): 595-610.
- Arias-Stella, J., P. H. Lieberman, R. A. Erlandson and J. J. Arias-Stella** (1986b). "Histology, immunohistochemistry, and ultrastructure of the verruga in Carrion's disease." American Journal of Surgical Pathology **10**(9): 595-610.
- Arrese Estrada, J. and G. E. Pierard** (1992). "Dendrocytes in verruga peruana and bacillary angiomatosis." Dermatology **184**(1): 22-5.
- Batterman, H. J., J. A. Peek, J. S. Loutit, S. Falkow and L. S. Tompkins** (1995). "Bartonella henselae and Bartonella quintana adherence to and entry into cultured human epithelial cells." Infect. Immun. **63**(11): 4553-4556.

- Battisti, J. M. and M. F. Minnick** (1999). "Development of a System for Genetic Manipulation of *Bartonella bacilliformis*." Appl. Environ. Microbiol. **65**(8): 3441-3448.
- Benson, L. A., S. Kar, G. McLaughlin and G. M. Ihler** (1986). "Entry of *Bartonella bacilliformis* into erythrocytes." Infect. Immun. **54**(2): 347-353.
- Berge, V., E. Johnson, K. Hogasen and G. Hetland** (1992). "Human umbilical vein endothelial cells synthesize S-protein (vitronectin) *in vitro*." Scandinavian Journal of Immunology **36**(1): 119-23.
- Birtles, R. J., T. G. Harrison, N. A. Saunders and D. H. Molyneux** (1995). "Proposals to unify the genera *Grahamella* and *Bartonella*, with descriptions of *Bartonella talpae* comb. nov., *Bartonella peromysci* comb. nov., and three new species, *Bartonella grahamii* sp. nov., *Bartonella taylorii* sp. nov., and *Bartonella doshiae* sp. nov." Int J Syst Bacteriol **45**(1): 1-8.
- Bliska, J. B., M. C. Copass and S. Falkow** (1993). "The *Yersinia pseudotuberculosis* adhesin YadA mediates intimate bacterial attachment to and entry into HEp-2 cells." Infect. Immun. **61**(9): 3914-3921.
- Booth, J. W., D. Telio, E. H. Liao, S. E. McCaw, T. Matsuo, S. Grinstein and S. D. Gray-Owen** (2003). "Phosphatidylinositol 3-Kinases in Carcinoembryonic Antigen-related Cellular Adhesion Molecule-mediated Internalization of *Neisseria gonorrhoeae*." J. Biol. Chem. **278**(16): 14037-14045.
- Brenner, D. J., S. P. O'Connor, D. G. Hollis, R. E. Weaver and A. G. Steigerwalt** (1991). "Molecular characterization and proposal of a neotype strain for *Bartonella bacilliformis*." J. Clin. Microbiol. **29**(7): 1299-1302.
- Brenner, D. J., S. P. O'Connor, H. H. Winkler and A. G. Steigerwalt** (1993). "43." **4** **777-86**.
- Brock, T. D.** (1999). "Robert Koch, a life in medicine and bacteriology." Washington DC, ASM Press.
- Brouqui, P. and D. Raoult** (1996). "*Bartonella quintana* invades and multiplies within endothelial cells *in vitro* and *in vivo* and forms intracellular blebs." Research in Microbiology **147**(9): 719-731.
- Bryant, P. A., D. Venter, R. Robins-Browne and N. Curtis** (2004). "Chips with everything: DNA microarrays in infectious diseases." The Lancet Infectious Diseases **4**(2): 100-111.
- Buckles, E. L. and E. McGinnis Hill** (2000). "Interaction of *Bartonella bacilliformis* with human erythrocyte membrane proteins." Microbial Pathogenesis **29**(3): 165-74.
- Burgess, A. W. O. and B. E. Anderson** (1998). "Outer membrane proteins of *Bartonella henselae* and their interaction with human endothelial cells." Microbial Pathogenesis **25**(3): 157-164.
- Burke, R.** (1999). "Invertebrate integrins: Structure, Function and Evolution." International Review of Cytology **191**: 257-284.
- Caceres-Rios, H., J. Rodriguez-Tafur, F. Bravo-Puccio, C. Maguina-Vargas, C. S. Diaz, D. c. Ramos and R. Patarca** (1995). "Verruga peruana: An infectious endemic angiomatosis." Critical Reviews in Oncogenesis **6**(1): 47-56.
- Cantley, L. C.** (2002). "The phosphoinositide 3-kinase pathway." Science **296**(5573): 1655-7.

- Cartwright, J. L., P. Britton, M. F. Minnick and A. G. McLennan** (1999). "The IalA Invasion Gene of *Bartonella bacilliformis* Encodes a (Di)Nucleoside Polyphosphate Hydrolase of the MutT Motif Family and Has Homologs in Other Invasive Bacteria." Biochemical and Biophysical Research Communications **256**(3): 474-479.
- Cascales, E. and P. J. Christie** (2003). "The versatile bacterial type IV secretion systems." Nat Rev Micro **1**(2): 137-149.
- Cerimele, F., L. F. Brown, F. Bravo, G. M. Ihler, P. Kouadio and J. L. Arbiser** (2003). "Infectious Angiogenesis: *Bartonella bacilliformis* Infection Results in Endothelial Production of Angiopoietin-2 and Epidermal Production of Vascular Endothelial Growth Factor." Am J Pathol **163**(4): 1321-1327.
- Chen, H.-C., P. A. Appeddu, J. T. Parsons, J. D. Hildebrand, M. D. Schaller and J.-L. Guan** (1995). "Interaction of Focal Adhesion Kinase with Cytoskeletal Protein Talin." J. Biol. Chem. **270**(28): 16995-16999.
- Cheng, T., M. Symons and T. Jou** (2004). "Regulation of anoikis by Cdc42 and Rac1." Experimental Cell Research **295**(2): 497-511.
- Coburn, J. and C. Cugini** (2003a). "Targeted mutation of the outer membrane protein P66 disrupts attachment of the Lyme disease agent, *Borrelia burgdorferi*, to integrin $\alpha v \beta 3$." Proceedings of the National Academy of Sciences **100**(12): 7301-7306.
- Coburn, J. and C. Cugini** (2003b). Targeted mutation of the outer membrane protein P66 disrupts attachment of the Lyme disease agent, *Borrelia burgdorferi*, to integrin $\alpha v \beta 3$. **100**: 7301-7306.
- Coburn, J. and C. Cugini** (2003c). "Targeted mutation of the outer membrane protein P66 disrupts attachment of the Lyme disease agent, *Borrelia burgdorferi*, to integrin $\alpha v \beta 3$." PNAS **100**(12): 7301-6.
- Coburn, J., L. Magoun, S. C. Bodary and J. M. Leong** (1998). "Integrins $\alpha v \beta 3$ and $\alpha 5 \beta 1$ Mediate Attachment of Lyme Disease Spirochetes to Human Cells." Infect. Immun. **66**(5): 1946-1952.
- Cockerell, C. J., M. A. Whitlow, G. F. Webster and A. E. friedman-kien** (1987). "Epithelioid angiomatosis: a distinct vascular disorder in patients with the acquired immunodeficiency syndrome or AIDS-related complex." Lancet **2**(8560): 654-6.
- Coleman, S. A. and M. F. Minnick** (2001). "Establishing a Direct Role for the *Bartonella bacilliformis* Invasion-Associated Locus B (IalB) Protein in Human Erythrocyte Parasitism." Infect. Immun. **69**(7): 4373-4381.
- Coombes, B. K. and J. B. Mahony** (2002). "Identification of MEK- and phosphoinositide 3-kinase-dependent signalling as essential events during *Chlamydia pneumoniae* invasion of HEp2 cells." Cellular Microbiology **4**(7): 447-460.
- Cox, D., C.-C. Tseng, G. Bjekic and S. Greenberg** (1999). "A Requirement for Phosphatidylinositol 3-Kinase in Pseudopod Extension." J. Biol. Chem. **274**(3): 1240-1247.
- Cox, D., C. Tseng, G. Bjeckic and S. Greenberg** (1999). "A requirement for phosphatidylinositol 3-kinase in pseudopod extension." The Journal of Biological Chemistry **274**(3): 1240-47.

- Crews, C. M., A. Alessandrini and R. L. Erikson** (1992). "The primary structure of MEK, a protein kinase that phosphorylates the ERK gene product." Science **258**(5081): 478-80.
- Cuadra, M.** (1956). "Salmonellosis complication in human bartonellosis." Texas Reports on Biology and Medicine **14**(2): 97-113.
- Cue, D., S. O. Southern, P. J. Southern, J. Prabhakar, W. Lorelli, J. M. Smallheer, S. A. Mousa and P. P. Cleary** (2000). A nonpeptide integrin antagonist can inhibit epithelial cell ingestion of *Streptococcus pyogenes* by blocking formation of integrin alpha 5 beta 1-fibronectin-M1 protein complexes. **97**: 2858-2863.
- Cuenda, A., J. Rouse, Y. N. Doza, R. Meier, P. Cohen, T. F. Gallagher, P. R. Young and J. C. Lee** (1995). "SB 203580 is a specific inhibitor of a MAP kinase homologue which is stimulated by cellular stresses and interleukin-1." FEBS Letters **364**(2): 229-233.
- Cueto, M.** (1996). "Tropical medicine and bacteriology in Boston and Peru: studies of Carrión's disease in the early twentieth century." Medical History **40**(3): 344-64.
- Dabo, S. M., A. W. Confer, J. T. Saliki and B. E. Anderson** (2006). "Binding of *Bartonella henselae* to extracellular molecules: Identification of potential adhesins." Microbial Pathogenesis **41**(1): 10-20.
- Dadgostar, H., S. E. Doyle, A. Shahangian, D. E. Garcia and G. Cheng** (2003). "T3JAM, a novel protein that specifically interacts with TRAF3 and promotes the activation of JNK." FEBS Letters **553**(3): 403-407.
- Datta, S. R., H. Dudek, X. Tao, S. Masters, H. Fu, Y. Gotoh and M. E. Greenberg** (1997). "Akt Phosphorylation of BAD Couples Survival Signals to the Cell-Intrinsic Death Machinery." Cell **91**(2): 231-241.
- Dehio, C., M. Meyer, J. Berger, H. Schwarz and C. Lanz** (1997). "Interaction of *Bartonella henselae* with endothelial cells results in bacterial aggregation on the cell surface and the subsequent engulfment and internalisation of the bacterial aggregate by a unique structure, the invasome." J Cell Sci **110**(18): 2141-2154.
- Dehio, M., O. G. Gomez-Duarte, C. Dehio and T. F. Meyer** (1998). "Vitronectin-dependent invasion of epithelial cells by *Neisseria gonorrhoeae* involves [alpha]v integrin receptors." FEBS Letters **424**(1-2): 84-88.
- Dehio, M., M. Quebatte, S. Foser and U. Certa** (2005). "The transcriptional response of human endothelial cells to infection with *Bartonella henselae* is dominated by genes controlling innate immune responses, cell cycle, and vascular remodelling." Thrombosis and Haemostasis **94**(2): 347-61.
- del Pozo, M. A., L. S. Price, N. B. Alderson, X. D. Ren and M. A. Schwartz** (2000). "Adhesion to extracellular matrix regulates the coupling of the small GTPase Rac to its effector PAK." EMBO J. **19**(9): 2008-14.
- Derrick, S. C. and G. M. Ihler** (2001). "Deformin, a substance found in *Bartonella bacilliformis* culture supernatants, is a small, hydrophobic molecule with an affinity for albumin." Blood, Cells, Molecules and Disease **27**(6): 1013-19.
- Draghici, S.** (2002). "Statistical intelligence: effective analysis of high-density microarray data." Drug Discovery Today **7**(11): S55-S63.
- Eide, B. L., C. W. Turck and J. A. Escobedo** (1995). "Identification of Tyr-397 as the primary site of tyrosine phosphorylation and pp60src association in the focal adhesion kinase, pp125FAK." Mol. Cell. Biol. **15**(5): 2819-2827.

- Ellington, J. K., A. Elhofy, K. L. Bost and M. C. Hudson** (2001). "Involvement of Mitogen-Activated Protein Kinase Pathways in Staphylococcus aureus Invasion of Normal Osteoblasts." Infection and Immunity **69**(9): 5235-5242.
- English, J. M., G. Pearson, T. Hockenberry, L. Shivakumar, M. A. White and M. H. Cobb** (1999). "Contribution of the ERK5/MEK5 Pathway to Ras/Raf Signaling and Growth Control." J. Biol. Chem. **274**(44): 31588-31592.
- Everest, P., J. Li, G. Douce, I. Charles, J. De Azavedo, S. Chatfield, G. Dougan and M. Roberts** (1996). "Role of the *Bordetella pertussis* P.69/pertactin and the P.69/pertactin RGD motif in the adhesion and invasion of mammalian cells." Microbiology **142**(11): 3261-68.
- Favata, M. F., K. Y. Horiuchi, E. J. Manos, A. J. Daulerio, D. A. Stradley, W. S. Feeser, D. E. Van Dyk, W. J. Pitts, R. A. Earl, F. Hobbs, R. A. Copeland, R. L. Magolda, P. A. Scherle and J. M. Trzaskos** (1998). "Identification of a Novel Inhibitor of Mitogen-activated Protein Kinase Kinase." J. Biol. Chem. **273**(29): 18623-18632.
- Forsberg, M., R. Blomgran, M. Lerm, E. Sarndahl, S. M. Sebti, A. Hamilton, O. Stendahl and L. Zheng** (2003). "Differential effects of invasion by and phagocytosis of Salmonella typhimurium on apoptosis in human macrophages: potential role of Rho-GTPases and Akt." J Leukoc Biol **74**(4): 620-629.
- Frankel, G., O. Lider, R. Hershkoviz, A. P. Mould, S. G. Kachalsky, D. C. A. Candy, L. Cahalon, M. J. Humphries and G. Dougan** (1996). The Cell-binding Domain of Intimin from Enteropathogenic Escherichia coli Binds to beta 1 Integrins. **271**: 20359-20364.
- Frost, J. A., H. Steen, P. Shapiro, T. Lewis, N. Ahn, P. E. Shaw and M. H. Cobb** (1997). "Cross-cascade activation of ERKs and ternary complex factors by Rho family proteins." EMBO J. **16**(21): 6426-38.
- Fuhrmann, O., M. Arvand, A. Gohler, M. Schmid, M. Krull, S. Hippenstiel, J. Seybold, C. Dehio and N. Suttorp** (2001). "Bartonella henselae Induces NF- κ B-Dependent Upregulation of Adhesion Molecules in Cultured Human Endothelial Cells: Possible Role of Outer Membrane Proteins as Pathogenic Factors." Infect. Immun. **69**(8): 5088-5097.
- Gailit, J. and E. Ruoslahti** (1988). "Regulation of the fibronectin receptor affinity by divalent cations." J. Biol. Chem. **263**(26): 12927-12932.
- Gao, H., Y. Wang, X. Liu, T. Yan, L. Wu, E. Alm, A. Arkin, D. K. Thompson and J. Zhou** (2004). "Global Transcriptome Analysis of the Heat Shock Response of Shewanella oneidensis." J. Bacteriol. **186**(22): 7796-7803.
- Garcia-Caceres, U. and F. U. Garcia** (1991). "Bartonellosis. An immunodepressive disease and the life of Daniel Alcides Carrion." American Journal of Clinical Pathology **95** (4 Suppl 1): S58-66.
- Garcia, F., J. Wojta and R. Hoover** (1992). "Interactions between Live *Bartonella bacilliformis* and Endothelial Cells." Journal of Infectious Diseases **165**: 1138-1141.
- Garcia, F. U., J. Wojta, K. N. Broadley, J. M. Davidson and R. L. Hoover** (1990). "Bartonella bacilliformis stimulates endothelial cells *in vitro* and is angiogenic *in vivo*." American Journal of Pathology **136**(5): 1125-35.

- Garcia, F. U., J. Wojta and R. L. Hoover** (1992). "Interactions between live *Bartonella bacilliformis* and endothelial cells." Journal of Infectious Diseases **165**(6): 1138-41.
- Gerber, H.-P., A. McMurtrey, J. Kowalski, M. Yan, B. A. Keyt, V. Dixit and N. Ferrara** (1998). "Vascular Endothelial Growth Factor Regulates Endothelial Cell Survival through the Phosphatidylinositol 3'-Kinase/Akt Signal Transduction Pathway. REQUIREMENT FOR Flk-1/KDR ACTIVATION." J. Biol. Chem. **273**(46): 30336-30343.
- Gibbs, J. B., M. S. Marshall, E. M. Scolnick, R. A. Dixon and U. S. Vogel** (1990). "Modulation of guanine nucleotides bound to Ras in NIH3T3 cells by oncogenes, growth factors, and the GTPase activating protein (GAP)." J. Biol. Chem. **265**(33): 20437-20442.
- Gum, R. J., M. M. McLaughlin, S. Kumar, Z. Wang, M. J. Bower, J. C. Lee, J. L. Adams, G. P. Livi, E. J. Goldsmith and P. R. Young** (1998). "Acquisition of Sensitivity of Stress-activated Protein Kinases to the p38 Inhibitor, SB 203580, by Alteration of One or More Amino Acids within the ATP Binding Pocket." J. Biol. Chem. **273**(25): 15605-15610.
- Halasz, P., G. Holloway, S. J. Turner and B. S. Coulson** (2008). "Rotavirus Replication in Intestinal Cells Differentially Regulates Integrin Expression by a Phosphatidylinositol 3-Kinase-Dependent Pathway, Resulting in Increased Cell Adhesion and Virus Yield." J. Virol. **82**(1): 148-160.
- Hamzaoui, N., S. Kerneis, E. Caliot and E. Pringault** (2004). Expression and distribution of beta1 integrins in *in vitro*-induced M cells: implications for *Yersinia* adhesion to Peyer's patch epithelium. **6**: 817-828.
- Han, J., J. D. Lee, L. Bibbs and R. J. Ulevitch** (1994). "A MAP kinase targeted by endotoxin and hyperosmolarity in mammalian cells." Science **265**(5173): 808-11.
- Harrison, R. E., B. A. Sikorski and J. Jongstra** (2004). "Leukocyte-specific protein 1 targets the ERK/MAP kinase scaffold protein KSR and MEK1 and ERK2 to the actin cytoskeleton." J Cell Sci **117**(10): 2151-2157.
- Hayashi, M., C. Fearn, B. Eliceiri, Y. Yang and J.-D. Lee** (2005). "Big Mitogen-Activated Protein Kinase 1/Extracellular Signal-Regulated Kinase 5 Signaling Pathway Is Essential for Tumor-Associated Angiogenesis." Cancer Res **65**(17): 7699-7706.
- Hendrix, L. R.** (2000). "Contact-dependent hemolytic activity distinct from deforming activity of *Bartonella bacilliformis*." FEMS Microbiology Letters **182**(1): 119-24.
- Herrer, A. and C. H. A.** (1975). "Implication of *Phlebotomus* sand flies as vectors of bartonellosis and leishmaniasis as early as 1764." Science **190**(4210): 154-5.
- Hertig, M.** (1942). "*Phlebotomus* and Carrion's disease." American Journal of Tropical Medicine **22**(Suppl 1-81).
- Higgins, J. A., S. Radulovic, D. C. Jaworski and A. F. Azad** (1996). "Acquisition of the cat scratch disease agent *Bartonella henselae* by cat fleas (Siphonaptera: Pulicidae)." Journal of Medical Entomology. **33**(3): 490-5.
- Hill, E. M., A. Raji, M. S. Valenzuela, F. Garcia and R. Hoover** (1992). "Adhesion to and invasion of cultured human cells by *Bartonella bacilliformis*." Infect. Immun. **60**(10): 4051-4058.

- Hobbie, S., L. M. Chen, R. J. Davis and J. E. Galan** (1997). "Involvement of mitogen-activated protein kinase pathways in the nuclear responses and cytokine production induced by Salmonella typhimurium in cultured intestinal epithelial cells." J Immunol **159**(11): 5550-5559.
- Hu, L., J. P. McDaniel and D. J. Kopecko** (2006). "Signal transduction events involved in human epithelial cell invasion by Campylobacter jejuni 81-176." Microbial Pathogenesis **40**(3): 91-100.
- Huang, C., K. Jacobson and M. D. Schaller** (2004). "MAP kinases and cell migration." J Cell Sci **117**(20): 4619-4628.
- Huang, X. Z., A. Chen, M. Agrez and D. Sheppard** (1995). "A point mutation in the integrin beta 6 subunit abolishes both alpha v beta 6 binding to fibronectin and receptor localization to focal contacts." American journal of respiratory cell and molecular biology **13**(2): 245-51.
- Hughes, P. E., F. Diaz-Gonzalez, L. Leong, C. Wu, J. A. McDonald, S. J. Shattil and M. H. Ginsberg** (1996). "Breaking the Integrin Hinge." J. Biol. Chem. **271**(12): 6571-6574.
- Hynes, R. O.** (2002). "Integrins: Bidirectional, Allosteric Signaling Machines." Cell **110**(6): 673-687.
- Hynes, R. O. and Q. Zhao** (2000). "The Evolution of Cell Adhesion." J. Cell Biol. **150**(2): 89F-96.
- Ihler, G. M.** (1996). "Bartonella bacilliformis: dangerous pathogen slowly emerging from deep background." FEMS Microbiology Letters **144**(1): 1-11.
- Inohara, I., L. Ding, S. Chen and G. Nunez** (1997). "Harakiri, a novel regulator of cell death, encodes a protein that activates apoptosis and interacts selectively with survival-promoting proteins Bcl-2 and Bcl-X(L)." EMBO J **16**(7): 1686-94.
- Ireton, K., B. Payrastre, H. Chap, W. Ogawa, H. Sakaue, M. Kasuga and P. Cossart** (1996). "A role of phosphoinositide 3-kinase in bacterial invasion." Science **274**(5288): 780-2.
- Ishibashi, Y. and A. Nishikawa** (2002). "Bordetella pertussis infection of human respiratory epithelial cells up-regulates intercellular adhesion molecule-1 expression: role of filamentous hemagglutinin and pertussis toxin." Microbial Pathogenesis **33**(3): 115-125.
- Ishibashi, Y., D. A. Relman and A. Nishikawa** (2001). "Invasion of human respiratory epithelial cells by Bordetella pertussis: Possible role for a filamentous hemagglutinin Arg-Gly-Asp sequence and [alpha]5[beta]1 integrin." Microbial Pathogenesis **30**(5): 279-288.
- Ishibe, S., D. Joly, X. Zhu and L. G. Cantley** (2003). "Phosphorylation-dependent paxillin-ERK association mediates hepatocyte growth factor-stimulated epithelial morphogenesis." Molecular Cell **12**(5): 1275-85.
- Jackson, T., D. Sheppard, M. Denyer, W. Blakemore and A. M. Q. King** (2000). "The Epithelial Integrin alpha v beta 6 Is a Receptor for Foot-and-Mouth Disease Virus." J. Virol. **74**(11): 4949-4956.
- Jaffe, E. A. and D. F. Mosher** (1978). "Synthesis of fibronectin by cultured human endothelial cells." Journal Experimental Medicine **147**(6): 1779-91.
- Johansson, S. and K. W. Gunbjørg Svineng, Annika Armulik, Lars Lohikangas** (1997). "Fibronectin-Integrin Interaction." Frontiers in Bioscience **2**: d:126-146.

- Johnson, G. L. and R. Lapadat** (2002). "Mitogen-Activated Protein Kinase Pathways Mediated by ERK, JNK, and p38 Protein Kinases." Science **298**(5600): 1911-1912.
- Jonsson, K., C. Signas, H.-P. Muller and M. Lindberg** (1991a). Two different genes encode fibronectin binding proteins in *Staphylococcus aureus*. The complete nucleotide sequence and characterization of the second gene. **202**: 1041-1048.
- Jonsson, K., C. Signas, H.-P. Muller and M. Lindberg** (1991b). "Two different genes encode fibronectin binding proteins in *Staphylococcus aureus*. The complete nucleotide sequence and characterization of the second gene." European Journal of Biochemistry **202**(3): 1041-1048.
- Kato, Y., R. I. Tapping, S. Huang, M. H. Watson, R. J. Ulevitch and J.-D. Lee** (1998). "Bmk1/Erk5 is required for cell proliferation induced by epidermal growth factor." Nature **395**(6703): 713-716.
- Kempf, V. A. J., B. Volkmann, M. Schaller, C. A. Sander, K. Alitalo, T. Riess and I. B. Autenrieth** (2001). "Evidence of a leading role for VEGF in *Bartonella henselae*-induced endothelial cell proliferations." Cellular Microbiology **3**(9): 623-632.
- Kennedy, S. G., A. J. Wagner, S. D. Conzen, J. Jordan, A. Bellacosa, P. N. Tsichlis and N. Hay** (1997). "The PI 3-kinase/Akt signaling pathway delivers an anti-apoptotic signal." Genes Dev. **11**(6): 701-713.
- Kierbel, A., A. Gassama-Diagne, K. Mostov and J. N. Engel** (2005a). The Phosphoinositol-3-Kinase-Protein Kinase B/Akt Pathway Is Critical for *Pseudomonas aeruginosa* Strain PAK Internalization. **16**: 2577-2585.
- Kierbel, A., A. Gassama-Diagne, K. Mostov and J. N. Engel** (2005b). "The Phosphoinositol-3-Kinase-Protein Kinase B/Akt Pathway Is Critical for *Pseudomonas aeruginosa* Strain PAK Internalization." Mol. Biol. Cell **16**(5): 2577-2585.
- Kim, I., J. H. Kim, S. O. Moon, H. J. Kwak, N. G. Kim and G. Y. Koh** (2000). "Angiopoietin-2 at high concentration can enhance endothelial cell survival through the phosphatidylinositol 3'-kinase/Akt signal transduction pathway." Oncogene **19**(39): 4549-4552.
- Kirby, J. E. and D. M. Nekorchuk** (2002a). "Bartonella-associated endothelial proliferation depends on inhibition of apoptosis." Proceedings of the National Academy of Sciences **99**(7): 4656-4661.
- Kirby, J. E. and D. M. Nekorchuk** (2002b). "Bartonella-associated endothelial proliferation depends on inhibition of apoptosis." PNAS **99**(7): 4656-4661.
- Kohlhorst, D. and B. Baumstark** (2007). Unpublished data.
- Kordick, D. L., K. H. Wilson, D. J. Sexton, T. L. Hadfield, H. A. Berkhoff and E. B. Breitschwerdt** (1995). "Prolonged *Bartonella* bacteremia in cats associated with cat-scratch disease patients." J. Clin. Microbiol. **33**(12): 3245-3251.
- Kotani, K., K. Hara, K. Yonezawa and M. Kasuga** (1995). "Phosphoinositide 3-Kinase as an Upstream Regulator of the Small GTP-Binding Protein Rac in the Insulin Signaling of Membrane Ruffling." Biochemical and Biophysical Research Communications **208**(3): 985-990.

- Ku, H. and K. E. Meier** (2000). "Phosphorylation of Paxillin via the ERK Mitogen-activated Protein Kinase Cascade in EL4 Thymoma Cells." J. Biol. Chem. **275**(15): 11333-11340.
- Kyriakis, J. M. and J. Avruch** (2001). Mammalian Mitogen-Activated Protein Kinase Signal Transduction Pathways Activated by Stress and Inflammation. **81**: 807-869.
- Leroy-Dudal, J., H. Gagniere, E. Cossard, F. Carreiras and P. Di Martino** (2004). "Role of $\alpha_5\beta_1$ integrins and vitronectin in *Pseudomonas aeruginosa* PAK interaction with A549 respiratory cells." Microbes and Infection **6**(10): 875-881.
- Liberto, M. C., G. Matera, A. G. Lamberti, G. S. Barreca, D. Foca, A. Quirino, M. R. Soria and A. Foca** (2004). "Bartonella quintana-induced apoptosis inhibition of human endothelial cells is associated with p38 and SAPK/JNK modulation and with stimulation of mitosis." Diagnostic Microbiology and Infectious Disease **50**(3): 159-166.
- Liberto, M. C., G. Matera, A. G. Lamberti, G. S. Barreca, A. Quirino and A. Foca** (2003). "In vitro Bartonella quintana infection modulates the programmed cell death and inflammatory reaction of endothelial cells." Diagnostic Microbiology and Infectious Disease **45**(2): 107-115.
- Luo, Y. and G. L. Radice** (2005). "N-cadherin acts upstream of VE-cadherin in controlling vascular morphogenesis." J. Cell Biol. **169**(1): 29-34.
- Maiti, D., A. Bhattacharyya and J. Basu** (2001). "Lipoarabinomannan from Mycobacterium tuberculosis Promotes Macrophage Survival by Phosphorylating Bad through a Phosphatidylinositol 3-Kinase/Akt Pathway." J. Biol. Chem. **276**(1): 329-333.
- Martinez, J. J. and S. J. Hultgren** (2002). "Requirement of Rho-family GTPases in the invasion of Type 1-piliated uropathogenic Escherichia coli." Cellular Microbiology **4**(1): 19-28.
- Maurin, M., F. Eb, J. Etienne and D. Raoult** (1997). "Serological cross-reactions between Bartonella and Chlamydia species: implications for diagnosis." J. Clin. Microbiol. **35**(9): 2283-2287.
- Minnick, M. F., S. J. Mitchell and S. J. McAllister** (1996). "Cell entry and the pathogenesis of Bartonella infections." Trends in Microbiology **4**(9): 343-347.
- Minnick, M. F., L. S. Smitherman and D. S. Samuels** (2003). "Mitogenic Effect of Bartonella bacilliformis on Human Vascular Endothelial Cells and Involvement of GroEL." Infect. Immun. **71**(12): 6933-6942.
- Mirzapoiazova, T., I. A. Kolosova, L. Romer, J. G. Garcia and A. D. Verin** (2005). "The role of caldesmon in the regulation of endothelial cytoskeleton and migration." Journal of Cellular Physiology **203**(3): 520-528.
- Mitchell, S. J. and M. F. Minnick** (1995). "Characterization of a two-gene locus from Bartonella bacilliformis associated with the ability to invade human erythrocytes." Infect. Immun. **63**(4): 1552-1562.
- Miyamoto, S., H. Teramoto, O. A. Coso, J. S. Gutkind, P. D. Burbelo, S. K. Akiyama and K. M. Yamada** (1995). "Integrin function: molecular hierarchies of cytoskeletal and signaling molecules." J. Cell Biol. **131**(3): 791-805.

- Moser, I., W. Schroeder and J. Salnikow** (1997). "Campylobacter jejuni major outer membrane protein and a 59-kDa protein are involved in binding to fibronectin and INT 407 cell membranes." *FEMS Microbiology Letters* **157**(2): 233-238.
- Musso, T., R. Badolato, D. Ravarino, S. Stornello, P. Panzanelli, C. Merlino, D. Savoia, R. Cavallo, A. N. Ponzi and M. Zucca** (2001). "Interaction of Bartonella henselae with the Murine Macrophage Cell Line J774: Infection and Proinflammatory Response." *Infect. Immun.* **69**(10): 5974-5980.
- Naranatt, P. P., S. M. Akula, C. A. Zien, H. H. Krishnan and B. Chandran** (2003). Kaposi's Sarcoma-Associated Herpesvirus Induces the Phosphatidylinositol 3-Kinase-PKC- ζ -MEK-ERK Signaling Pathway in Target Cells Early during Infection: Implications for Infectivity. **77**: 1524-1539.
- Naumann, M., T. Rudel, B. Wieland, C. Bartsch and T. F. Meyer** (1998). "Coordinate Activation of Activator Protein 1 and Inflammatory Cytokines in Response to Neisseria gonorrhoeae Epithelial Cell Contact Involves Stress Response Kinases." *J. Exp. Med.* **188**(7): 1277-1286.
- Ohnishi, Y., T. Beppu and S. Horinouchi** (1997). "Two genes encoding serine protease homologues in *Serratia marcescens* and characterization of their products in *Escherichia coli*." *Journal of Biochemistry* **121**(5): 902-13.
- Owen, P., M. Meehan, H. de Loughry-Doherty and I. Henderson** (1996). "Phase-variable outer membrane proteins in *Escherichia coli*." *FEMS Immunology and Medical Microbiology* **16**(2): 63-76.
- Ozeri, V., I. Rosenshine, D. F. Mosher, R. Fassler and E. Hanski** (1998). "Roles of integrins and fibronectin in the entry of *Streptococcus pyogenes* into cells via protein F1." *Molecular Microbiology* **30**(3): 625-637.
- Padmalayam, I., T. Kelly, B. Baumstark and R. Massung** (2000a). "Molecular Cloning, Sequencing, Expression and Characterization of an Immunogenic 43-Kilodalton Lipoprotein of Bartonella bacilliformis that has Homology to NlpD/LppB." *Infection and Immunity* **68**(9): 4972-4979.
- Padmalayam, I., T. Kelly, B. Baumstark and R. Massung** (2000b). "Molecular Cloning, Sequencing, Expression, and Characterization of an Immunogenic 43-Kilodalton Lipoprotein of Bartonella bacilliformis That Has Homology to NlpD/LppB." *Infect. Immun.* **68**(9): 4972-4979.
- Padmalyam, I., K. Karem, B. Baumstark and R. Massung** (2000). "The gene encoding the 17-kDa antigen of Bartonella henselae is located within a cluster of genes homologous to the virB virulence operon." *DNA and Cell Biology* **19**(6): 377-82.
- Peacock, S. J., T. J. Foster, B. J. Cameron and A. R. Berendt** (1999). "Bacterial fibronectin-binding proteins and endothelial cell surface fibronectin mediate adherence of *Staphylococcus aureus* to resting human endothelial cells." *Microbiology* **145**(12): 3477-3486.
- Pelech, S. L. and J. S. Sanghera** (1992). "MAP kinases: charting the regulatory pathways." *Science* **257**(5075): 1355-56.
- Peterson, K., J. Baseman and J. Alderete** (1983). "Treponema pallidum receptor binding proteins interact with fibronectin." *J. Exp. Med.* **157**(6): 1958-1970.

- Pi, X., C. Yan and B. C. Berk** (2004). "Big Mitogen-Activated Protein Kinase (BMK1)/ERK5 Protects Endothelial Cells From Apoptosis." *Circ Res* **94**(3): 362-369.
- Pottratz, S. T. and W. J. I. Martin** (1990). "Role of fibronectin in *Pneumocystis carinii* attachment to cultured lung cells." *Journal of Clinical Investigation* **85**(2): 351-356.
- Purushothaman, S. S., B. Wang and P. P. Cleary** (2003). "M1 Protein Triggers a Phosphoinositide Cascade for Group A Streptococcus Invasion of Epithelial Cells." *Infect. Immun.* **71**(10): 5823-5830.
- Qi, J.-H., T. Matsumoto, K. Huang, K. Olausson, R. Christofferson and L. Claesson-Welsh** (1999). "Phosphoinositide 3 kinase is critical for survival, mitogenesis and migration but not for differentiation of endothelial cells." *Angiogenesis* **3**(4): 371-380.
- Qian, Y., X. Zhong, D. C. Flynn, J. Z. Zheng, M. Qiao, C. Wu, S. Dedhar, X. Shi and B.-H. Jiang** (2005). "ILK mediates actin filament rearrangements and cell migration and invasion through PI3K//Akt//Rac1 signaling." **24**(19): 3154-3165.
- Raingeaud, J., S. Gupta, M. Dickens and J. Han** (1995). "Pro-inflammatory Cytokines and Environmental Stress Cause p38 Mitogen-activated Protein Kinase Activation by Dual Phosphorylation on Tyrosine and Threonine." *J. Biol. Chem.* **270**(13): 7420-7426.
- Raoult, D., M. Drancourt, A. Carta and J. A. Gastaut** (1994). "Bartonella (Rochalimaea) quintana isolation in patient with chronic adenopathy, lymphopenia, and a cat." *Lancet* **343**(8903): 977.
- Raoult, D. and V. Roux** (1999). "The body louse as a vector of reemerging human disease." *Clinical and Infectious Diseases* **29**(4): 888-911.
- Relman, D. A., S. Falkow, P. E. LeBoit, L. A. Perchocha, K. W. Min, D. F. Welch and L. N. Slater** (1991). "The organism causing bacillary angiomatosis, peliosis hepatis, and fever and bacteremia in immunocompromised patients." *New England Journal of Medicine* **324**(21): 1514.
- Ren, X. D., W. B. Kiosses, D. J. Sieg, C. A. Otey, D. D. Schlaepfer and M. A. Schwartz** (2000). "Focal adhesion kinase suppresses Rho activity to promote focal adhesion turnover." *J Cell Sci* **113**(20): 3673-3678.
- Resto-Ruiz, S. I., M. Schmiederer, D. Sweger, C. Newton, T. W. Klein, H. Friedman and B. E. Anderson** (2002). "Induction of a Potential Paracrine Angiogenic Loop between Human THP-1 Macrophages and Human Microvascular Endothelial Cells during Bartonella henselae Infection." *Infect. Immun.* **70**(8): 4564-4570.
- Riess, T., S. G. E. Andersson, A. Lupas, M. Schaller, A. Schafer, P. Kyme, J. Martin, J.-H. Walzlein, U. Ehehalt, H. Lindroos, M. Schirle, A. Nordheim, I. B. Autenrieth and V. A. J. Kempf** (2004). "Bartonella Adhesin A Mediates a Proangiogenic Host Cell Response." *J. Exp. Med.* **200**(10): 1267-1278.
- Riess, T., G. Raddatz, D. Linke, A. Schafer and V. A. J. Kempf** (2006). "Analysis of Bartonella adhesin A-expression reveals differences between various B. henselae strains." *Infect. Immun.* **75**(1): 35-43.
- Riess, T., G. Raddatz, D. Linke, A. Schafer and V. A. J. Kempf** (2007). "Analysis of Bartonella Adhesin A Expression Reveals Differences between Various B. henselae Strains." *Infect. Immun.* **75**(1): 35-43.

- Rosen, L. B., D. D. Ginty, M. J. Weber and M. E. Grennberg** (1994). "Membrane depolarization and calcium influx stimulate MEK and MAP kinase via activation of Ras." *Neuron* **12**(6): 1207-21.
- Rousseau, S., F. Houle, J. Landry and J. Huot** (1997). "p38 MAP kinase activation by vascular endothelial growth factor mediates actin reorganization and cell migration in human endothelial cells." *Oncogene* **15**(18): 2169-77.
- Ruggieri, R., C. Y. Y. and M. Symons** (2001). "The small GTPase Rac suppresses apoptosis caused by serum deprivation in fibroblasts." *Molecular Medicine* **7**(5): 293-300.
- Ruoslahti, E. and M. D. Pierschbacher** (1987). "New perspectives in cell adhesion: RGD and integrins." *Science* **238**(4826): 491-7.
- Sa, G., G. Murugesan, M. Jaye, Y. Ivashchenko and P. L. Fox** (1995). "Activation of Cytosolic Phospholipase A(2) by Basic Fibroblast Growth Factor via a p42 Mitogen-activated Protein Kinase-dependent Phosphorylation Pathway in Endothelial Cells." *J. Biol. Chem.* **270**(5): 2360-2366.
- Saenz, H. L., P. Engel, M. C. Stoeckli, C. Lanz, G. Raddatz, M. Vayssier-Taussat, R. Birtles, S. C. Schuster and C. Dehio** (2007). "Genomic analysis of Bartonella identifies type IV secretion systems as host adaptability factors." *Nat Genet* **39**(12): 1469-1476.
- Sakai, A., T. Koga, J.-H. Lim, H. Jono, K. Harada, E. Szymanski, H. Xu, H. Kai and J.-D. Li** (2007). "The bacterium, nontypeable Haemophilus influenzae, enhances host antiviral response by inducing Toll-like receptor expression. Evidence for negative regulation of host antiviral response by CYLD." *FEBS Journal* **274**(14): 3655-3668.
- Salameh, A., F. Galvagni, M. Bardelli, F. Bussolino and S. Oliviero** (2005). "Direct recruitment of CRK and GRB2 to VEGFR-3 induces proliferation, migration, and survival of endothelial cells through the activation of ERK, AKT, and JNK pathways." *Blood* **106**(10): 3423-3431.
- Schaller, M. D., C. A. Otey, J. D. Hildebrand and J. T. Parsons** (1995). "Focal adhesion kinase and paxillin bind to peptides mimicking beta integrin cytoplasmic domains." *J. Cell Biol.* **130**(5): 1181-1187.
- Scherer, D. C., I. DeBuron-Connors and M. F. Minnick** (1993). "Characterization of Bartonella bacilliformis flagella and effect of anti-flagellin antibodies on invasion of human erythrocytes." *Infect. Immun.* **61**(12): 4962-4971.
- Schmid, M. C., F. Scheidegger, M. Dehio, N. Balmelle-Devaux, egrave, ge, R. Schulein, P. Guye, C. S. Chennakesava, B. Biedermann and C. Dehio** (2006). "A Translocated Bacterial Protein Protects Vascular Endothelial Cells from Apoptosis." *PLoS Pathogens* **2**(11): e115.
- Schmid, M. C., R. Schulein, M. Dehio, G. Denecker, I. Carena and C. Dehio** (2004). "The VirB type IV secretion system of Bartonella henselae mediates invasion, proinflammatory activation and antiapoptotic protection of endothelial cells." *Molecular Microbiology* **52**(1): 81-92.
- Schmiederer, M., R. Arcenas, R. Widen, N. Valkov and B. Anderson** (2001). "Intracellular Induction of the Bartonella henselae virB Operon by Human Endothelial Cells." *Infect. Immun.* **69**(10): 6495-6502.

- Schulein, R. and C. Dehio** (2002). "The VirB/VirD4 type IV secretion system of Bartonella is essential for establishing intraerythrocytic infection." Molecular Microbiology **46**(4): 1053-1067.
- Schulein, R., P. Guye, T. A. Rhomberg, M. C. Schmid, G. Schroder, A. C. Vergunst, I. Carena and C. Dehio** (2005). "A bipartite signal mediates the transfer of type IV secretion substrates of Bartonella henselae into human cells." Proceedings of the National Academy of Sciences **102**(3): 856-861.
- Schulein, R., A. Seubert, C. Gille, C. Lanz, Y. Hansmann, Y. Piemont and C. Dehio** (2001). "Invasion and Persistent Intracellular Colonization of Erythrocytes: A Unique Parasitic Strategy of the Emerging Pathogen Bartonella." J. Exp. Med. **193**(9): 1077-1086.
- Schulte, B., D. Linke, S. Klumpp, M. Schaller, T. Riess, I. B. Autenrieth and V. A. J. Kempf** (2006). "Bartonella quintana Variably Expressed Outer Membrane Proteins Mediate Vascular Endothelial Growth Factor Secretion but Not Host Cell Adherence." Infect. Immun. **74**(9): 5003-5013.
- Scibelli, A., S. Roperto, L. Manna, L. M. Pavone, S. Tafuri, R. D. Morte and N. Staiano** (2007). "Engagement of integrins as a cellular route of invasion by bacterial pathogens." The Veterinary Journal **173**(3): 482-491.
- Secott, T. E., T. L. Lin and C. C. Wu** (2004). "Mycobacterium avium subsp. paratuberculosis Fibronectin Attachment Protein Facilitates M-Cell Targeting and Invasion through a Fibronectin Bridge with Host Integrins." Infect. Immun. **72**(7): 3724-3732.
- Severa, M., M. E. Remoli, E. Giacomini, V. Annibali, V. Gafa, R. Lande, M. Tomai, M. Salvetti and E. M. Coccia** (2007). "Sensitization to TLR7 Agonist in IFN-beta-Preactivated Dendritic Cells." J Immunol **178**(10): 6208-6216.
- Sokolova, O., N. Heppel, R. Jagerhuber, K. S. Kim, M. Frosch, M. Eigenthaler and A. Schubert-Unkmeir** (2004). "Interaction of Neisseria meningitidis with human brain microvascular endothelial cells: role of MAP- and tyrosine kinases in invasion and inflammatory cytokine release." Cellular Microbiology **6**(12): 1153-1166.
- Stockbauer, K. E., L. Magoun, M. Liu, E. H. Burns, Jr., S. Gubba, S. Renish, X. Pan, S. C. Bodary, E. Baker, J. Coburn, J. M. Leong and J. M. Musser** (1999). "A natural variant of the cysteine protease virulence factor of group A Streptococcus with an arginine-glycine-aspartic acid (RGD) motif preferentially binds human integrins alpha vbeta 3 and alpha IIb beta 3." Proceedings of the National Academy of Sciences **96**(1): 242-247.
- Strieter, R. M., S. L. Kunkel, M. D. Burdick, P. M. Lincoln and A. Walz** (1992). "The detection of a novel neutrophil-activating peptide (ENA-78) using a sensitive ELISA." Immunological Investigations **21**(6): 589-96.
- Strong, R. P., E. E. Tyzzer, C. T. Brues, A. W. Sellards and J. C. Gastiaburu** (1915). "Report of the first expedition to South America." Havard University Press, Cambridge, MA.
- Sukumaran, S. K. and N. V. Prasadarao** (2002). "Regulation of Protein Kinase C in Escherichia coli K1 Invasion of Human Brain Microvascular Endothelial Cells." J. Biol. Chem. **277**(14): 12253-12262.

- Tang, P., I. Rosenshine and B. B. Finlay** (1994). "Listeria monocytogenes, an invasive bacterium, stimulates MAP kinase upon attachment to epithelial cells." Mol. Biol. Cell **5**(4): 455-464.
- Tang, P., C. L. Sutherland, M. R. Gold and B. B. Finlay** (1998). "Listeria monocytogenes Invasion of Epithelial Cells Requires the MEK-1/ERK-2 Mitogen-Activated Protein Kinase Pathway." Infect. Immun. **66**(3): 1106-1112.
- Townsend, C. H.** (1913). "A Phlebotomus the practically certain carrier of verruga." Science **38**(971): 194-5.
- Unkmeir, A., K. Latsch, G. Dietrich, E. Wintermeyer, B. Schinke, S. Schwender, K. S. Kim, M. Eigenthaler and M. Frosch** (2002). "Fibronectin mediates Op-dependent internalization of Neisseria meningitidis in human brain microvascular endothelial cells." Molecular Microbiology **46**(4): 933-946.
- Valbuena, G., H. M. Feng and D. H. Walker** (2002). "Mechanisms of immunity against rickettsiae. New perspectives and opportunities offered by unusual intracellular parasites." Microbes and Infection **4**(6): 625-633.
- van der Flier, A. and A. Sonnenberg** (2001). "Function and interactions of integrins." Cell and Tissue Research **305**(3): 285-298.
- Vercellotti, G. M., D. Lussenhop, P. K. Peterson, L. T. Furcht, J. B. McCarthy, H. S. Jacob and C. F. Moldow** (1984). "Bacterial adherence to fibronectin and endothelial cells: A possible mechanism for bacterial tissue tropism." Journal of Laboratory and Clinical Medicine **103**(1): 34-43.
- Verma, A., G. E. Davis and G. M. Ihler** (2000). "Infection of Human Endothelial Cells with Bartonella bacilliformis Is Dependent on Rho and Results in Activation of Rho." Infect. Immun. **68**(10): 5960-5969.
- Verma, A., G. E. Davis and G. M. Ihler** (2001). "Formation of stress fibres in human endothelial cells infected with Bartonella bacilliformis is associated with altered morphology, impaired migration and defects in cell morphogenesis." Cellular Microbiology **3**(3): 169-180.
- Verma, A. and G. Ihler** (2002a). "Activation of Rac, cdc42 and other downstream signalling molecules by Bartonella bacilliformis during entry into human endothelial cells." Cellular Microbiology **4**(9): 557-569.
- Verma, A. and G. M. Ihler** (2002b). "Activation of Rac, Cdc42 and other downstream signalling molecules by Bartonella bacilliformis during entry into human endothelial cells." Cellular Microbiology **4**(9): 557-569.
- Vinogradova, O., T. Haas, E. F. Plow and J. Qin** (2000). "A structural basis for integrin activation by the cytoplasmic tail of the alpha IIb-subunit." Proceedings of the National Academy of Sciences **97**(4): 1450-1455.
- Wagner, V. T. and A. G. Matthyse** (1992). "Involvement of a vitronectin-like protein in attachment of Agrobacterium tumefaciens to carrot suspension culture cells." J. Bacteriol. **174**(18): 5999-6003.
- Wang, B., R. S. Yurecko, S. Dedhar and P. P. Cleary** (2006). "Integrin-linked kinase is an essential link between integrins and uptake of bacterial pathogens by epithelial cells." Cellular Microbiology **8**(2): 257-266.
- Watanabe, K., O. Yilmaz, S. F. Nakhjiri, C. M. Belton and R. J. Lamont** (2001). "Association of Mitogen-Activated Protein Kinase Pathways with Gingival

- Epithelial Cell Responses to Porphyromonas gingivalis Infection." Infect. Immun. **69**(11): 6731-6737.
- Watarai, M., S. Funato and C. Sasakawa** (1996). Interaction of Ipa proteins of Shigella flexneri with alpha5beta1 integrin promotes entry of the bacteria into mammalian cells. **183**: 991-999.
- Watarai, M., S. Funato and C. Sasakawa** (1996). "Interaction of Ipa proteins of Shigella flexneri with alpha5beta1 integrin promotes entry of the bacteria into mammalian cells
10.1084/jem.183.3.991." J. Exp. Med. **183**(3): 991-999.
- Weitzman, J. B., L. Fiette, K. Matsuo and M. Yaniv** (2000). "JunD Protects Cells from p53-Dependent Senescence and Apoptosis." Molecular Cell **6**(5): 1109-1119.
- Wennstrom, S., A. Siegbahn, K. Yokote, A. K. Arvidsson, C. H. Heldin, S. Mori and L. Claesson-Welsh** (1994). "Membrane ruffling and chemotaxis transduced by the PDGF beta-receptor require the binding for phosphatidylinositol 3' kinase." Oncogene **9**(2): 651-60.
- Williams-Bouyer, N. M. and E. M. Hill** (1999). "Involvement of host cell tyrosine phosphorylation in the invasion of HEp-2 cells by Bartonella bacilliformis." FEMS Microbiology Letters **171**(2): 191-201.
- Williams, C. H., T. Kajander, T. Hyypia, T. Jackson, D. Sheppard and G. Stanway** (2004). "Integrin $\alpha_v\beta_6$ Is an RGD-Dependent Receptor for Coxsackievirus A9." J. Virol. **78**(13): 6967-6973.
- Xu, Y. H., Z. Y. Lu and G. M. Ihler** (1995). "Purification of deformin, an extracellular protein synthesized by Bartonella bacilliformis which causes deformation of erythrocyte membranes." Biochimica et Biophysica Acta **1234**(2): 173-83.
- Yamazaki, S., T. Muta and K. Takeshige** (2001). "A Novel Ikappa B Protein, Ikappa B-zeta, Induced by Proinflammatory Stimuli, Negatively Regulates Nuclear Factor-kappa B in the Nuclei." J. Biol. Chem. **276**(29): 27657-27662.
- Yilmaz, O., T. Jungas, P. Verbeke and D. M. Ojcius** (2004). "Activation of the Phosphatidylinositol 3-Kinase/Akt Pathway Contributes to Survival of Primary Epithelial Cells Infected with the Periodontal Pathogen Porphyromonas gingivalis." Infect. Immun. **72**(7): 3743-3751.
- Yilmaz, O., K. Watanabe and R. J. Lamont** (2002). "Involvement of integrins in fimbriae-mediated binding and invasion by Porphyromonas gingivalis." Cellular Microbiology **4**(5): 305-314.
- Yu, C., Y. Minemoto, J. Zhang, J. Liu, F. Tang, T. N. Bui, J. Xiang and A. Lin** (2004). "JNK Suppresses Apoptosis via Phosphorylation of the Proapoptotic Bcl-2 Family Protein BAD." Molecular Cell **13**(3): 329-340.
- Zhang, P., B. B. Chomel, M. K. Schau, J. S. Goo, S. Droz, K. L. Kelminson, S. S. George, N. W. Lerche and J. E. Koehler** (2004). "A family of variably expressed outer-membrane proteins (Vomp) mediates adhesion and autoaggregation in Bartonella quintana." Proceedings of the National Academy of Sciences **101**(37): 13630-13635.